A TECHNIQUE TO UTILIZE SMART METER LOAD INFORMATION FOR ADAPTING OVERCURRENT PROTECTION FOR RADIAL DISTRIBUTION SYSTEMS WITH DISTRIBUTED GENERATIONS

A Thesis

by

FRED AGYEKUM ITUZARO

Submitted to the Office of Graduate Studies of
Texas A&M University
in partial fulfillment of the requirements for the degree of

MASTER OF SCIENCE

May 2012

Major Subject: Electrical Engineering

A TECHNIQUE TO UTILIZE SMART METER LOAD INFORMATION FOR ADAPTING OVERCURRENT PROTECTION FOR RADIAL DISTRIBUTION SYSTEMS WITH DISTRIBUTED GENERATIONS

A Thesis

by

FRED AGYEKUM ITUZARO

Submitted to the Office of Graduate Studies of
Texas A&M University
in partial fulfillment of the requirements for the degree of

MASTER OF SCIENCE

Approved by:

Chair of Committee,	Karen L. Butler-Purry
Committee Members,	Mehrdad Ehsani
	Deepa Kundur
	Lewis Ntaimo
Head of Department,	Costas Georghiades

May 2012

Major Subject: Electrical Engineering

ABSTRACT

A Technique to Utilize Smart Meter Load Information for Adapting Overcurrent Protection for Radial Distribution Systems with Distributed Generations. (May 2012)

Fred Agyekum Ituzaro, B.S., Kwame Nkrumah University of Science & Technology, Ghana

Chair of Advisory Committee: Dr. Karen L. Butler-Purry

Smart radial distribution grids will include advanced metering infrastructure (AMI) and significant distributed generators (DGs) connected close to loads. DGs in these radial distribution systems (RDS) introduce bidirectional power flows (BPFs) and contribute to fault current. These BPFs may cause unwanted tripping of existing overcurrent (OC) protection devices and result in permanent outages for a large number of customers. This thesis presents a protection approach that modified an existing overcurrent protection scheme to reduce the number of customers affected by faults in RDS with DGs. Further, a technique is presented that utilizes customers loading information from smart meters in AMI to improve the sensitivity of substation OC relays by adaptively changing the pickup settings. The modified protection approach involves predefining zones in RDS with DGs and installing directional OC relays and circuit breakers at the zonal boundaries. Zonal boundary relays determine faulted zones by sharing information on the direction of detected faults current using binary state signals over a communication medium. The technique to adapt the substation relay pickup settings uses the demand measurements from smart meters for two 12-hour intervals from the previous day to determine the maximum diversified demand at the relay's location. The pickup settings of the substation relay for the two 12-hour intervals during the following day for the zone supplied by the substation are adaptively set based on the current that corresponds to the maximum diversified demand from the previous day.

The techniques were validated through simulations in EMTP™/PSCAD® using an expanded IEEE 34 node radial test feeder that included DGs and a secondary distribution level. By decentralizing the control of the zonal boundary breakers, the single point of failure was eliminated in the modified protection approach. The cases studied showed that the modified protection approach allows for selective identification and isolation of the faulted zones. Also, the sensitivity of the substation OC relay was improved by at least 24% by using the pickup settings for the two 12-hour intervals from the smart meter demand measurements compared to the pickup settings computed using the conventional methodology based on the maximum loading of the zone.

DEDICATION

This thesis is proudly dedicated to my parents and siblings. Without their encouragement and assistance, I would never have gotten this far.

ACKNOWLEDGEMENTS

I would like to express my deepest gratitude to my advisor, Dr. Karen Butler-Purry, for her guidance and encouragement throughout the course of my research work. Dr. Butler-Purry's guidance and financial assistance have been instrumental during my graduate study at Texas A&M University.

I want to thank my committee members, Dr. Mehdrad Ehsani, Dr. Deepa Kundur, and Dr. Lewis Ntaimo for their valuable time. My appreciation also goes to the Electrical/Computer Engineering faculty and staff for making my time at Texas A&M University a great experience.

Thank you to my fellow researchers at the Power System Automation Lab for their amity. Finally, credits go to my parents and siblings for their love, inspiration and patience.

TABLE OF CONTENTS

Page

LIST OF FIGURES

Page

Page

Page

LIST OF TABLES

Page

1 INTRODUCTION

1.1 Background

The Electric Power Grid since its inception has greatly revolutionized our way of life and improved productivity. By virtue of its physical layout, the electric power grid consists of three major systems: generation, transmission and distribution. This classification of the grid has allowed for the development of solutions that tailors to the specific needs and challenges of operating each of these three major systems. Traditionally the generation systems, usually bulky for purposes of economies of scale, are located at remote locations away from the load centers and supply the needed energy. Power from the generating stations is transported on high voltage lines of the transmission systems to distribution substations. The distribution substation transformers step down the voltages to utilization levels for consumers. Fig. 1 shows the structure of an electric power grid [1].

The distribution system (DS) has both a primary and a secondary section with the distinction mainly due to the voltage levels. The primary DS, usually 3-phase with a voltage range of 69kV – 2.4kV, consists of feeders that radiate from the substation and supply power to the customers at the secondary level. High capacity industrial and commercial loads are sometimes served by the feeders at the primary level. The secondary distribution, which branches off from the main feeders at the primary section has distribution transformers that further reduce the primary voltage to 120/240 single phase, 120/208 or 277/480 3-phase depending on the loads served.

The topologies of the DS can be classified into three major categories: radial, loop and network [2]. A utility's choice of a particular topology is often influenced by cost and degree of reliability needed by its customers. The radial topology is the most commonly used in the US and is also the least ranked in terms of service reliability.

This thesis follows the style of *IEEE Transactions on Power Systems*.

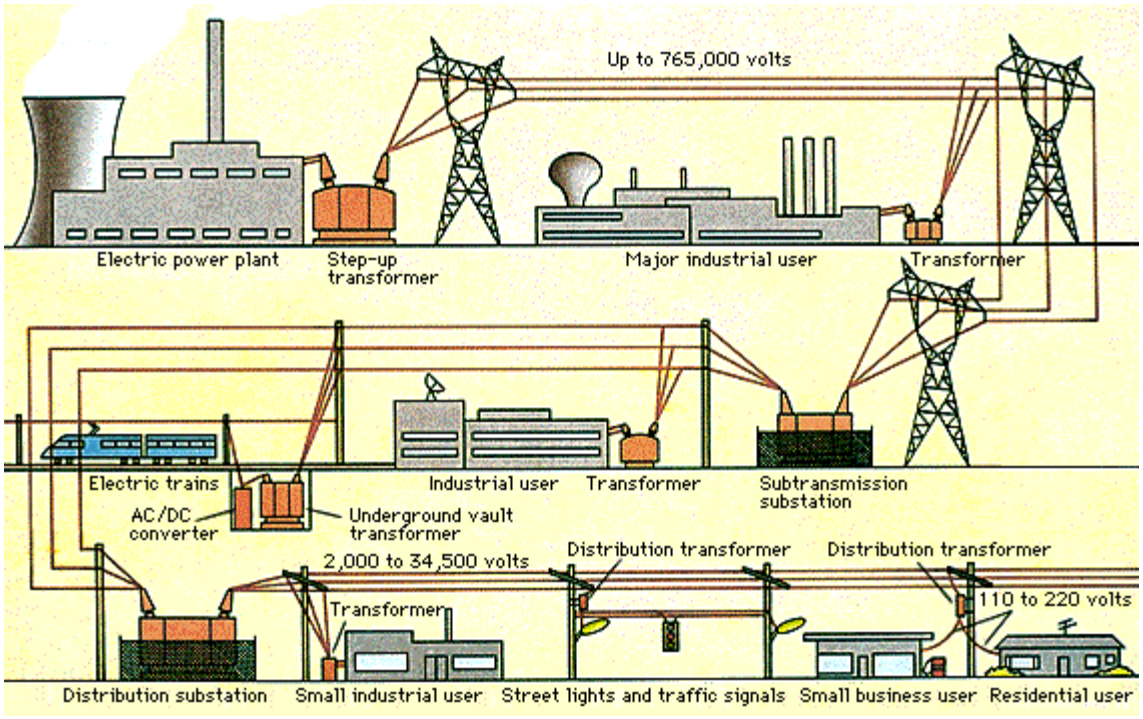

Fig. 1 The Electric Power Grid [1]

In radial DS, power flows from the substation to customers in one direction. The loop and network arrangement have increased levels of reliability due to the possible supply paths from other connected distribution lines.

Radial DS have a main feeder that serves as the backbone of the distribution circuit and has laterals from which power is tapped to supply various customers. The laterals can be single phase, two-phase or three-phase. By virtue of the radial nature of most DS, overcurrent (OC) protection is relatively simple to implement. Fuses, reclosers, sectionalizers and relays are the commonly used overcurrent protection devices.

1.2 Problem Definition

Presently, the distribution systems are experiencing a number of challenges. Firstly, the infrastructure is aging and deteriorating thereby making it hard to meet the increasing load growth. This is further complicated by the inability of utilities to obtain

right-of-ways to build new transmission lines to transport more power from remote generation stations to major load centers. Distributed generators (DGs) are therefore been introduced close to the load centers. In addition, the lack of adequate real time data also causes the operation of the DS to be based on past grid topologies, historical load profiles, and statistical studies. These challenges have caused many countries around the world to take a fresh look at their DS and have resulted in the concept of the smart grid.

The DS currently accommodates a small amount of distributed generators (DGs) due to its robust design. However, under the smart grid concept, more DGs and demand side response programs are anticipated to be implemented at the DS level. Such increased penetration levels of DGs will result in significant bidirectional flows in radial DS, which are detrimental to the conventional OC protection schemes. The power flows arising from the DGs cause selectivity losses among the various OC protective devices as fault currents are altered. Moreover, the implementation of demand side programs will make maximum loading of the DS to be even more rarely used. Sensitivity of phase OC relays will further reduce under such circumstances. Hence it is prudent to have a protection scheme that takes into consideration the added DGs and is also reflective of the varying system loading.

1.3 Objective and Research Approach

There were two objectives of the research reported in this thesis. First, an overcurrent protection scheme was to be developed for a radial distribution system (RDS) with DGs by modifying an existing protection scheme. The second objective was to investigate the utilization of load data from smart meters available through advanced metering infrastructure (AMI) system to adapt the settings of the substation relays in the modified overcurrent protection approach. To validate and study the approach developed to achieve the two objectives, the IEEE 34 Node Radial Test Feeder was selected as the test system. The actual test feeder was modified to represent a two feeder system. A dual bus radial multi-feeder design was adopted. DGs were connected at select nodes at the primary distribution level. OC relay protection was added to the multi-feeder. Also, the

primary level of the multi-feeder was extended to the secondary distribution level to model customer consumption and smart meters. The secondary distribution level customers were classified as residential, commercial and industrial for the identification of the appropriate type of smart meter device. The load data measured by the smart meters at the respective customer locations was used to compute the adaptive OC substation relay pick up settings for a zone directly connected to the substation. The multi-feeder test system and the smart meters were implemented and the simulation studies were performed using EMTP™/PSCAD® software.

1.4 Summary

The work in this thesis is organized into six sections. Section 2 presents a review of radial distribution system protection approach. Further in that section, the impacts of DGs to DS protection are discussed and various approaches proposed in the literature to mitigate these effects are presented. In section 3, an overview of smart grid and advanced metering infrastructure is given. The key technology areas that have been identified by industry experts to make the current grid smarter are examined.

Section 4 states the problems that were addressed by this thesis work. In section 5, the solution methodologies are outlined. The first part of section 5 focuses on the methodology for the modified protection approach. The IEEE 34 Node Radial Test Feeder is introduced and the modifications made for the purpose of testing the modified protection approach are shown. Results of case studies of the protection approach are also presented. In the second part of section 5, the approach for utilizing the load measurements from smart meters in adapting the settings of the substation OC relay is presented. Additional changes that were made to the IEEE 34 node radial test feeder to study the adaptive approach are expounded, and the results of case studies are discussed. Finally, section 6 gives conclusions from the research findings. Future research efforts that can be pursued to improve the findings are also suggested.

2 REVIEW OF DISTRIBUTION SYSTEM PROTECTION APPROACHES

2.1 Introduction

Distribution Systems (DSs) are comprised of a vast number of components connected either overhead or underground. Therefore, protecting the various components from damage is very critical in maintaining high reliability levels. The protection philosophy for DSs is based on isolating permanent faults such that minimal customers are affected, with sensitivity levels that promote personnel and public safety. DS protection is achieved through the use of various fault interrupting elements such as fuses, automatic reclosers, sectionalizers, relays and circuit breakers.

Most faults that occur on overhead radial DSs are temporary, 50-90% [3], and as a result the main feeders of radial DSs are often protected by a recloser. The recloser is used to clear temporary faults on the feeder and locks out after a set number of shots on a permanent fault. Breakers are also typically located at the substations and are used for interrupting larger fault currents. Fuses, however, are used to protect laterals or taps and in some cases on the high voltage side of distribution substation transformers.

In this section conventional protection schemes for radial distribution systems are discussed. A literature review of existing protection methods when DGs are connected to radial distribution systems is also presented.

2.2 Conventional Protection Schemes for Radial Distribution Systems

Faults that occur on the DS subject the components to high short circuit currents. This makes radial distribution protection to be predominantly overcurrent (OC). Fig. 2 shows a simple radial distribution feeder with typical OC devices. The supply represents the sub-transmission network that delivers power to the DS via the substation transformer. The feeder as shown has a relay, R1 that serves as the primary protective device for lines 1 and 2. In radial distribution systems (RDS), R1 is typically called a recloser as it will have a reclosing function with predetermined sequence of operations (e.g. two fast and two slow operations). The recloser in this example serves as the back-

up protective device for lines 3 and 4. Fuse 1 and fuse 2 are the main protective devices for lines 3 and 4, respectively. The feeder as shown has 4 loads and all lines are 3-phase.

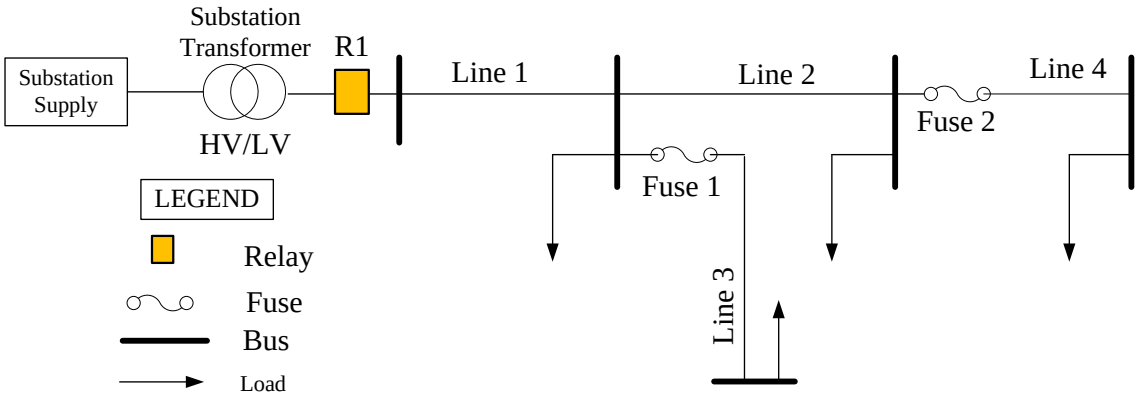

Fig. 2 A Simple Radial Distribution Feeder with Overcurrent Protection.

2.2.1 Overcurrent Protection Based on Fuses and Reclosers

Fuse based protection is often used in conjunction with reclosers. A recloser is a specialty distribution protective device capable of interrupting fault current and automatically reclosing while a fuse is a low cost fault current interrupter that are easily replaced [3]. Two time-current curves describe a fuse: minimum melt curve (MMC) and total clear curve (TCC). The MMC time is 90% of the average-melt time so as to account for manufacturing tolerances. The TCC is the summation of the average melting time, the arcing time, and the manufacturing tolerances [3]. Fuse based protection schemes can be either a fuse saving or fuse blowing scheme. The distinguishing feature between these two schemes is based on how quick the sequence of operation of the recloser is allowed to interrupt a given fault current [4].

In a fuse blowing scheme, the fuse operates and isolates the faulted area for any fault occurring on the system before any recloser operation. This is achieved by setting the recloser fast curve above the MMC and the TCC of the fuse. The scheme is applied

in areas (urban or industrial plants) of the distribution feeder where loads are sensitive to momentary service interruption. The drawback of this scheme is that the line fuses have to be replaced frequently as they operate for all fault conditions, both temporary and permanent. In reference to Fig. 2, the implementation of a fuse blowing scheme will be such that for any fault on line 3, fuse 1 melts and eventually isolates that section of the feeder before R1 operates. A coordination curve for this fuse blowing scheme is depicted in Fig. 3. For every value of current on the x-axis between points A and B on the figure, the fuse curve is always below the recloser curve. This means that fuse 1 operates before R1 in all fault conditions.

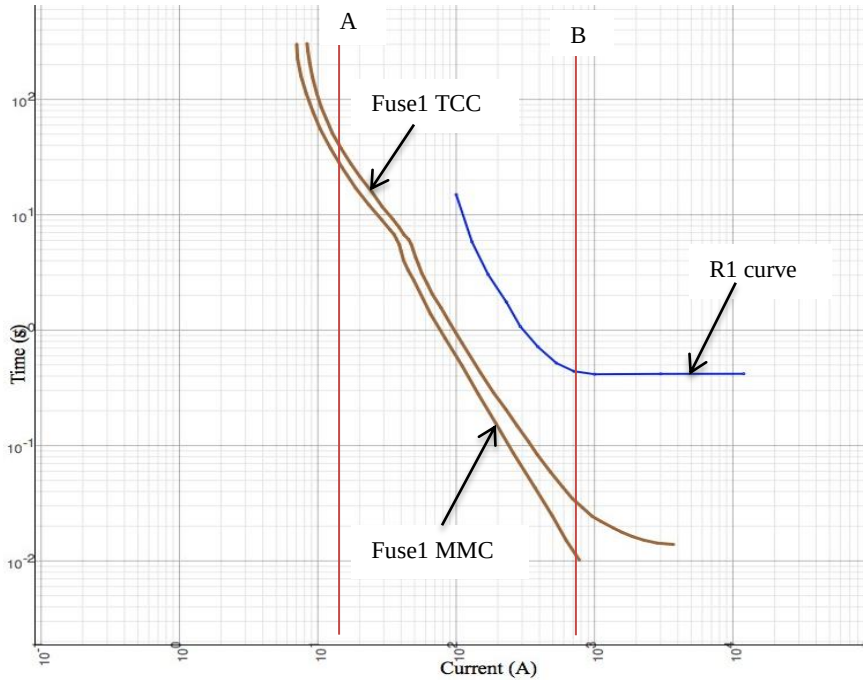

Fig. 3 A Typical Fuse Blowing Coordination Curve for Fig. 2 System.

Experience has shown that most distribution faults in DSs with overhead lines are temporary in nature; and therefore making the fuse operate at the incidence of every fault affects the requirement of service continuity. The fuse saving scheme therefore

ensures that the recloser operates for a specified number of times on its fast response curve to clear all momentary faults that occur downstream a fused protected line. If for some reason, the fault persists after the recloser's operation on its fast curve, the fuse blows to clear the fault. In the event that the fuse is unable to clear the fault due to a malfunction, the recloser will proceed to operate on its slow response curve to permanently isolate the faulted line segment. Therefore, for this scheme, the fuse characteristic curves falls between the recloser's fast and slow response curves for coordination purposes. The scheme is mostly applicable to multi-tap rural distribution networks where loads may not be very sensitive to temporary faults. Fig. 4 shows a fuse saving coordination curve for the system in Fig. 2. As shown in the figure, R1 fast curve occurs before fuse 1 curves for all currents between A and B. This approach ensures that R1 operates before fuse 1 does within the coordination interval between A and B.

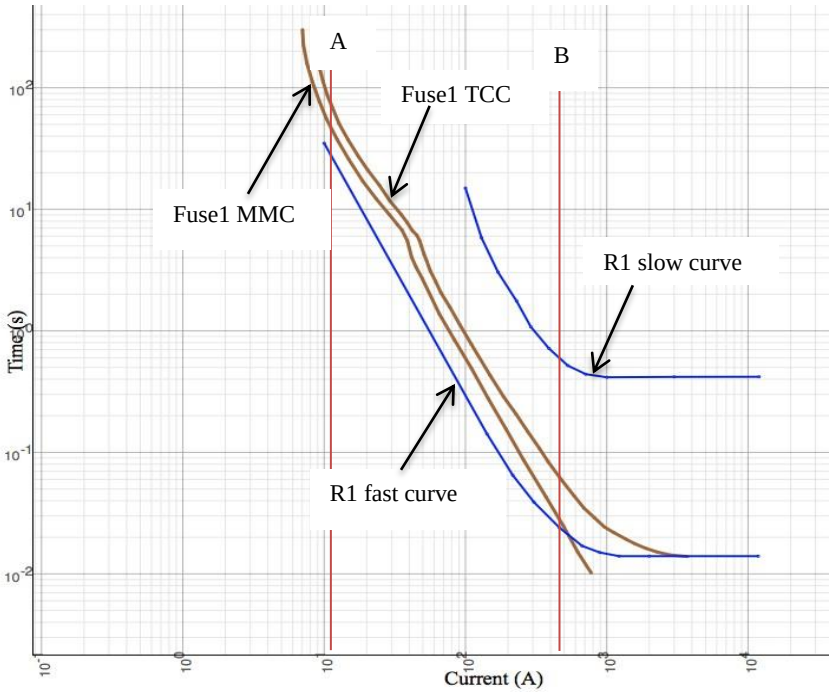

Fig. 4 A Typical Fuse Saving Coordination Curve for Fig. 2 System

2.2.2 Overcurrent Protection Based on Relays

Relays are the brains in controlling circuit breaker operations. IEEE defines a circuit breaker as a device designed to open and close a circuit by non-automatic means, and to open the circuit automatically on a predetermined overload of current, without injury to itself when properly applied within its rating. IEEE again defines a relay as an electric device designed to respond to input conditions in a prescribed manner and, after specified conditions are met, to cause contact operation or similar abrupt change in associated electric control circuits [5]. The inputs to the relay are supplied through either a current transformer or voltage transformer or both depending on the relay's application. Relays exist in different forms including overcurrent (OC), differential, overvoltage, impedance etc. In RDS, OC relays are often used and could be phase, ground or negative sequence type [4]. These OC devices react when the current sensed by the relay exceeds a predetermined threshold either instantaneously or for some duration of time. The set threshold for phase OC relays is normally between twice the maximum load current and a third of the minimum fault current value [6]. Thus, the reach (protection coverage) of phase OC relay is defined between the maximum load current and minimum fault current. For ground and negative sequence relays, the threshold is respectively set to be above the zero sequence and negative sequence currents due to loading and feeder unbalance. The characteristics curve of the relays can be instantaneous, definite or inverse time depending on the application requirement and available fault current magnitudes.

Instantaneous OC relays are applied in parts of the RDS where there are significant changes in fault current magnitudes as one moves away from the relay location towards the end of the feeder. The operating time of the instantaneous OC relay is constant for a given fault current once the set threshold is exceeded. The setting of this relay's threshold does not take into consideration the maximum load current but rather transient overreach arising from transformer inrush and cold load pick up. Another requirement considered is to set the instantaneous relays such that they do not overreach the end of their protected line.

For definite time OC relay applications, the relay operating time is independent of the level of fault current. Coordination among these relays is achieved by assigning appropriate time delay setting to each available relay such that the relay closest to the fault operates. Fig. 5 shows a radial distribution feeder where fuse 1 in Fig. 2 is replaced by a relay, R2.

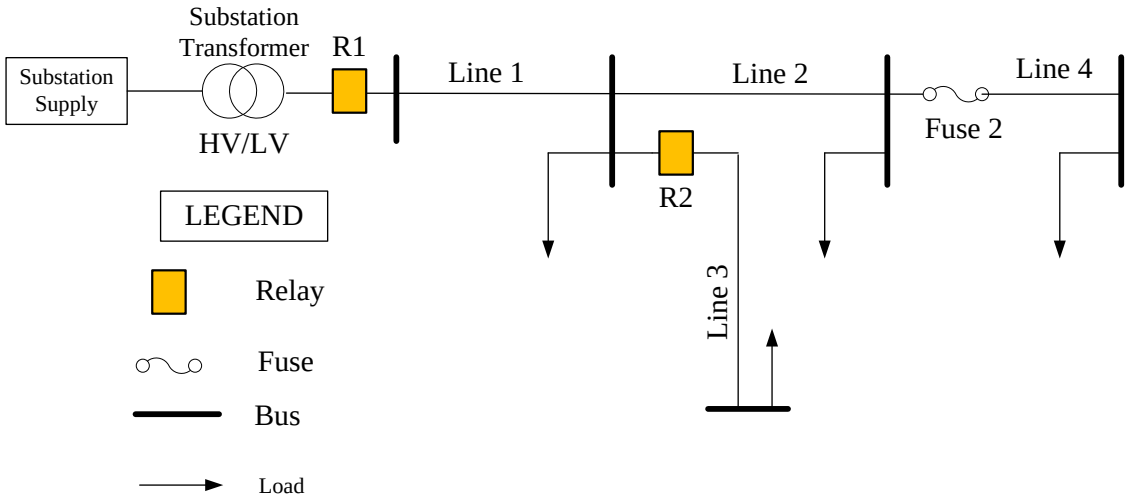

Fig. 5 A Simple Radial Distribution Feeder with Overcurrent Protection (Adapted from Fig. 2)

In Fig. 5, assuming R1 and R2 are definite OC relays, coordination is obtained by setting R2 to operate at t secs and R1 at t+τ secs. The time delay value τ is usually long enough to prevent the upstream relay (R1) from operating until the downstream relay (R2) has reacted. A drawback to this coordination approach is that there is a long delay to clear faults close to the source point, which also happen to be of the highest current magnitude.

To overcome the shortcomings of the above two relay types, inverse time relays are used. These relays have their time of operation to be inversely proportional to the available fault current. Two settings are required: pickup and time dial. The pickup value serves as the threshold beyond, which the relay operates for any given fault

current. The appropriate time dial setting is used to establish coordination among the relays. A typical coordination curve for the relays R1 and R2 in Fig. 5 assuming inverse curve characteristics is shown in Fig. 6, which is adapted from [7]. The coordination time interval (CTI) allows for selectivity between the two relays.

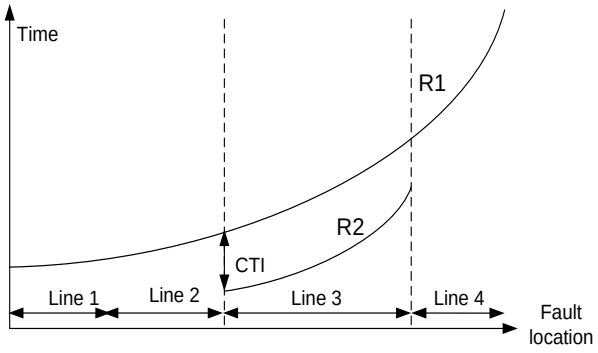

Fig. 6 Time Coordination Curve of Inverse Time OC Relays for Fig. 5 System

2.2.3 Directional Overcurrent and Distance Relays

Directional overcurrent relays usually consist of a directional element and an OC relay. The directional element discriminates the direction of current flow to a fault in a way that permits the OC relay to operate for faults in one direction, and hinders the relay operation for faults in the opposite direction. Traditionally, the direction of the fault current is achieved through a comparison of the phase angle of the operating current phasor, which is dependent on a fault, to a polarizing quantity independent of the fault location [6]. The polarizing quantity is commonly the system voltage for phase overcurrent relays. The addition of the directional functionality to the OC relay, can take the form of a directional control or a directional supervision. Directional control prevents the relay from picking up until the directional element has correctly indicated the path of the fault current. This approach is safer as it prevents the race between the resetting of the OC relay and the directional element. For directional supervision, the relay can pick

up for all currents but cannot initiate a trip of the circuit breaker before the directional element has detected the fault current path.

Distance relay protection is mostly applicable in transmission systems. However, it is gaining popularity in medium and low voltage DSs. For normal system conditions, the ratio of a node voltage to a line current gives the line impedance. A fault, on the other hand, is characterized by a reduction in a node voltage and an increase in line current. As a result, the impedance of a line computed by a distance relay decreases in the presence of a fault. Thus the distance relay operates by comparing the calculated apparent impedance to the reach point impedance of the relay [8]. Protection coverage zones are defined for distance relays. The zones are often defined as an instantaneous zone 1 reach, and time delayed zone 2 and zone 3. If the line impedance computed by the relay falls within a given zone the relay trips the circuit breaker otherwise the relay restraints the breaker. A sample distribution feeder with distance relay protection is shown in Fig. 7. The feeder consists of three buses A, B and C and two line segments shown as line 1 and line 2. The distance relay D1 provides primary protection to line 1 and back up protection to line 2. D2 is the primary protective device for line 2.

A distance protection scheme for the line 1 segment of the system of Fig. 7 will comprise a zone 1 reach typically set to cover 80% of the positive sequence impedance of the protected line. The 80% coverage is due to uncertainties associated with the line parameters, fault studies and relay design. Zone 2 setting will cover the whole length of line 1 and 20% of line 2 segment. The coverage area of zone 3 will span the entire lengths of lines 1 and 2, and 20% into the adjacent line beyond bus C.

The characteristic of a distance relay is presented usually in an impedance R-X diagram. R is the resistance and forms the abscissa, while X is the reactance which constitutes the ordinate. The origin of the impedance diagram is where the relay is located with operation normally in the first quadrant [8]. Fig. 8 shows a mho characteristic of the distance relay, D1, set to protect line 1 of Fig. 7. A mho is a circle through the origin of the R-X diagram. The impedance of the line segments from bus A to bus C is represented as the straight line |AC|. Any fault, F, on line 1 whose impedance

falls in zone 1 will be instantaneous cleared. For those faults beyond the reach of zone 1, either zone 2 or zone 3 operates depending on where the faults fall on line |AC|.

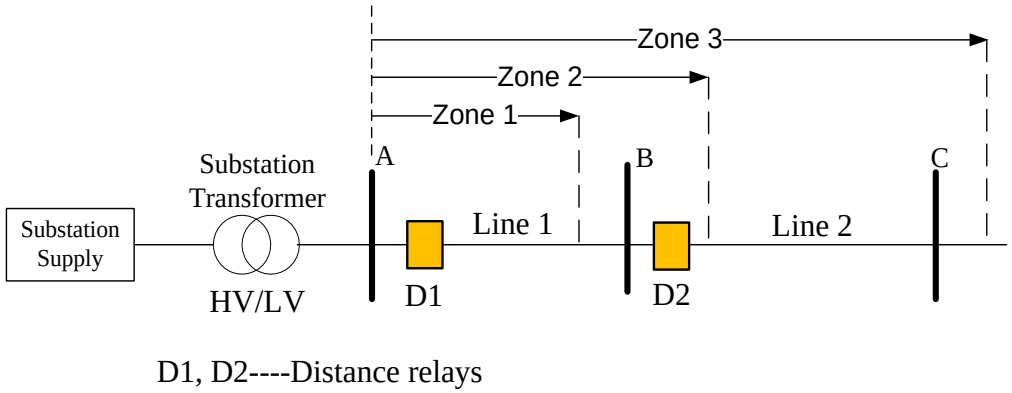

Fig. 7 A Sample Distribution Feeder with Distance Protection

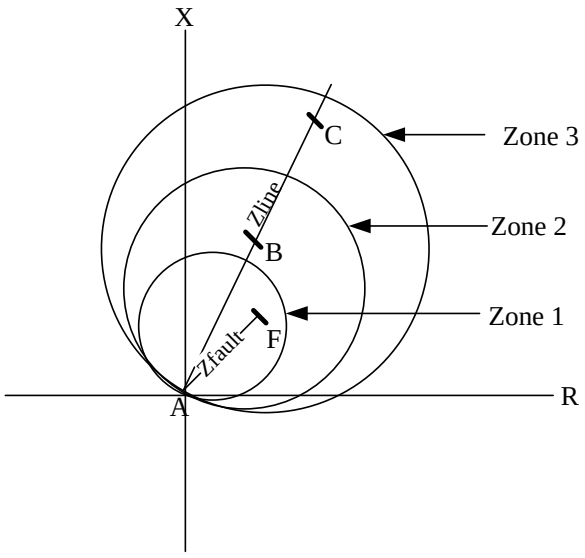

Fig. 8 Mho Impedance Diagram for Distance Relay at Bus A of System in Fig. 7

2.2.4 Distributed Generators in Radial Distribution Systems

Distributed generators (DGs) have no universal definition. IEEE defines DGs as the generation of electricity by facilities that are sufficiently smaller than generating plants so as to allow interconnection at nearly any point in a power system [9]. The International Council on Large Electric Systems (CIGRE) Working Group, in contrast, defines DGs as generation sources that are not centrally planned or dispatched, have capacity less than 50-100MW, and are usually connected at the distribution level [9]. Some authors define it based on the voltage level, others based on its proximity to the consumer or the type of prime mover.

DGs may be powered by either renewable or non-renewable sources. Non-renewable types include reciprocating engine generator sets, fuel cells, micro-turbines, gas turbines and hybrid fuel cells. The reciprocating engine set is dominated by synchronous generators. Renewable DG types include wind turbines, biogas and concentrated photovoltaic units. Some renewable types are connected through power electronics inverters to the distribution system.

Connecting DGs at the distribution level introduces some challenges especially to protection. Several authors have investigated the effects of DGs on radial distribution protection and have concluded that protective devices, such as reclosers and fuses may mis-coordinate depending on type, size, and placement of the DGs [10]-[15]. Fault currents at the point of tie of the DG increase and these higher currents have the potential to redistribute among the various parts of the networks, causing stress and damage to components and danger to personnel. For some instances, the in-feed contributed by DGs on a healthy feeder to a faulted feeder may cause sympathetic tripping. Sympathetic tripping is undesirable as it causes service interruption to customers who under normal circumstances should not have been affected. Reclosing functions which are applied to a large extent on radial DS to clear temporary faults also become infeasible without disconnecting the DGs.

2.3 Protection Approaches for Distribution Systems with or without DGs

To address the protection challenges that arise from connecting DGs to DS, various approaches have been proposed in the literature. These approaches range from the use of fault current limiters, to microprocessor reclosers, as well as adaptive protection schemes. Adaptive protection, according to [16], is the ability to automatically make real-time adjustments to power system protection schemes in response to changing system conditions. Adaptive protection can be divided into adaptive protection device and adaptive protection system depending on the functions and information involved [17]. Adaptive protection device uses local information only and can adapt to changes of operating mode of less area while the adaptive protection system involves a larger operating area requiring high communication channel bandwidth. Table 1 shows a review of various approaches in the literature that seek to address the protection challenges pertaining to RDS with DGs. The table also has some protection schemes that do not address DGs impact but rather adapting OC protection due to varying loads on RDS.

In [18] and [19], it was proposed to minimize the contribution of DGs during fault through the use of fault current limiters without jeopardizing the network under no fault conditions. No changes were made to the existing OC protection scheme in the system. The use of the fault current limiters offers simplicity in tackling the problem of reducing the DGs current contribution. However, fault current limiters are characterized by power electronics which may affect power quality. To solve the problem of fuse-recloser coordination, [20], and [21] suggested to use a microprocessor recloser that allows for implementing user-defined curves. The microprocessor recloser provides flexibility in maintaining OC coordination between fuses and the recloser. On the other hand, the requirement of having to check for protection coordination in order to select the appropriate recloser curve may prove to be difficult as the number of DGs increase. [22] addressed the issues of nuisance fuse blowing and fuse fatigue on laterals with DGs by replacing the lateral fuses with a multi-function recloser. The method works best for

nuisance fuse blowing but not so well for fuse fatigue as there exist instances for which a fuse can begin melting before a recloser's fast operation is initialized.

References [17, 23, 24] presented approaches for changing relay pick up in response to varying load current. However, these approaches presented do not take into consideration conditions when DGs are connected to the system. The scheme presented in [25] for adapting the zone 2 distance relay setting works best for inverter interfaced DGs and does not hold for synchronous DG type. The adaptive technique for current protection scheme presented in reference [26], which was based on a directional approach has some limitations as it is more suitable for systems where the DG is connected near the grid or at the bus bar.

The approaches presented in [27]-[30] established protection zones in the distribution system. The zones were separated by circuit breakers that had the capability to receive control signals from a central relay at the substation. The zones were formed with a balance between generations and load in a way that allowed for unfaulted zones to be operated as intentional islands. For those zones that had no DGs, they became dead during fault. In [31]-[33], the overcurrent relay pick up setting was changed based on the contribution from the DGs. These methods were adaptive as it involved appropriate choice of relay settings that matched the network conditions. In [34], when a fault occurred on an area of a feeder operated as a loop, a distance relay employing a modified permissive overreach transfer trip (POTT) scheme was used to break up the loop by disconnecting the appropriate circuit breakers. The DG(s) in the faulted area were disconnected but those on the unfaulted areas of the feeder remain connected. Conventional OC protection cleared the fault once the loop was broken and the faulted area's DG(s) were disconnected. [35]-[37] presented communication assisted overcurrent protection schemes where relays were tripped based on the directional information it receives from other relays on the distribution system. Specifically in [35], a master relay at the substation controlled all the relays on the radial distribution system based on the response to queries it frequently sent out to these relays.

Table 1 Review of Protection Approaches for Radial Distribution Systems with DGs or Adaptive

#	Protection Approach / Method	Protective Elements	Protection Type	DG (Yes/No)	Adaptive (Yes/No)	Ref.
1	A fault current limiter was proposed to be placed between the DG and the interconnection point to the distribution system to reduce the fault current contribution that emanates from the DG.	Fault current limiter, relays	Overcurrent	Yes	No	[18]
2	Fault current limiter impedance was optimally determined to restore coordination among protective elements in the presence of DGs. Impedance of the limiter was increased in steps following a fault calculation such that coordination was maintained between the primary and back relays.	Fault current limiter, relays	Overcurrent	Yes	No	[19]
3	The scheme entailed using a microprocessor based recloser that enabled switching from one curve to the other during fault. A user defined recloser curve to maintain fuse-recloser coordination in the presence of DG was obtained by scaling any suitable recloser curve using the ratio of fuse to recloser current.	Microprocessor based recloser, fuses	Overcurrent	Yes	Yes	[20]
4	The paper proposed to use a microprocessor recloser to revise the recloser's fast characteristic curve. The revision was done by shifting the fast curve down by the lowest value of the ratio of the recloser fault current to the fuse current. Feeder relay had directional elements to mitigate false tripping.	Microprocessor based recloser, fuses	Overcurrent	Yes	Yes	[21]
5	For mitigating fuse fatigue and nuisance fuse blowing in RDS with DGs, the author suggested replacing fuses on a lateral with DG with a multifunction recloser and adding a relay at the DG point of connection.	Microprocessor based recloser, fuses, relays	Overcurrent	Yes	No	[22]

Table 1 Continued

#	Protection Approach / Method	Protective Elements	Protection Type	DG (Yes/No)	Adaptive (Yes/No)	Ref.
6	The operating status of the system, loading and fault conditions are determined and the real time settings of the protection devices are computed. The method employed was an adaptive three-step current protection comprised of adaptive current fast tripping, adaptive current fast tripping with time limit and adaptive over current protection.	Relays	Overcurrent	No	Yes	[17]
7	The paper introduced a new logic for the setting of the pickup current of an OC relay, which was a function of the load current with an added margin of 15% of the maximum load current.	Relays	Overcurrent	No	Yes	[23]
8	Pickup values of OC relay were dynamically varied in response to load variation to achieve coordination among relays.	Relays	Overcurrent	No	Yes	[24]
9	An adaptive mathematical formulation for computing the zone II settings of distance relays was presented that took into consideration the fault type. The method used the positive sequence current from inverter interfaced DGs.	Relays	Distance protection	Yes	Yes	[25]
10	The method involved a directional protection that used the system equivalent phase voltage, system composite impedance and line impedance to estimate the fault current. Depending on the location of the protection relative to the DG position, the line current was enhanced or reduced through a line compensation coefficient. No changes were made to the protection settings when DGs were absent.	Relays	Directional overcurrent protection	Yes	Yes	[26]

Table 1 Continued

#	Protection Approach / Method	Protective Elements	Protection Type	DG (Yes/No)	Adaptive (Yes/No)	Ref.
11	The distribution system was divided into zones that maintained a load and generation balance. Zones with DG(s) were capable of islanding. . Circuit breakers were installed to separate the zones. A centralized computer based relay at the substation determined the faulted zone and isolated it by comparing offline measurements of main source and DG currents contribution to faults in a look table with their real time equivalents.	Fuses, circuit breakers, relays	Comm. assisted overcurrent	Yes	Yes	[27]
12	The basic idea was again based on dividing the distribution system into zones considering DG and load requirements. Each zone had two breakers whose decision to open or close was determined by a centralized computer relay at the substation. The relay used a look up table that stored the offline currents of main source, DGs and laterals for all fault types and locations and compared these currents to their online counterparts to identify faulted zones.	Relays, circuit breakers	Comm. assisted overcurrent	Yes	No	[28]
13	The protection was based on the zoning concept with remotely controlled switches placed between two zones. Zones that had no DG and were located downstream a faulted zone were switched to connect zones with DGs.	Relays, circuit breakers	Comm. assisted overcurrent	Yes	No	[29]
14	The approach divided the distribution system into zones; upstream and downstream from the DG point of location. The zones upstream of the DGs were protected by directional pilot protection and OC protection. The zone downstream, as it appeared as a single source, used definite-time overcurrent protection. For multiple DGs connected to various buses, the feeder was divided into several zones with directional pilot protection and directional definite OC in the upstream zones from each DG point. Downstream zones were protected with definite-time OC relays.	Relays, circuit breakers	Overcurrent and pilot protection.	Yes	No	[30]
15	Relay pickup setting was changed as the total amount of power injected by all DGs increased to address the problem of reduced reach.	Relays	Overcurrent	Yes	Yes	[31]

Table 1 Continued

#	Protection Approach / Method	Protective Elements	Protection Type	DG (Yes/No)	Adaptive (Yes/No)	Ref.
16	Discussed an algorithm that calculated the actual short circuit current contribution from the grid and all DGs connected to the appropriate feeder and adapted the settings of the high set OC element. Real time data involving monitoring grid conditions, breaker statuses as well as non-real time data that involved the prediction of distributed energy resources were used to confirm the selectivity of tripping characteristic for each fault condition and the choice of the relay settings.	Relays, circuit breakers	Overcurrent	Yes	Yes	[32]
17	Pickup setting of overcurrent relay was changed based on the increase or decrease short circuit current contribution from the DG.	Relay, circuit breakers	Overcurrent	Yes	Yes	[33]
18	The DG was connected to two radial feeders that could be operated in a loop by closing a normally open switch. For a given feeder fault, connection of the DG was switched to the unfaulted feeder, and conventional OC protection scheme was applied to clear the fault on the faulted feeder.	Sectionalizers, fuses, relays	Overcurrent and distance protection with POTT scheme.	Yes	No	[34]
19	This method was based on a longitudinal comparison principle with a master-slave communication structure. Each slave relay had directional element. Master relay at substation queried all slaves and used their responses to identify the faulted section and isolated the section accordingly.	Relays	Directional overcurrent protection	Yes	No	[35]
20	Relays issued a binary state signal to indicate the possibility of a fault nearby based on the magnitude of the current entering the associated area from the upper system. Corresponding relay received such signals from other relays and simultaneously utilized binary state signals, to determine whether it should trip its breaker or not. This method was for selective disconnection of faulted area and DG on a particular feeder.	Relays, circuit breakers	Comm. assisted overcurrent protection.	Yes	No	[36]
21	Communication assisted scheme that allowed for fast tripping of faulted zones based on traditional three step current protection scheme. The main protection concept was to add directional elements and communication channel to traditional protection scheme. The directional element is to avoid improper tripping for reverse faults, and the communication channel is used for remote tripping and blocking.	Relays, circuit breakers	Comm. assisted overcurrent	Yes	No	[37]

The approaches [27]-[29] that divide the distribution system into zones and use circuit breakers on the zonal boundaries provide an efficient means of containing and limiting the extent of fault damage. However, relying on one central relay to control the breakers that separate the zones can impair the performance of the protection approach in the event of losing the relay due to a cyber-attack or malfunctioning of the component. High processing power is also needed to store the large amount of lookup table data that is needed by this central relay. A protection approach was developed which modifies the work of [27] and [28]. The approach proposes to decentralize the control of the zonal circuit breakers via relay with zone breakers to eliminate the single point of failure the central relay presents. A binary state signal is used as the means of sharing the fault information among the relays that are added. The idea to use binary state signals originates from [36] to help reduce the amount of information that will be exchanged in the modified protection approach.

2.4 Summary

In this section, the conventional radial distribution protection (RDS) philosophy has been presented and a discussion of various overcurrent protective devices and how they are applied to RDS is given. The section also provides a review of various distribution protection schemes in the literature that address some of the challenges caused by integrating DGs. Microprocessor based protective relays are providing new ways to ensure coordination in the face of DGs in radial distribution feeders. Adaptive and communication assisted schemes have also been utilized to some extent that take into consideration the changing network conditions. Existing protection approaches that separate RDS with DGs into zones have been selected for modification.

3 SMART GRID OVERVIEW AND ADVANCED METERING INFRASTRUCTURE

3.1 Introduction

Over the years and around the world, the need to reduce carbon emissions from the power industry while meeting the increasing customer reliability and power quality needs continues to cause a tremendous stress on the existing power system infrastructure. The current grid is not equipped to deal with renewable energy integration and at the same time allow for consumer flexibility on energy usage. Political and tight regulatory measures further aggravate the issue in an attempt to meet energy policy goals. As a result, the power grid is now subject to challenges and conditions, which were never envisioned when it was designed several decades ago. A power grid that provides a means for meeting the emerging trends and also allows for efficient and effective automatic controls as operational decision times reduces has been envisioned. This vision has led to the birth of the smart grid that has attracted a lot of attention.

In this section, the smart grid concept is introduced along with the technologies required to drive this concept. Advanced metering infrastructure which is considered a cornerstone for a smarter distribution grid is also discussed. Distribution system protection technologies developed for the smart grid are also briefly introduced.

3.1.1 Smart Grid

A smart grid is essentially adding ‘intelligence’ to the power grid. Although some forms of intelligence currently exist in the power grid, they are often local and decisions are made without adequate inputs from other parts of the system. Such approaches have been known to be the cause of major system outages. The ability to take into consideration decision parameters from various parts of the system will be very critical in meeting the power needs of the 21st century. The smart grid is at its nascent form, and like any emerging trend there is no clear consensus as to what exactly the smart grid is, and the path to which it will eventually evolve. Fig. 9 depicts the

intricacies of a conceptual smart grid as envisioned by [38]. It illustrates a number of sources and sinks of the data that will be generated in a smart grid environment. The sources are projected to be located at various places in the network and will consist of both conventional and non-conventional sources. The non-conventional sources as shown in the figure will consist of both renewable energy sources such as wind and solar. The solar sources will span from large solar farms to small household rooftops. Electric vehicles and rechargeable battery will also be part of the energy mix with the capability to receive and supply to the power network at the same time. Communication is also expected to play a major role in the smart grid. The communication link can take the forms of wireless, wired or power line carriers. Intelligent household appliances will be interacting with the smart grid network through the communication links by way of the smart meters. The control and system management consoles will have a complete oversight of the activities occurring on the system by monitoring the data emanating from all the components of the grid.

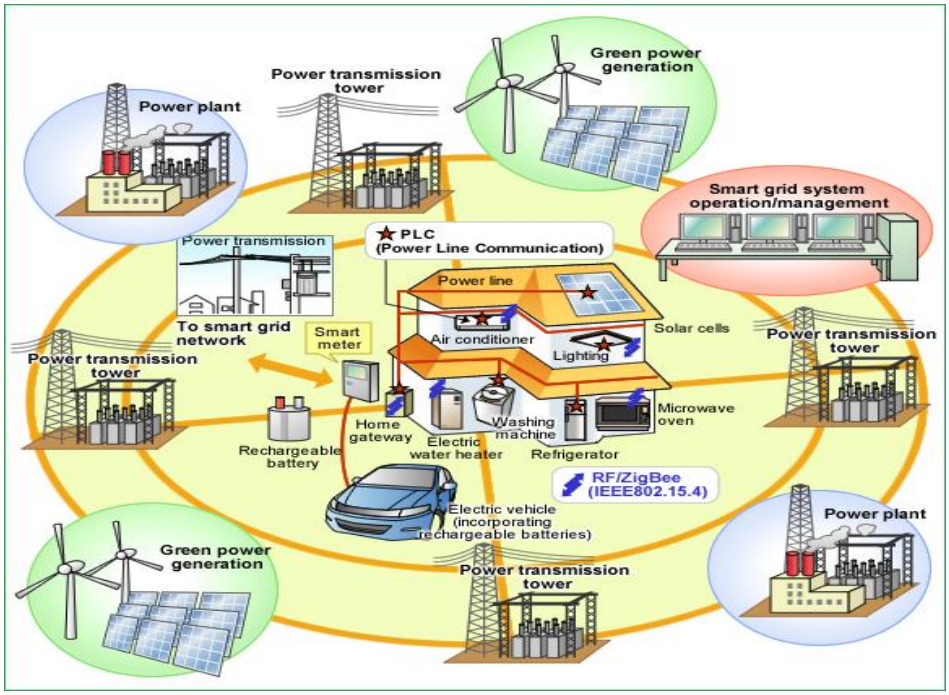

Fig. 9 A Conceptual Smart Grid System [38]

The US Department of Energy (DOE) defines the smart grid as the use of digital technology to improve the reliability, efficiency and security of the current grid [39]. DOE suggests that the modern smart grid should [40]:

1. Have a self-healing capability. The grid through the continuous use of measurement from intelligent electronic devices should be able to detect faults, mitigate the impacts and restore network components following an outage.
2. Encourage active customer participation. Through the bidirectional flow of information, customers should be able to respond to electricity pricing signals by controlling their in-house equipment. Customers should also be able to sell excess power emanating from any distributed energy resources (DERs) they have to the utility. These DERs could be plug-in-hybrid vehicles, roof top solar panels or small wind units.
3. Resilient to attack. The modern grid should be reconfigurable to provide continuous services in the event of natural disasters or cyber-attacks.
4. Accommodate all generation forms. Integration of DERs with plug-and-play capabilities must be possible in the future smart grid. This is to help improve reliability, reduce generation cost, and energy losses and introduce a niche market system for renewable generation currently inexistent.
5. Improve the power quality needs of the 21st century. The grid must support the digital needs of the emerging industrial and commercial processes so as to minimize downtimes and maximize productivity.
6. Enable new markets. The generation sources, be it centralized or distributed, should be able to sell power to customers wherever they are located. The market must therefore encompass a variety of stakeholder groups (consumers, distribution companies, generation companies). This means that the financial and regulatory environment must provide a fair access to electricity market.
7. Optimize assets and operate efficiently. Use of advanced monitoring techniques should allow for optimal loading of assets while reducing their out-of-service times.

The smart grid is also considered to be the application of technologies from the telecommunication and information technology industry to the electric grid [41]. Thus, in a smart grid system, the transmission and distribution network of the power grid will serve as the physical layer, while data control and transport will be realized through the communication layer. The information systems will be used to process the data gathered through the communication network and present them in comprehensible formats so that stakeholders of the grid can make timely and better informed decisions. Stakeholders of the power grid recognize that adopting technologies from the communication and the information industry in itself present challenges that will have to be solved through proper use and development of standards across the board.

3.2 Smart Grid Technology Development

The technologies that are anticipated to propel the current power grid into the smart grid of the future have been identified in [40]. These technologies comprise the following key areas: advanced components, advanced control, improved interface and decision support, and sensing and measurements. Fig. 10 shows the merging of these key areas under the smart grid umbrella.

The requirement of the smart grid to be resilient and self-heal itself is in part dependent on it being able to acquire the necessary data for the appropriate control and protection systems. A fully integrated communication network standardized across the industry will ensure that such actions are possible. The integrated approach is to allow for bidirectional flow of information, and just like the internet, provide a plug-and-play environment among the various components of the grids. Integrated communication forms the basis on which other functions of the smart grid will be developed. Confidentiality, integrity and authentication of the communication networks will be essential in preventing intruders from gaining access to vital systems in order to inflict damages.

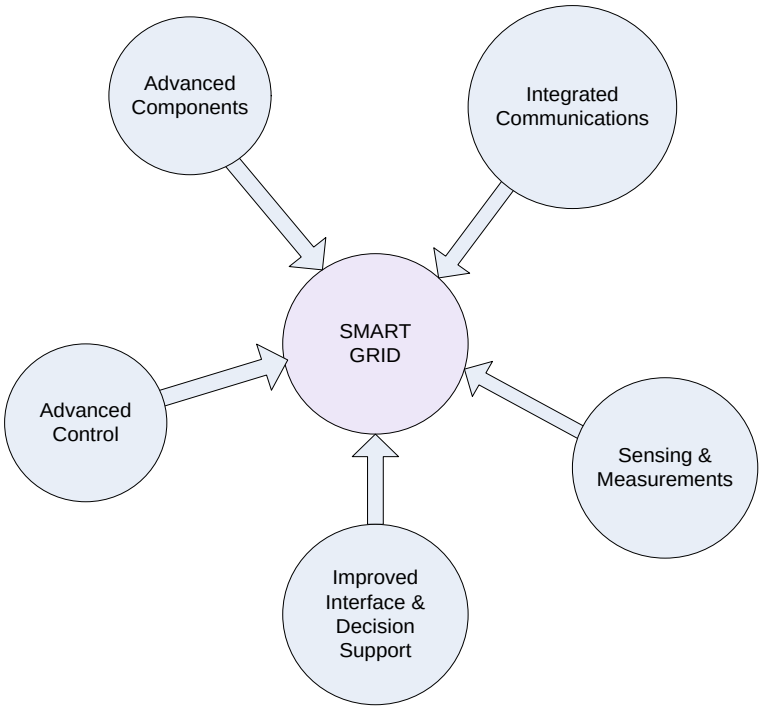

Fig. 10 Smart Grid Key Technology Areas

Similarly, advanced power electronics components, high temperature superconductors, distributed energy resources, and intelligent components are considered some of the next generation assets that will allow for delivery of high power quality services and optimum reliability levels of operation. Pilot phase testing of some of the advanced components are currently underway and mass adoption is soon to be expected.

Without sensing and measurements, the integrated communication networks have no data to transport. Phasor measurement units, advance metering infrastructure, synchrophasors, line sag monitors, electronic instrument transformers, and advanced protective elements will provide real time data acquisition for monitoring the power system states. These sensing and measurements units will help to improve the

performance of preventive and corrective actions while providing a system wide view of the power grid.

By the same token, advanced control technology is of necessity for the realization of efficient control of the transmission, distribution and consumer levels. Analytical tools, distributed intelligent agents, human machine automation network etc. will allow for quick diagnosis and restoration of the network following system disturbance. These processes will utilize the data acquired from sensors and measuring devices together with the integrated communication to achieve the prospective goals.

Finally, the ability to make any meaning of the voluminous data gathered from the sensing and measurement units, to an operator will be dependent on the ability of information systems to reduce them into readable forms so that timely decisions can be made. Intelligent alerting systems, and advanced visual techniques are some of the tools expected to provide active assistance to human operators.

3.3 Advanced Metering Infrastructure

Historically, sensing and measurement of customer energy have evolved from in person reading to automated meter reading and now smart metering, which is achievable through an advanced metering infrastructure (AMI) [42]. Automated meter reading only involves unidirectional flow of information and therefore fell short of the needed smart grid attribute that will allow for bidirectional information flow. With the smart grid euphoria, the fundamental assumption is that improving the sensing and measurement capabilities at the distribution level will eventually provide added benefits that will offset the cost of maintenance. This has seen many electric utilities implementing AMI on their systems. Some utilities are deploying the AMI in a gradual manner while others are taking a more aggressive approach. A few decades ago, this would have been an acrimonious step due to the comparable cost of maintaining and planning the distribution system to the need for real time data and analysis expected from the AMI. The roll out is expected to set the stage for more innovative measures needed in a smart distribution grid. AMI is anticipated to allow for active customer participation in the electricity

market. This will give customers choices thereby helping them reduce their energy usage and ultimately save money. Through the AMI energy measurements, it is expected that utilities will have an accurate estimate of the loading on their network at any point in time. Table 2 summarizes the benefits that AMI is expected to bring to both the utility and the customer [43].

Table 2 Advanced Metering Infrastructure (AMI) Benefits

Utility	Consumer
Ability to collect a variety of data on consumers' power usage to provide more fine grained services.	Access to information that will allow consumers to make timely decision concerning their energy usage.
Reduction in the man power hours needed to read consumers' energy usage data.	Participate in demand side management programs such as rate plans and expanded product option.
Combat power theft.	Ability to use in-home monitors.
Ability to disconnect and reconnect customers depending on their fulfillment of an obligation.	Accurate energy billing compared to the sometimes estimated or manual meter reads.
Service interruption can be detected more quickly without have to rely on customer calls.	Improved service and reliability.

The basic components that constitute the AMI are: Smart meters, AMI Communication Network, Customer Gateway, and AMI Headend [44]. Smart meters come in different types and models with the basic functionality for a two-way communication between the utility and the customer. Residential smart meters are single-phase devices and that of commercial and industrial customers are three-phase devices. The smart meters can measure energy consumptions in almost real time and communicate the data to the utility at regular intervals of 15, 30 or 60 minutes. Through the smart meters, remote control of customer equipment (e.g. adjusting temperature setting of air conditioners) can be done by the utility. The smart meters also have the ability to measure the energy supplied to the distribution systems by distributed generation sources that may be connected. A study conducted by Navigant Consulting for the Public Utility Commission of Texas explored the benefits of smart meters over

electromagnetic meters. Accuracy tests of a sample of smart meters were found to be within +/- 0.5% and showed better performance in most cases over their electromechanical counterpart [45]. The leading manufacturers of smart meters in the United States currently include Echelon, Elster, GE, Itron, LandisGyr, and Sensus. Table 3 shows a comparison of certain features for some of the smart meters developed by these major manufacturers.

The AMI communication network serves as the neural paths for information exchange between the customer and utility and comprises of both Wide Area Network (WAN) and Large Area Network (LAN). Data gathered from the smart meters through the communication network are made available to other systems at the AMI headend usually located at the distribution or the transmission control center. These systems can include the outage management, meter data management, operator consoles and market simulator. The AMI headend therefore serves as the power house of the metering systems. To fully maximize the benefits of AMI, Home Area networks (HAN) and Building Management Systems (BMS) deployed in homes are made to interface the AMI communication network through the customer gateway.

Table 3 Comparison of Smart Meters by Major Manufacturers

Manufacturer / Feature	Itron [46]	GE [47]	Elster [48]	Sensus [49]	LandisGyr [50]	Echelon [51]
Model	Open-Way Centron®	I-210+c	AS 220	iCon A Residential	FOCUS AX SD	2S
Capabilities	-Bi-directional metering. -Provides over one year of 15-minute load profile data storage. -200A remote disconnect and reconnect switch optional feature. -Tamper detection.	-Supports delivered, received, and net metering for distributed generation. -Power quality. -Load profile recording. -Time of Use Billing Measures. -Tamper detection.	-Power quality measurement. -Load profile for billing data. -Integrated connect and disconnect relay up to 100A.	-Power outage and restoral notification. -Full net metering. -Load profile and time-of-Use. -Remote disconnect capability. -Power quality reporting. -Meter tamper detection.	-Proactive outage and restoration notification. -200A remote load control and disconnect. -Time of use and demand billing.	-Integrated 200A switch can be locally or remotely controlled. - Power quality analysis. -Demand metering. - Load profile and time-of-use.
Data Measured	-Instantaneous voltage. -Wh (delivered, received, net, unidirectional). -VAh (delivered arithmetic, received arithmetic, Lag). -W (max delivered, max received, max net, max unidirectional).	-Maximum and minimum voltage. -kVAR, kVA, demand.	-Measurement of active, reactive and apparent demand.	-Instantaneous and average voltage and current. -kWh and kVAh energy measurements over customer selectable intervals.	-kWh delivered, kWh received and net kWh -Full function meters measure and display instantaneous and average power.	-Forward, reverse, and net active energy. - KVARh import and export.

Table 3 Continued

Manufacturer / Feature	Itron [46]	GE [47]	Elster [48]	Sensus [49]	LandisGyr [50]	Echelon [51]
Demand Interval length	-Programmable 5, 6, 10, 12, 15, 20, 30 and 60 minutes. -Single channel 30-minute data 753 days. -Two channels 30-minute data 501 days.	-Event logging up to 200 events of 15 minutes intervals.	-Load profile interval data every 15, 30, or 60 minutes.	-Meter is customer selectable to report its information from every 15 minutes, 1, 1-1/2, 2, 4, 6, 8, 12, and 24 hour -Up to two seasons of Time-of-use in up to 5 tiers of data	-Interval data of 1, 5, 15, 30 or 60 minutes -5-minute interval data is available for a minimum of 45 days for two channels	-Data can be captured at programmable intervals from 5 minutes to once a day. - Single-channel, 1-hour data can be retained for 180 days.
Communication	-ZigBee radio for interfacing with the HAN, in-home displays and load control devices.	-Radio Frequency Mesh (RF Mesh). - Power Line Communications (PLC). - Cellular (GPRS/CDMA) - Ethernet	-WAN using GSM/GPRS - HAN communication for gas & water meter reading using wireless M-Bus, 868MHz	- ZigBee with PKI authentication - IP addressable through FlexNet.	-GSM/GPRS technology -Ethernet -PSTN, low or medium voltage PLC or a combination.	-Power line communication. - Internal slot to house an optional ZigBee radio card for communication with in-home devices.
Voltage Class	120/240V	120/240 V	220/240V	120/ 240V	120/ 240 V	120/240V

A typical AMI infrastructure and how data collected at the smart meters is made available to the utility operator is shown in Fig. 11 [52]. The meters can communicate using either wired or wireless medium. Data gathered by the meters are relayed to a collector typically installed on poles and then transmitted to the utility. The extent of travel of the metered data is enhanced through a repeater. Depending on the topography of the service area, each smart meter can either transmit its data directly to the collector or the data may hop from one smart meter to the other until the data makes its way to the collector. The collectors connect to a WAN where the data is transmitted wirelessly to the utility control computers.

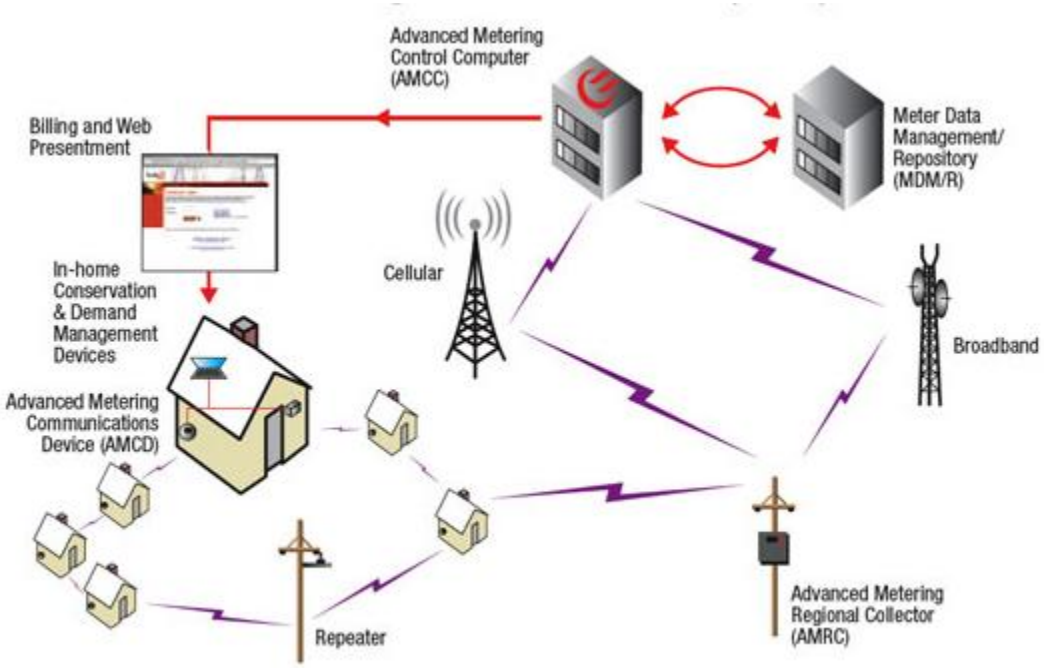

Fig. 11 Advanced Metering Infrastructure System[52]

3.3.1 Smart Grid Technology in Relation to Distribution System Protection

Smart grids will require smarter protection that can respond to network topology changes during operation. A smarter protection is expected to consider the network flows arising from all the added generation sources, the load variability ensuing from demand response, and the need to optimize the assets and system.

In [53], a novel current only directional relay concept is presented that will reduce the cost of applying directional relaying elements to distribution systems in a smart grid environment. The novel technology eliminates the need of the voltage polarizing element in traditional directional relays. The scheme employs the pre-fault current as the polarizing quantity and identifies the forward and reverse fault direction based on significant phase angle changes.

Beckwith Electric recently introduced a state-of-the-art feeder protection relay (M-7651) with 18 protective relaying functions and sync-check with four step recloser capabilities [54]. The relay has a smart grid ready platform with communication protocols such as DNP 3.0, Smart P2P, and Modbus. The high sampling rate of 128 samples per cycle provides advanced metering, power quality, THD and load profiling capabilities.

RadioRanger® wireless fault indication system developed by Schweitzer Engineering Laboratories (SEL) is being used by utilities in their effort towards the smart grid to reduce fault finding times. While driving the device around the distribution system, the device communicates the fault status back to a central location allowing engineers to pinpoint where the fault has occurred on the system [55].

A list of other advanced protection technology systems being developed for the smart grid is presented in Table 4 [40].

Table 4 Advanced Protection Systems

System	Description
Fault-testing recloser	-Applies a very fast, low-energy pulse to the line to determine if a fault is still present. -Minimizes damage caused by reclosing into faulted lines. -Significantly reduces damaging fault-current and voltage sags on the faulted line and adjacent feeders. -Substation transformers experience fewer through-faults, thus extending service life. -Cables, overhead conductors, splices, and terminations experience less thermal and mechanical stress from through-fault currents.
Special protection system	-Real-time monitoring of key generation assets or transmission lines and their associated power flows. -Upon a change of status (like loss of generation and/or loss of transmission), a pre-programmed set of actions takes place (e.g., wide-area load shed, generator re-dispatch, separation of interties). -Allows power transfers across the grid that would not comply with single or multiple contingencies under normal criteria. -Allows operators to load transmission lines closer to thermal limits or beyond normal voltage or system stability limits

3.4 Summary

The aging infrastructures of the power grid are without adequate intelligence to meet the needs of 21st century. Smart grid brings the needed intelligence through metering, communication and information system technology to the power grid. The smart grid is at a nascent state and therefore its success depends on the industries' ability to develop some key technologies, which have been identified to include: advanced components, improved interface and decision support, advanced control, sensing and measurements. Advanced metering infrastructure system and some novel distribution protections are currently being implemented to set the stage for a smart distribution grid.

4 PROBLEM FORMULATION FOR OVERCURRENT PROTECTION AND SMART METER INFORMATION USAGE

4.1 Introduction

The design of the distribution system (DS) since the genesis of the electric power grid was made without thought of connecting generation sources close to the loads. However, in a smart distribution grid more distributed generators (DGs) will be connected at various locations close to loads. The addition of DGs changes the topology of radial distribution systems (RDS). This causes the power flow in the RDS to change from being unidirectional to bidirectional. Such flow alterations affect overcurrent (OC) protection in RDS, which is often based on one direction of power flow. More DGs will also increase the short circuit current in certain parts of the system while reducing the reach of some protective devices. Unwanted tripping and mis-coordination may occur between the primary devices and the backup devices on the system. Thus, the selectivity and security of OC protection in RDS can be greatly affected in a smart grid environment.

This section states the overcurrent protection problem of RDS with DGs to be addressed and the need to have protection settings that are adaptive to system loading.

4.2 Problem Formulation

Fig. 12 shows a radial distribution feeder with three generation sources, DG1, DG2 and DG3. The current flow through relays R2 and R3 can be either from the substation and the downstream DGs depending on the capacity of the downstream DGs. This potential bidirectional flow undermines the unidirectional principle on which the settings of these devices are based. R2 and R3 may misoperate for faults outside of their protected area due to the contribution from the DGs that are connected downstream of their positions. These unwanted trippings reduce the service reliability of the customers on those sections of the feeder. The contributions from DG1, DG2 and DG3 to a fault on line 2 may cause the fault current flowing through R1 to be reduced. Such a condition

may affect the reach of R1 thereby making it unable to provide the desired protection for line 2. The cumulative effects of not having the overcurrent protection operate as desired subjects the general public and utility personnel to potential hazards. For a fault on line 1, where R1 operates, reclosing functions performed by the relay may be connecting two energized systems if proper synchronization with the DGs is not performed.

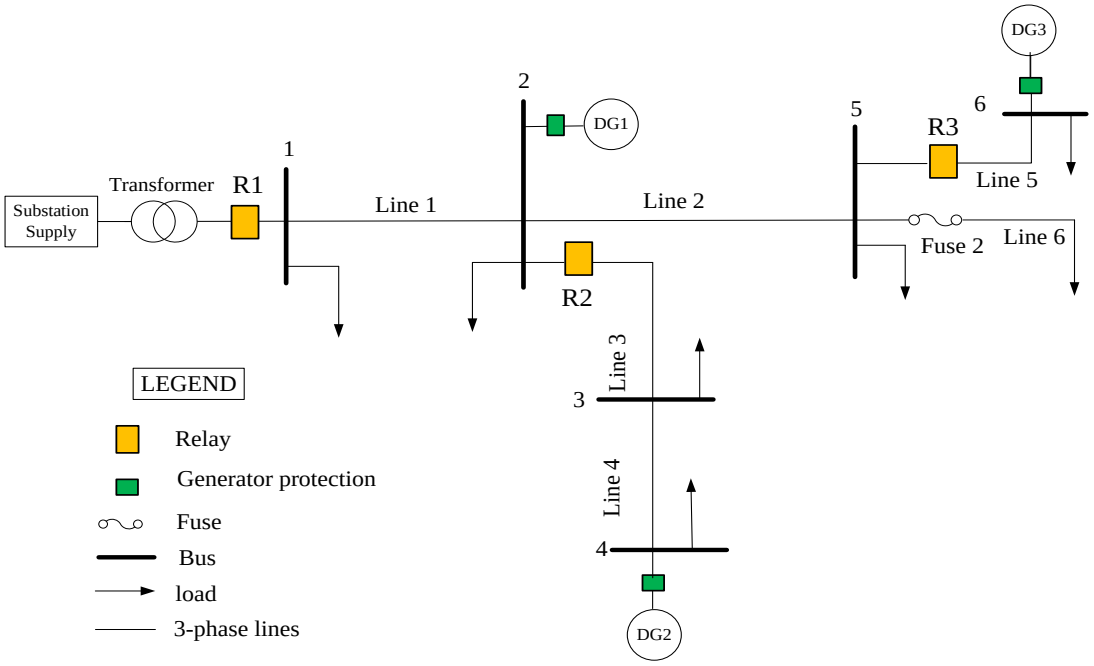

Fig. 12 A Radial Distribution Feeder with Interconnected DGs

If faults occur on the feeder and the DGs contribute to the fault, IEEE STD [56] guide requires that those DGs be disconnected from the feeder circuit. To mitigate unwanted tripping of the protective devices, while allowing the DGs to continue to supply the unfaulted sections of the feeder, [27] and [28] presented an approach that uses a zonal concept to isolate a faulted area in RDS with DGs. The authors in [27] first proposed and showed how the zone concept can be applied to RDS with DGs to isolate faulted sections. The zone concept has the property of limiting disturbances to a

confined area of the network. This is important in RDSs where the de-energization of a fault should be as selective as possible. In [28], systematic procedures for the formation of zones on a radial distribution network with DGs were outlined. The procedure for forming zones [28] follows the steps listed below

1. One zone is considered for each DG. A zone starts from DG bus and extends towards the end of the feeder. Using the example system of Fig. 13, a zone starts at bus 2 and extends along line segment 2, and another zone begins at bus 5 and proceeds along line 5.
2. Coverage area of a zone on the feeder continues downstream until the DG's capacity matches the total average load within its zone. Continuing with the example of Fig. 13, a zone started at bus 2 will have its loads matched to DG1's capacity.
3. In the course of a zone's expansion towards the end of the feeder for a given DG, if a second DG is encountered before exceeding the balance between the first DG's capacity and the total average load, then the second DG is regarded as part of the first DG's zone.
4. A zone's coverage area is extended upwards in the event that the zone formed by the DG reaches the end of the feeder and the DG's capacity is still larger than the total average load located in the DG's zone. For example, the zone formed by DG2 may extend upwards to line 4 if DG2 still has excess capacity.

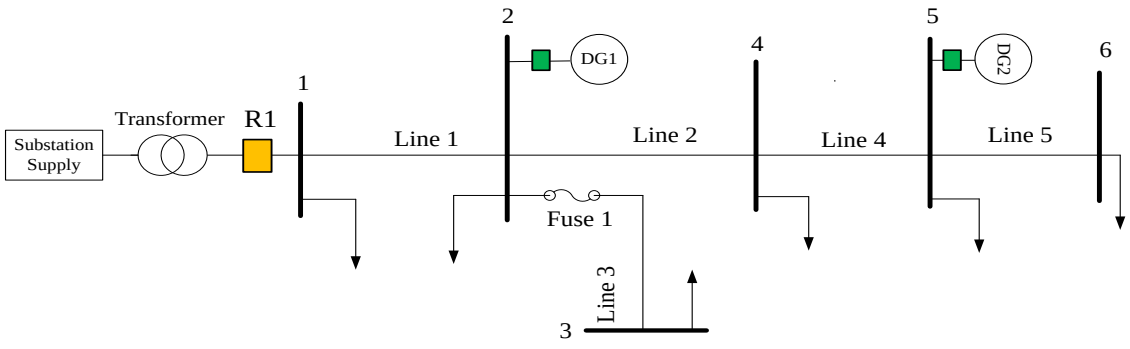

Fig. 13 An Example Radial Distribution Feeder for Zone Formation

Applying the zone formation steps to Fig. 13, each zone starts from the respective DG's bus. Fig. 14 shows the zone boundaries defined for the example system of Fig. 13. B1, B2, and B3 are the breakers installed to separate each of the established zones following the method outlined in [27] and [28]. These breakers will then be controlled by a central computer relay located at the substation. Each breaker is capable of opening and closing based on the received signals from the central relay and has a check-synchronization function. The central relay houses a look up table that is acquired through offline calculations. The table contains the current contributions from the main source and the DGs for all fault types and their locations in the network. Online measurements of these currents are compared by the relay to their corresponding offline values in the lookup table to help identify the faulted section and, consequently, the faulted zone. After identifying the faulted zone, the central relay sends tripping signals to the appropriate breakers to isolate the zone while the remaining unfaulted zones operate as intentional islands. The difference in the methods of [27] and [28] is that the lookup table in [28] also includes current through laterals for the various fault types and locations.

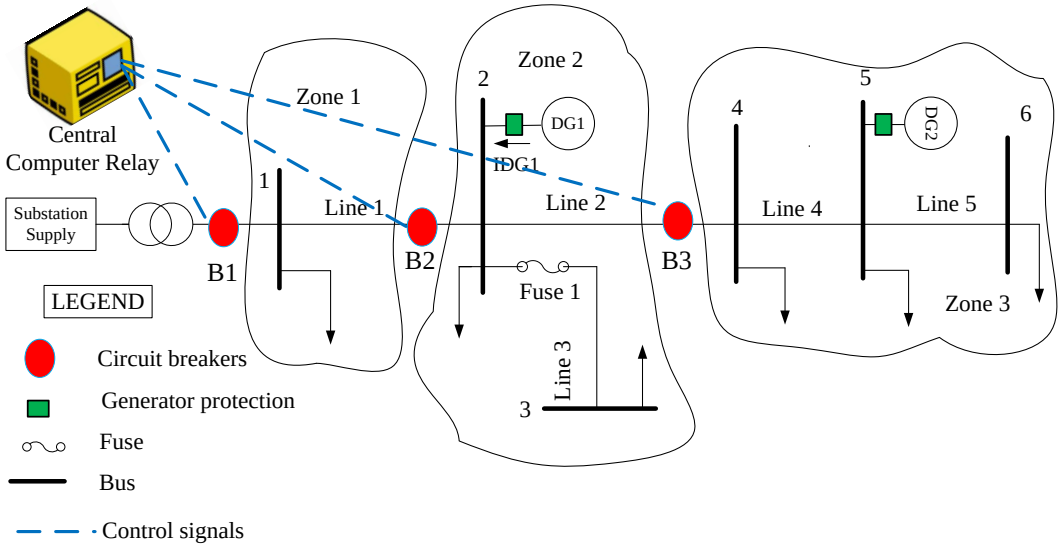

Fig. 14 The Example Radial Distribution Feeder in Fig. 13 with Zones Defined

Cyber security issues are of a major concern due the increased dependency on computerized technology and the eventual evolution of the electric power grid to the smart grid. Therefore, relying on one central relay, as presented in [27] and [28], to trigger the control of all zonal breakers can cause much damage if the central relay is lost due to a cyber-attack or malfunction of the component. For example, a denial-of-service attack on the central relay will produce a delay of the signal transmitted to the circuit breakers. As a result, breakers may fail to operate in a timely manner causing the fault to persist for a longer period of time. Thus, it is prudent to be able to perform the same protection functions without having to rely on one central component.

Disconnecting a faulted zone reduces the total loading on the feeder. This means the protective relays of the unfaulted zones especially those that remain grid connected see a reduction in nominal load current. In general, the ways in which overcurrent relays respond to faults depend on prefault conditions and the type of fault. Therefore, for prefault conditions where the loading of the isolated unfaulted zone(s) connected to the substation are low and the substation OC relay retain the pickup setting that corresponds to the maximum loading of the zone(s), the response of the substation relay may not be very sensitive. By adapting the pickup setting of the substation OC relay to the new loading of the zone(s), the sensitivity of the substation relay can be increased. Acknowledging that the new loading on which the unfaulted zones' substation relay pickup setting will be based on is also ephemeral, it is proposed to operationally adapt the settings. Some distribution systems will have two peaks that may show significant difference: morning and evening. Therefore, for operational adaptive pickup setting and the fact that utilities will have access to the consumption information of customers by way of smart metering, the day-to-day loading can be determined and used in the OC protection setting for the substation relay.

5 SOLUTION METHODOLOGY FOR OVERCURRENT PROTECTION AND SMART METER INFORMATION USAGE

5.1 Introduction

The solution methodologies developed to address the stated problems in section 4 are outlined in this section. First, the work focuses on addressing some of the overcurrent protection challenges that arise from connecting DGs to radial distribution systems (RDS). The proposed solution focuses on decentralizing the control of the zonal breakers used in the methods of [27] and [28] to eliminate the single point of failure that a central relay may present. Also, the IEEE 34 node radial test feeder and its modifications made to examine the response of the proposed protection approach are presented in section 5.2.2. The results of case studies are discussed in section 5.3.

Secondly, the step-by-step method developed to use smart meter load information to adapt the overcurrent pickup setting for the substation overcurrent (OC) relay of zone 1 is presented in section 5.5. A secondary distribution design for the multi-feeder test system is presented to allow for the allocation of the smart meters among the individual customers defined for the test system. The responses of the adaptive pick setting for the substation relay for a select portion of the multi-feeder test system are presented for a number of fault types and locations.

5.2 Proposed Directional Overcurrent Protection Approach

The proposed overcurrent protection approach presented in this thesis expands on the work of [27] and [28] which use a zone concept to isolate a faulted area in RDS with DGs. The zone formation follows the steps presented in [28] which were discussed in section 4. However, in the proposed approach, the zones are separated by zonal boundary protective elements that are comprised of both a directional overcurrent (OC) relay and a circuit breaker. The directional OC element is composed of negative and positive sequence elements to detect the fault current direction. The negative sequence element operates for unbalanced faults while the positive sequence element activates for

balanced faults. The control of the breakers separating the zones is decentralized by eliminating the central relay concept used in the methods of [27] and [28].

Each directional overcurrent relay at a zonal boundary location controls its respective zone breaker. The zonal boundary OC relays communicate with one another about the direction of their detected fault current using binary state signals. The use of a binary state signal, initially proposed by [57], as opposed to actual fault current values reduces the amount of information communicated across the channel to neighboring zonal relays. Therefore, a low cost, small bandwidth communication design will help reduce the capital needed to implement this protection approach. The shared fault direction information is used by the boundary relays in a directional comparison blocking scheme to decide a trip or block operation of their boundary breakers. The communication between the relays takes into consideration the scale of the network as there may be redundancy in the communicated information. For instance, zones separated by two or more other zones may not need to have a communication link. This is because the relays of the zones innermost may have already communicated the correct fault direction information to the relays in the end zones. Two adjoining zones whose relays produce an incongruity on the direction of the fault current provide an indication of the faulted zone. This faulted zone detection is made by the relays at the boundary of a zone by utilizing the fault direction information received from the neighboring zone relays. Once a faulted zone is identified, the relays at the respective ends of the zone send commands to trip their breakers. Within the faulted zone, the local protection of the DGs trips the DGs to prevent them from sourcing the fault following the tripping of the zone's breakers. This means that zones downstream of the faulted zone will be operated as intentional islands and the zones upstream of the faulted zone will be energized by the substation and any DGs that may be present.

The assumptions made in the proposed directional overcurrent protection approach were:

1. The radial distribution system includes two or more radial feeders on which DGs have been connected.

2. The DGs are either located on the main or the three phase laterals of the radial feeders.
3. The DGs are synchronous based machines with automatic controls to regulate both the output real and reactive powers to maintain the voltage and frequency within acceptable limits.
4. The DGs have their own protection.
5. All protective devices on the radial feeders are relay controlled circuit breakers.
6. Each zonal boundary protective element has both a receiving and a transmitting port for communication.
7. Each zonal boundary protective element has the ability to perform both reclosing and synchronization functions.
8. Each directional element determines the fault type by using the current and voltage it samples at its location to activate the required sequence element.
9. A reliable and secure communication medium exists.

The proposed approach can be applied to the radially interconnected DG system of Fig. 12 by establishing the four zones as shown in Fig. 15. ZB1, ZB2, ZB3 and ZB4 are the zonal boundary protective elements that separate the individual zones. Fig. 16 shows the topology for communicating the binary state signals among the various zonal boundary protective elements of Fig. 15. An example of a binary signal information exchange for a fault in zone 2 takes the form of ZB2 transmitting a binary bit to ZB3 and ZB4 indicating that its sequence element has detected a forward fault. ZB3 and ZB4 in return respond with a binary bit that indicates a reverse direction as would be seen by an observer looking into the network. The information transmitted by ZB1 to ZB3 and ZB4 will be redundant as ZB2 also shares the same information. When each relay compares its own fault direction to the direction received from the neighboring relays, the fault is found to be in zone 2, and zone 2 will be isolated. For a fault in zone 1, the forward fault direction of ZB1 in contrast to the reverse direction indicated by the ZB2 will allow only zone 1 to be isolated while the other zones stay connected and operate as islands.

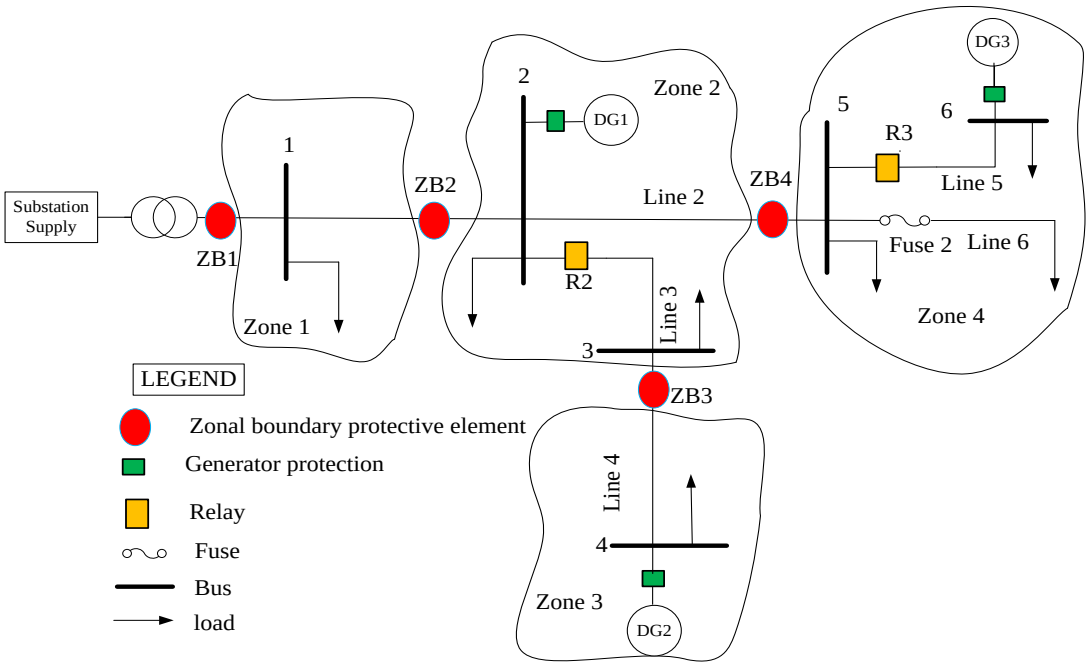

Fig. 15 Zone Formation for Fig. 12 System Using the Proposed Directional OC Protection Approach

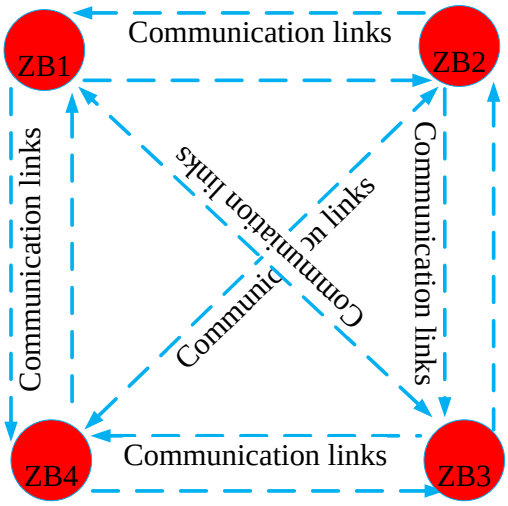

Fig. 16 Zonal Boundary Protective Elements Communication Topology for Fig. 12 System

5.2.1 The IEEE 34 Node Radial Test Feeder

The IEEE 34 Node Radial Test Feeder [58], Fig. 17, is based on an actual feeder located in rural Arizona. The feeder as presented in [58] consists of one 2.5 MVA, 69/24.9 kV step down transformer located at the substation and one 24.9/4.16 kV in-line transformer located for a short section of the feeder on lateral 5. Two in-line voltage regulators are included to restore the voltage within acceptable limits. The loading on the system is light and characteristically unbalanced with wye and delta configurations. All loads are of the static type with representations as either constant current, constant impedance or constant power. The feeder loading is classified as either spot or distributed. Capacitor banks are located at nodes 844 and 848.

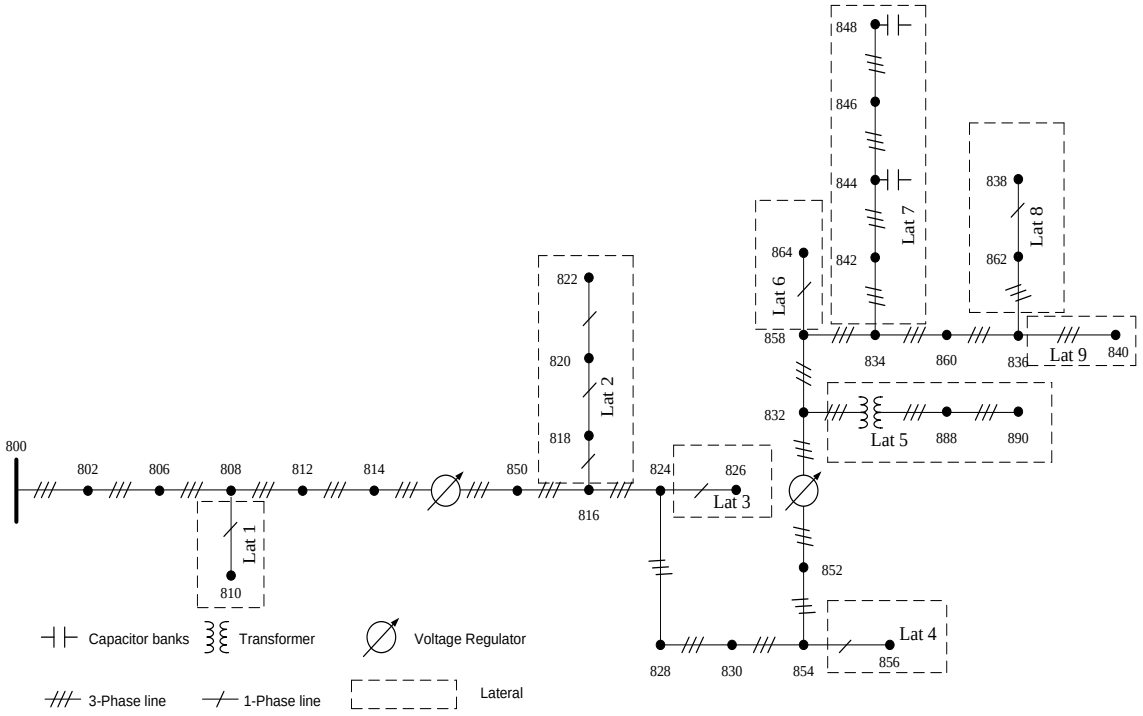

Fig. 17 The IEEE 34 Node Radial Test Feeder (Adapted from [59])

5.2.2 Revised IEEE 34 Node Radial Test Feeder for Testing Proposed Directional Overcurrent Protection Approach

Coherent with the objectives of this thesis, the IEEE 34 node radial test feeder was revised into a multi-feeder test system that preserved the structure of the original test feeder. A dual bus substation configuration was adopted for the purpose of this work. For simplicity and reliability reasons, the multi-feeder was designed as two single radial feeders that were connected by a normally opened switch at node 800. Fig. 18 shows the multi-feeder configuration adopted. Five synchronous based DGs were introduced on the multi-feeder test system; three on feeder 1, and two on feeder 2. The DGs were placed both on the mains and on the laterals of the multi-feeder. The DGs on feeder 1 were connected at nodes 840, 848 and 854. On feeder 2, the DGs were located at nodes 858 and 862. The individual ratings of the DGs are given in Table 5. Overcurrent protection using relays were added to the multi-feeder both at the laterals and at the substation.

Table 5 Synchronous DG Ratings

Feeder #	Feeder Node	DG Number	S Rated (kVA)	VLN rated (kV)
1	854	1	610	13.8
1	840	2	1000	13.8
1	848	3	1500	13.8
2	858	4	1100	13.8
2	862	5	1400	13.8

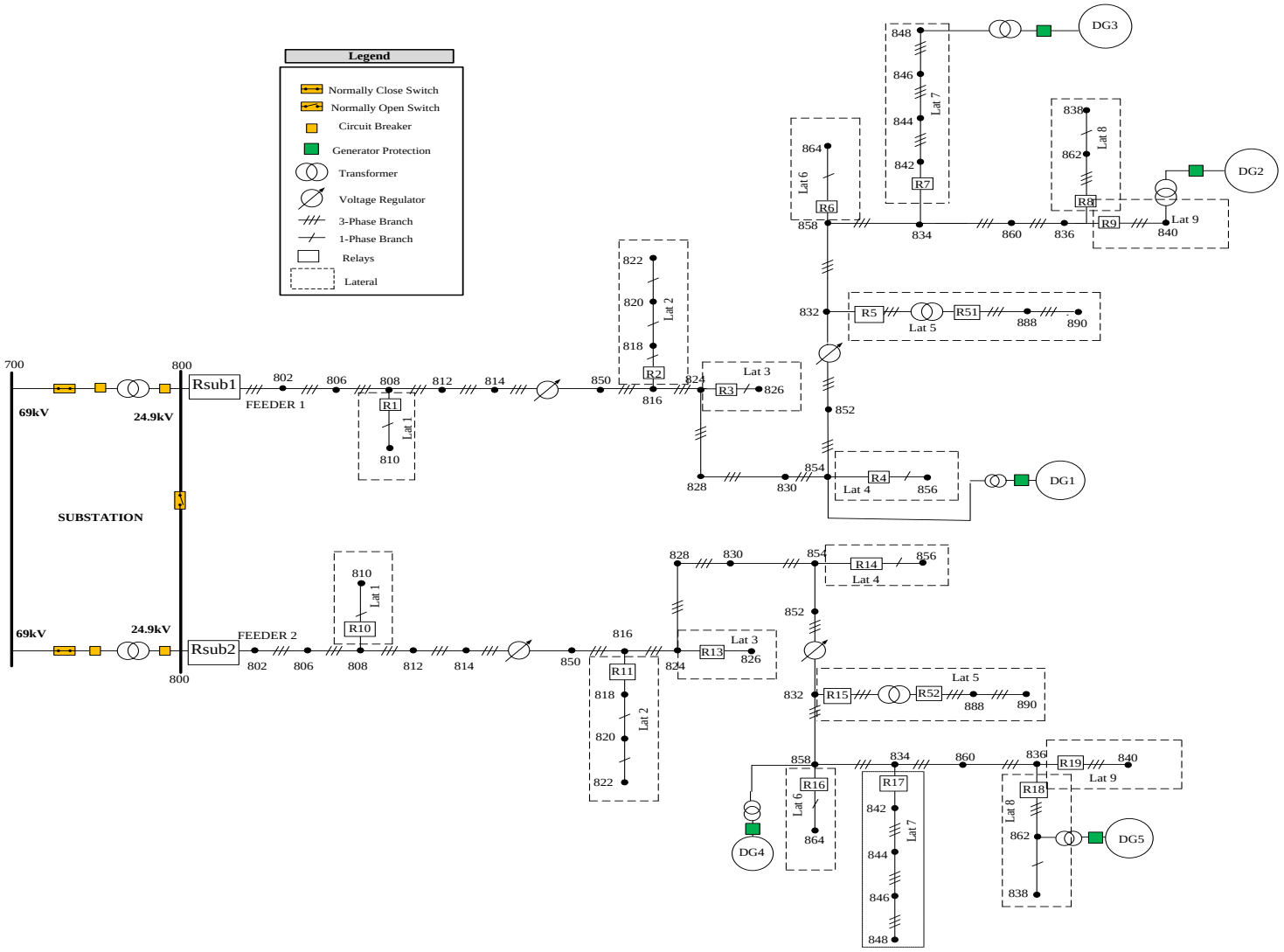

Fig. 18 IEEE 34 Node Radial Test Feeder Revised to a Two Feeder Test System with DGs.

5.2.3 Estimation of Secondary Load Ratings for the Multi-feeder Test System

The loads were modeled in the multi-feeder test system as distributed and spot loads. The average and maximum power requirements for each individual customer at the secondary distribution level were estimated to size the secondary distribution transformers. The secondary load ratings estimation process for the distributed loads utilized the energy consumption data provided in [60] from customer billing records for a particular month. As the distributed loads represented monthly energy consumption of a number of customers with unequal load values between the various phases, they were classified as residential customers. The maximum active and reactive powers provided in the same reference paper [60] for the spot loads were maintained. The balanced nature of the spot loads coupled with the fact that only their maximum demand was reported suggested that they could be either commercial or industrial type loads. Thus, the spot loads were designated as commercial or industrial depending on their maximum powers. Table 6 shows the kW and kVAR ratings of the spot loads. The ratings of the distributed loads for the specific month of recording as reported in [60] are shown in Table 7. The loads on the two feeders of the multi-feeder test system were a duplicate of each other.

Table 6 Ratings for Spot Loads on the Two Feeder Test System

Node	Phase A		Phase B		Phase C	
	kW	kVAR	kW	kVAR	kW	kVAR
860	24.57	18.43	24.57	18.43	24.57	18.43
840	10.93	8.2	10.93	8.2	10.93	10.93
844	164.69	123.52	164.69	123.52	164.69	123.52
848	24	18	24	18	24	18
890	33.33	25	33.33	25	33.33	25
Total	257.52	193.15	257.52	193.15	257.52	193.15

Table 7 Kilowatt Hour Ratings for Distributed Loads on the Two Feeder Test System

Node A	Node B	Phase A		Phase B		Phase C	
		# Of Customers	Total kWh Energy	# Of Customers	Total kWh Energy	# Of Customers	Total kWh Energy
802	806	0	0	68	10375	67	8465
808	810	0	0	7	3415	0	0
818	820	6	7706	0	0	0	0
820	822	101	53860	0	0	0	0
816	824	0	0	1	39	0	0
824	826	0	0	36	14325	0	0
824	828	0	0	0	0	3	390
828	830	5	1073	0	0	0	0
854	856	0	0	1	500	0	0
832	858	10	1420	2	127	4	864
858	864	2	69	0	0	0	0
858	834	11	813	15	3205	14	3233
834	860	13	3980	14	5602	104	42985
860	836	16	7844	8	2235	14	12369
836	840	4	3294	8	5077	0	0
862	838	0	0	34	8840	0	0
842	844	1	1380	0	0	0	0
844	846	0	0	61	7928	35	6934
846	848	0	0	2	3953	0	0

Using the kWh energy consumption data and the number of customers representing each distributed load, the consumption of each individual customer household between any two nodes A and B was randomized around the average consumption. The randomization of the individual energy consumption around the average was performed based on the assumption that rarely will individual households within a neighborhood have the same energy consumption per month. Using typical load factors for each class of load type and assumed diversity factors from [61], the secondary distribution transformers were sized appropriately. The steps below summarize the procedure used in establishing the ratings for the secondary distributed loads. The steps

used in determining the phase-A secondary loads between nodes 860 and 836 are given as an example. The same procedure was followed for the other loads. The data for the secondary distributed loads are given in appendix A.

Step 1: The average energy consumption per phase of the distributed loads between nodes 860 and 836 was calculated using the data in Table 7.

$$\text{Average Energy Consumption} = \frac{\text{Total kWh Energy Consumption}}{\text{Number of Customers}} = \frac{7844}{16} = 490.25 \text{ kWh} \quad (1)$$

Step 2: The energy consumption for each customer, i, for a phase was estimated to be within ±25% around the average energy consumption. As a check, the sum of the individual customer energy consumption for the given phase must equal the total kWh energy consumption. Table 8 shows the calculated values for the energy consumption.

$$\text{Total kWh Energy Consumption} = \sum_{i=1}^{16} \text{Energy Consumption}_i$$

Table 8 Energy Consumption for Each Customer of Phase-A for Nodes 860-836

Customer #	Energy Consumption (kWh)
1	536
2	500
3	457
4	458
5	498
6	459
7	500
8	488
9	506
10	453
11	461
12	459
13	523
14	518
15	513
16	515

Step 3: The average demand in kW for each customer was calculated from the energy consumption data in step 2 assuming a 30-day billing cycle. The average demand for each customer using 720 hours of consumption is shown in Table 9.

$$\text{Average Demand}_i = \frac{\text{Energy Consumption}_i}{\text{Hours of Consumption}} \quad (2)$$

Table 9 Average Demand for Each Customer of Phase-A for Nodes 860-836

Customer #	Average Demand (kW)
1	0.744
2	0.694
3	0.635
4	0.636
5	0.692
6	0.638
7	0.694
8	0.678
9	0.703
10	0.629
11	0.640
12	0.638
13	0.726
14	0.719
15	0.713
16	0.715

Step 4: The maximum demand for each customer was estimated using assumed load factors. The typical load factor for residential customers is 10-15%, commercial customers is 25-30%, and industrial customers is 70-80% [62]. Random values of the load factors within the ranges were determined for each customer. The maximum demand for each customer was calculated using (3). A list of the maximum demand calculated for each customer is shown in Table 10

$$\text{Maximum Demand}_i = \frac{\text{Average Demand}_i}{\text{Load Factor}_i} \quad (3)$$

Table 10 Maximum Demand for Each Customer of Phase-A for Nodes 860-836

Customer #	Average Demand (kW)	Load Factor	Maximum Demand (kW)
1	0.744	0.13	5.726
2	0.694	0.11	6.313
3	0.635	0.11	5.770
4	0.636	0.10	6.361
5	0.692	0.10	6.917
6	0.638	0.12	5.313
7	0.694	0.10	6.944
8	0.678	0.11	6.162
9	0.703	0.14	5.020
10	0.629	0.12	5.243
11	0.640	0.15	4.269
12	0.638	0.11	5.795
13	0.726	0.13	5.588
14	0.719	0.11	6.540
15	0.713	0.14	5.089
16	0.715	0.12	5.961

Step 5: The mean length of displacement for each distributed load from a given transformer location was computed using (4). The mean length of displacement represents the distance the customers were assumed to be spaced from one another for them to be supplied by one transformer.

$$\text{Mean Length of displacement} = \frac{\text{Length of Line Segment}}{\text{Number of Customers}} \tag{4}$$

One common secondary transformer was assigned to a group of 12 customers if the mean length was less than 250 ft until the total number of customers has all been assigned a transformer. If the mean length is greater than 250 ft, a transformer was assigned to each individual customer with the assumption that the customers were remotely located from one another. The lengths of the line segments for the multi-feeder test system are given in appendix B. For nodes 860-836, the mean length is 167.5 ft which is less than 250 ft. Thus, two groups were obtained: Group 1 comprising of 12 customers and Group 2 comprising of the remaining 4 customers which is based on the assumed utility transformer allocation philosophy.

Step 6: The secondary distribution transformer size for each customer group, k, was determined using (5) from the maximum non-coincident computed demand, maximum demand, an assumed power factor of 0.9, and diversity factors from [61]. The closest standard overhead distribution transformer rating depending on the value obtained in (5) was then selected as the transformer size. Table 11 shows the computed transformer (X'fmer) ratings.

$$\text{Maximum KVA}_{\text{XFER, group k}} = \frac{\text{Maximum Non-Coincident Demand}_{\text{group k}}}{\text{Power Factor} \times \text{Diversity factor}} \qquad (5)$$

$$\text{Maximum Non-Coincident Demand}_{\text{group k}} = \sum_{i} \text{Maximum Demand}_{i}$$

Table 11 Secondary Load Ratings for Phase-A Loads between Nodes 860- 836

Group #	Customer #	Average Demand (kW)	Load Factor	Maximum Demand (kW)	Maximum Non-coincident Demand (kW)	Diversity Factor	X'fmer rating (kVA)
1	1	0.744	0.13	5.726	64.04	2.7	25
	2	0.694	0.11	6.313			
	3	0.635	0.11	5.770			
	4	0.636	0.10	6.361			
	5	0.692	0.10	6.917			
	6	0.638	0.12	5.313			
	7	0.694	0.10	6.944			
	8	0.678	0.11	6.162			
	9	0.703	0.14	5.020			
	10	0.629	0.12	5.243			
	11	0.640	0.15	4.269			
	12	0.638	0.11	5.795			
2	13	0.726	0.13	5.588	28.97	2.1	10
	14	0.719	0.11	6.540			
	15	0.713	0.14	5.089			
	16	0.715	0.12	5.961			

The secondary distributed load ratings together with their assigned transformer sizes are provided in appendix A. The secondary ratings of the multi-feeder test system were aggregated to the primary distribution level and used as the ratings for the distributed loads in the protection study. Table 12 provides the kW and KVAR ratings for the distributed loads on the multi-feeder test system.

The cables in the multi-feeder test system were changed to match the new loading of the system. Table 13 shows the overhead line configurations used. The line lengths were retained as they were in the original test feeder. The impedance and susceptance data for the cables are given in appendix B.

Table 12 kW and kVAR Ratings of the Distributed Loads in Multi-feeder Test System

Node A	Node B	PHASE A		PHASE B		PHASE C	
		P (kW)	Q (kVAR)	P (kW)	Q (kVAR)	P (kW)	Q (kVAR)
802	806	0	0	131	63	84	41
808	810	0	0	32	15	0	0
818	820	76	37	0	0	0	0
820	822	623	302	0	0	0	0
816	824	0	0	0.42	0.2	0	0
824	826	0	0	153	74	0	0
824	828	0	0	0	0	5	3
828	830	10	5	0	0	0	0
854	856	0	0	5	2	0	0
832	858	15	7	1.47	0.71	9	4
858	864	0.87	0.42	0	0	0	0
858	834	9	4	30	14	32	16
834	860	39	19	52	25	597	289
860	836	78	38	28	14	132	64
836	840	35	17	71	34	0	0
862	838	0	0	82	40	0	0
842	844	17	8	0	0	0	0
844	846	0	0	100	48	80	39
846	848	0	0	39	19	0	0

Table 13 Overhead Line Configurations for the Multi-feeder Test System

Configuration	Phasing	Phase ACSR	Neutral ACSR	Spacing ID
300	BACN	4/0	4/0	500
301	BACN	4/0	1/0	500
302	AN	1/0	1/0	505
303	BN	1/0	1/0	510
304	BN	1/0	1/0	510

5.2.4 Implementation of Multi-feeder Test System in EMTP™/PSCAD®

The multi-feeder test system was modeled in EMTP™/PSCAD® [63]. Voltage regulators and cables were modeled exactly as is reported in [64]. The voltage regulator model includes the following controls: set voltage, initial tap setting, bandwidth, out-of-band detector, control time delay, tap position calculator, timer reset, and line compensation. Table 14 provides the voltage regulator compensator settings.

Table 14 Voltage Regulator Compensator Settings

Regulator Data			
Regulator ID:	1		
Line Segment:	814 - 850		
Location:	814		
Phases:	A - B -C		
Connection:	3-Ph,LG		
Monitoring Phase:	A-B-C		
Bandwidth:	2.0 volts		
PT Ratio:	120		
Primary CT Rating:	100		
Compensator Settings:	Ph-A	Ph-B	Ph-C
R - Setting:	2.7	2.7	2.7
X - Setting:	1.6	1.6	1.6
Voltage Level:	122	122	122

Table 14 Continued

Regulator Data			
Regulator ID:	2		
Line Segment:	852 - 832		
Location:	852		
Phases:	A - B -C		
Connection:	3-Ph,LG		
Monitoring Phase:	A-B-C		
Bandwidth:	2.0 volts		
PT Ratio:	120		
Primary CT Rating:	100		
Compensator Settings:	Ph-A	Ph-B	Ph-C
R - Setting:	2.5	2.5	2.5
X - Setting:	1.5	1.5	1.5
Voltage Level:	124	124	124

The cable model from [64] addresses the tightly coupled nature of unbalanced distribution lines and allows for direct entry of impedance and susceptance values. For the load models, the exponential static model in [65] was implemented using PSCAD master library components. The exponential static model expressions of the load are given as in (6). For constant power, constant current and constant impedance load characteristics, both ‘a’ and ‘b’ are 0, 1 and 2, respectively.

$$P = P_0 \left(\frac{V}{V_0}\right)^a \qquad Q = Q_0 \left(\frac{V}{V_0}\right)^b \tag{6}$$

P and Q are the active and reactive components of the load

P_0 and Q_0 are the initial active and reactive power

V_0 and V are the initial and bus voltage

‘a’ and ‘b’ are the parameters

The master library synchronous machine model in PSCAD was used for the DG model. The DG model parameters are shown in Table 15.

Table 15 Synchronous Generator Parameters

Armature Time Constant [Ta]	0.0042 pu
Potier Reactance [Xp]	0.18 pu
D: Unsaturated Reactance [Xd]	1.25 pu
D: Unsaturated Transient Reactance [Xd']	0.24 pu
D: Unsaturated Transient Time (Open) [Tdo']	4.11 s
D: Unsaturated Sub-Transient. Reactance [Xd"]	0.19 pu
D: Unsaturated Sub-Transient Time (open) [Tdo"]	0.023 pu
Q: Unsaturated Reactance [Xq]	0.62 pu
Q: Unsaturated Transient Reactance [Xq']	0.228 pu
Q: Unsaturated Transient Time (Open) [Tqo']	0.85 s
Q: Unsaturated Sub-Transient. Reactance [Xq"]	0.26 pu
Q: Unsaturated Sub-Transient Time (open) [Tqo"]	0.061 s
Air Gap Factor	1

The OC protective relays used in the multi-feeder test system were moderately inverse Schweitzer Engineering Laboratories (SEL) relays. The SEL moderately inverse characteristic is defined in (7) [66].

$$T_p = TD \times \left(0.0226 + \frac{0.0104}{M^{0.02} - 1}\right) \tag{7}$$

T_p = Operating time in seconds

TD = Time dial setting

M = Multiples of pickup current

The directional capability of the relay was modeled to include both the negative and positive sequence directional elements. Fig. 19 shows the functional block of the directional OC relay model. The directional capability of the OC relay uses a directional supervision as can be seen in the figure. This supervision was implemented through the ‘Ctrl 3’ in the figure. The OC relay can sense fault currents, but it does not initiate a tripping of its circuit breaker unless the directional element has confirmed the direction of the fault current. The operating quantity of the relay is current.

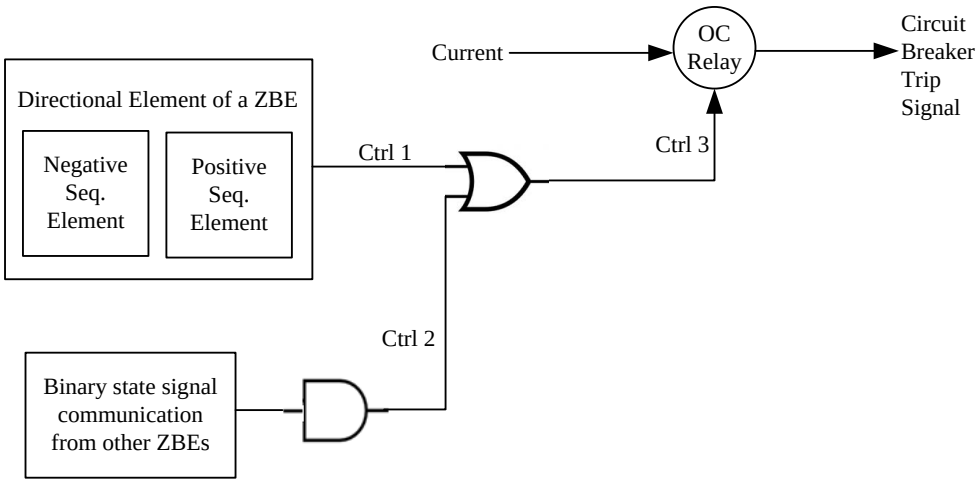

Fig. 19 Functional Block of Directional OC Relay Model in EMTP™/PSCAD®

The negative sequence directional element determines the direction of the fault current by computing the negative sequence impedance value, which is the ratio of the negative sequence voltage and negative sequence current. The negative sequence voltage for a forward or reverse fault is always negative. However, the negative sequence current is positive for a forward fault and negative for a reverse fault. Thus, for a forward fault the negative sequence impedance is negative, and for a reverse fault, the negative sequence impedance is positive [67]. EMTP™/PSCAD® master library component for negative sequence element was used to implement this function of the directional element.

The modeled positive sequence directional element of the OC relay detects faults in the forward direction by comparing the phase angle difference between the positive sequence current and voltage to a defined forward range given in (8) using a range comparator. The forward and reverse operating zones of the positive sequence element are depicted in Fig. 20.

$$-\frac{\pi}{2}+\theta<\beta<\frac{\pi}{2}+\theta \tag{8}$$

β = Angle difference between positive sequence voltage and current

θ = Positive sequence line angle

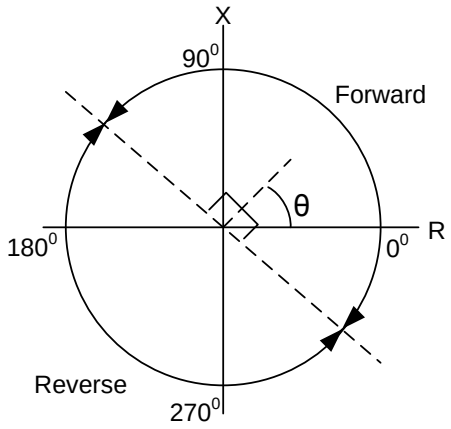

Fig. 20 Direction of Positive Sequence Element

The logic flow for the complete directional element of the relay is shown in Fig. 21. The ‘Pos’ and ‘Neg’ inputs to the AND gates in the figure enable the directional OC element to determine the fault current direction depending on the type of fault. The forward direction or reverse direction form the ‘Ctrl’ in Fig. 19. The negative sequence directional element was given the essential function of detecting and making the fault direction decision for unbalanced faults types while the positive sequence directional element made the direction decision for balanced fault types. Thus, if an unbalanced fault is detected by the negative sequence element to be forward, OR1 output will be 1, which consequently drives the output of OR2 to high. The output of OR3 and OR4 will both be zero thereby driving the reverse status to low. In the case of a balanced three phase fault, the negative sequence element is disabled thus, making both AND2 and AND5 output zero. This then translates to a zero output for both OR1 and OR3, leaving the fault direction detection solely to be made by the positive sequence directional element. For a forward fault, AND1 and AND3 output will be high and vice-versa for a reverse fault condition. The opposite holds for AND4 and AND6, which are high for reverse fault and low for forward faults.

Although both positive and negative sequence current and voltage exist in unbalanced fault conditions, the negative sequence directional element was made to have

a higher priority in controlling the overcurrent (OC) relays. This choice was to prevent the positive sequence directional element from making erroneous decision for magnitudes of faults currents comparable to the load current.

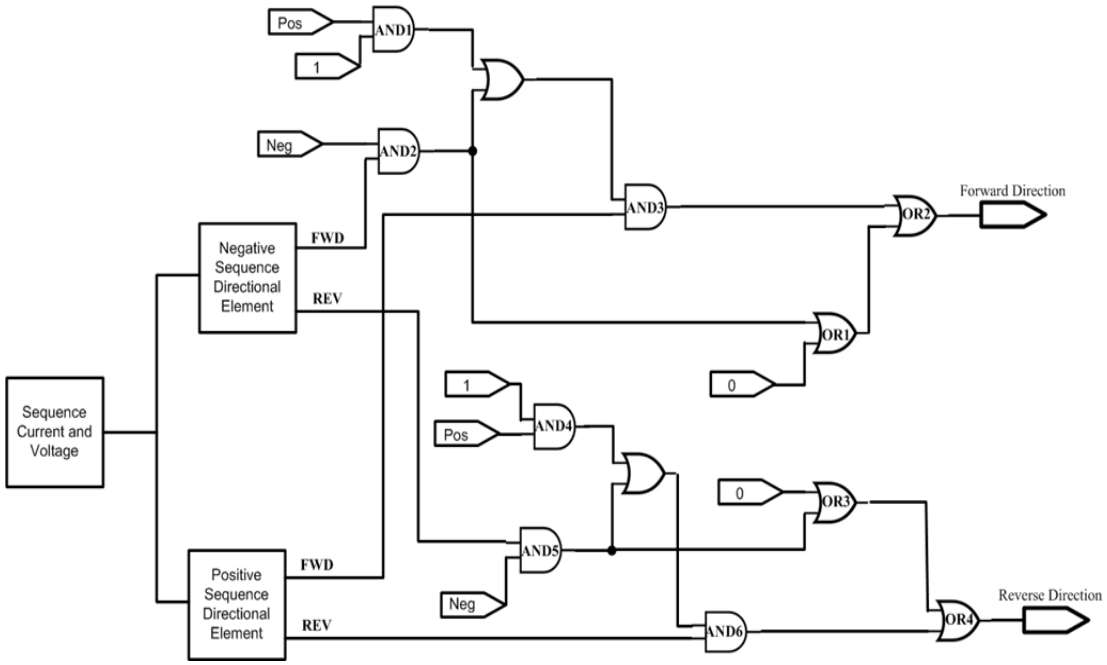

Fig. 21 Logic Flow for Directional Element Model in EMTP™/PSCAD®

5.2.5 Multi-feeder Test System Model

The individual component models were integrated to form the multi-feeder test system model in PSCAD. Transient analysis was performed in PSCAD using the maximum load values in Table 6 and Table 12. The simulation was run and after 4s, the steady state phase voltages at the primary nodes were recorded. The per-unit (p.u.) node phase voltages for the system without DGs are shown in Table 16. The voltages as seen in the table are roughly within ±5% of the nominal. Table 17 shows the per phase real and reactive powers of the line segments on the multi-feeder test system. The values

shown in the table are the sending powers from node A to B. The receiving powers are the negative of those reported in the table.

Table 16 Node Voltages of Multi-feeder Test System without DGs

Node	Feeder 1			Feeder 2		
	Phase A V(p.u.)	Phase B V(p.u.)	Phase C V(p.u.)	Phase A V(p.u.)	Phase B V(p.u.)	Phase C V(p.u.)
800	1.0500	1.0520	1.0410	1.0500	1.0530	1.0440
802	1.0460	1.0520	1.0400	1.0480	1.0530	1.0380
806	1.0350	1.0530	1.0060	1.0520	1.0520	1.0360
808	1.0350	1.0530	1.0060	1.0340	1.0520	1.0060
810	0.0000	1.0530	0.0000	0.0000	1.0520	0.0000
812	1.0380	1.0290	1.0270	1.0160	1.0400	0.9765
814	0.9982	1.0510	0.9535	1.0030	1.0400	0.9503
850	1.0330	1.0340	1.0380	1.0340	1.0350	1.0350
816	1.0320	1.0370	1.0350	1.0310	1.0360	1.0370
818	1.0300	0.0000	0.0000	1.0320	0.0000	0.0000
820	0.9757	0.0000	0.0000	0.9841	0.0000	0.0000
822	0.9677	0.0000	0.0000	0.9761	0.0000	0.0000
824	1.0380	1.0290	1.0270	1.0360	1.0280	1.0290
826	0.0000	1.0310	0.0000	0.0000	1.0270	0.0000
828	1.0330	1.0330	1.0330	1.0320	1.0290	1.0320
830	1.0380	1.0260	1.0100	1.0370	1.0250	1.0130
854	1.0390	1.0220	1.0100	1.0370	1.0210	1.0160
856	0.0000	1.0260	0.0000	0.0000	1.0200	0.0000
852	1.0140	0.9853	0.9669	1.0400	1.0140	0.9853
832	1.0440	1.0410	1.0530	1.0460	1.0390	1.0530
888	0.9650	0.9953	0.9789	0.9829	1.0400	1.0020
890	0.9650	0.9953	0.9789	0.9577	1.0180	0.9713
858	1.0350	1.0390	1.0500	1.0490	1.0350	1.0510
864	1.0450	0.0000	0.0000	1.0470	0.0000	0.0000

Table 17 Line Segment Powers of Multi-feeder Test System without DGs

Node A	Node B	Phase A (MW)	Phase A (MVAR)	Phase B (MW)	Phase B (MVAR)	Phase C (MW)	Phase C (MVAR)
800	802	1.3370	0.5780	1.2580	0.4531	1.3450	0.6870
802	806	1.3310	0.5530	1.1850	0.3861	1.3307	0.6630
806	808	1.3310	0.5146	1.0410	0.3290	1.3208	0.6530
808	810	0.0000	0.0000	0.0330	0.0140	0.0000	0.0000
808	812	1.3240	0.5030	1.0200	0.3180	1.3130	0.6430
812	814	1.3140	0.4536	1.0930	0.3086	1.3010	0.5956
814	850	1.3030	0.4389	1.0320	0.3020	1.2985	0.5803
850	816	1.3030	0.4393	1.0320	0.3020	1.2864	0.5806
816	818	0.7550	0.3480	0.0000	0.0000	0.0000	0.0000
818	820	0.7541	0.3474	0.0000	0.0000	0.0000	0.0000
820	822	0.6389	0.2948	0.0000	0.0000	0.0000	0.0000
816	824	0.6448	0.5027	1.0220	0.3007	1.2802	0.5728
824	826	0.0000	0.0000	0.1684	0.0691	0.0000	0.0000
824	828	0.6414	0.0903	0.8489	0.1919	1.2790	0.5659
828	830	0.6388	0.0945	0.8358	0.2144	1.2800	0.5533
830	854	0.6286	0.0931	0.8185	0.1766	1.2720	0.5487
854	856	0.0000	0.0000	0.0054	0.0025	0.0000	0.0000
854	852	0.6180	0.0981	0.8113	0.2373	1.1400	0.4254
852	832	0.5947	0.0764	0.8458	0.2049	1.2640	0.3562
832	888	0.1444	0.0742	0.1633	0.0751	0.1355	0.0748
888	890	0.1444	0.0742	0.1633	0.0751	0.1355	0.0748
832	858	0.4588	-0.0209	0.6960	0.0895	1.0320	0.3325
858	864	0.0011	0.0001	0.0000	0.0000	0.0000	0.0000
858	834	0.4295	-0.0095	0.6076	0.0916	1.1300	0.3096
834	842	0.2145	-0.1131	0.3626	-0.0615	0.2934	-0.0712
842	844	0.2240	-0.1120	0.3255	-0.0552	0.2840	-0.0835
844	846	0.0318	-0.1495	0.0712	-0.1226	0.0163	-0.1430
846	848	0.0183	-0.1481	0.0249	-0.1444	0.0343	-0.1423
834	860	0.1666	0.0738	0.2100	0.1105	0.1884	0.0984
860	836	0.0505	0.0262	0.1776	0.0780	0.0117	0.0086
836	862	0.0008	0.0000	0.0870	0.0416	0.0009	-0.0003
862	838	0.0000	0.0000	0.0790	0.0381	0.0000	0.0000
836	840	0.0130	0.0086	0.0110	0.0089	0.0112	0.0085

Prior to the addition of DGs to the multi-feeder test system, the relay settings for the multi-feeder were determined. Table 18 provides the settings of the individual lateral and substation relays. The substation relay was the primary protective element for the mains and served as back-up to the other lateral relays. Column 1 represents the locations of the relays. Column 2 of the table shows the corresponding pickup settings for 1.5 times the nominal load current at the relay location. The last column of the table provides the time dial values of the relays that provided coordination between the lateral and substation relays. Due to the transformer between nodes 832 and 888, an independent OC protection was provided for lateral 5. This protection involved coordinating just the primary and the secondary sides of the transformer.

Table 18 Protection Device Settings on Multi-feeder Test System without DGs

Relay Location	**Pickup Setting (A)**	**Time Dial**
Lat. 1	3.8	0.5
Lat. 2	83.8	0.5
Lat. 3	17.7	0.5
Lat. 4	0.6	0.5
Lat. 5 (pri)	17.5	1.0
Lat. 5 (sec)	106.1	0.5
Lat. 6	9.3	0.5
Lat. 7	35.3	0.5
Lat. 8	9.3	0.5
Lat. 9	9.8	0.5
Substation	174	2.5

The DGs in Table 5 were connected on the multi-feeder test system for all studies in the remainder of this thesis. The multi-feeder test system was divided into 7 zones following the zone approach discussed in section 4. The multi-feeder test system with the zone divisions is shown in Fig. 22. Four zones can be seen on feeder 1, and three zones are observable on feeder 2. Each zone is separated by the boundary

protective elements, comprising of a directional overcurrent relay and a circuit breaker. On feeder 1, the boundary protective elements are designated as CB1, CB2, CB3 and CB4, and CB5, CB6 and CB7 on feeder 2. The locations of the boundary protective elements are as shown on the figure.

The settings of the negative sequence directional component of each of the boundary protective elements are presented in Table 19. Column 1 of the table indicates the parameter of interest. CTR is the per phase current transformer ratio for a 5A secondary relay current. PTR is the selected voltage transformer ratio for 115V secondary relay operating voltage. The length values signify the extent of coverage of the directional element. Z2 is the negative sequence impedance of the protected line. Z2 FWD and Z2 REV are the forward and reverse impedance thresholds, respectively. The line angle is the positive sequence angle for the protected lines. The CBs' are the names of the zonal boundary protective elements (relay and circuit breaker combined).

Table 19 Settings of Negative Sequence Directional Element

Element / Parameter	**CB1**	**CB2**	**CB3**	**CB4**	**CB5**	**CB6**	**CB7**
CTR	20	20	30	20	20	20	20
PTR	125	125	125	125	125	125	125
Length (mi)	25.78	9.01	1.10	1.11	33.68	2.20	1.05
Z2 (per mi)	0.63	0.63	0.63	0.63	0.63	0.63	0.63
Z2 FWD	2.58	0.90	0.16	0.11	3.37	0.22	0.11
Z2 REV	2.68	1.00	0.26	0.21	3.47	0.32	0.21
Line Angle	72.69	72.69	72.69	72.69	72.69	72.69	72.69

Equation (8) was used to set the forward operating regions of the positive sequence directional component of all the boundary protective elements with $\theta=72.9^0$ as:

$$-17.31^0 < \beta < 162.9^0$$

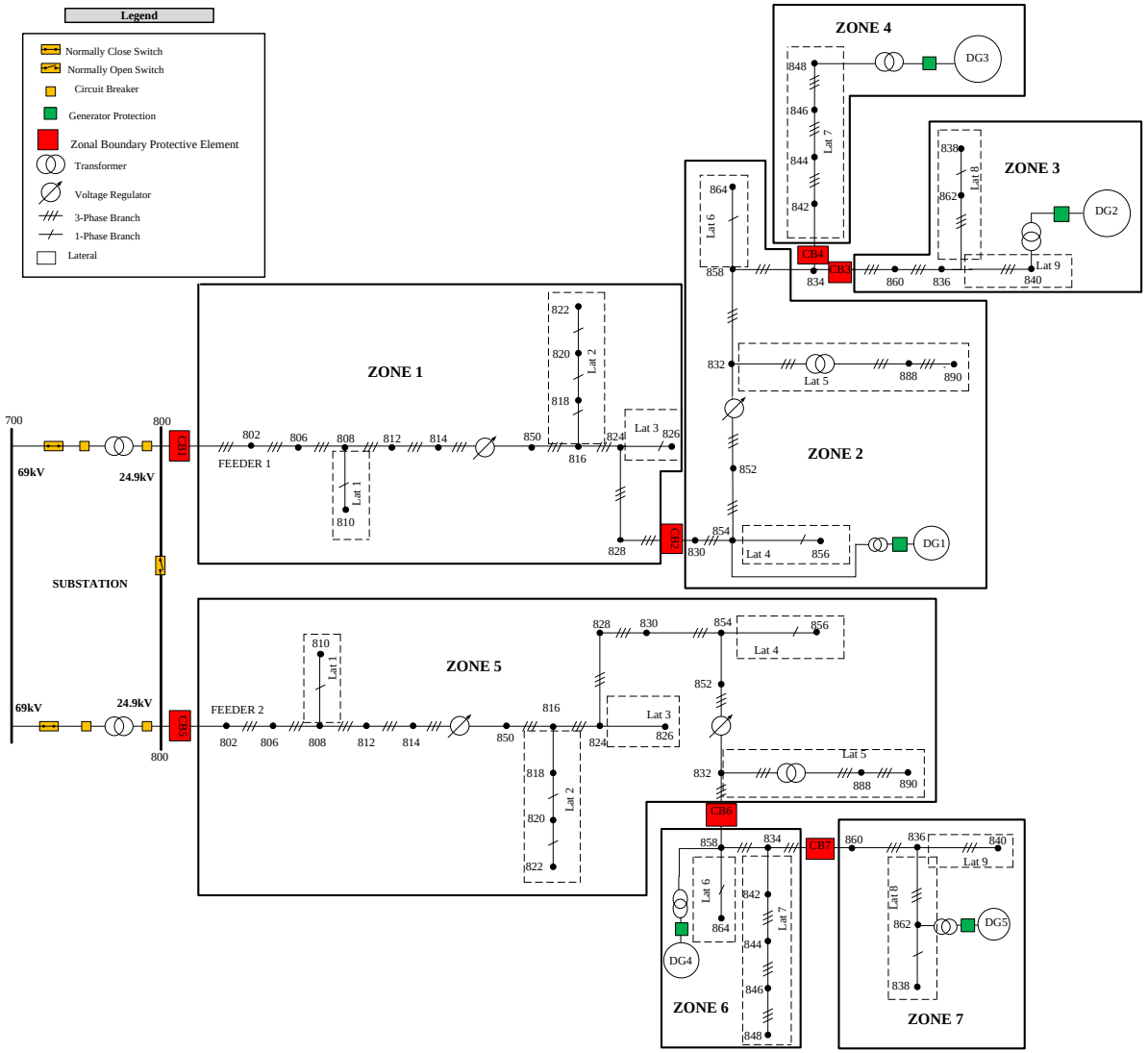

Fig. 22 The Multi-feeder Test System with DGs and Zone Divisions

The forward and reverse fault current directions were defined with respect to the relay location. Forward current for boundary protective relays on the mains designated flow from left to right. Reverse current for boundary relays on mains designated flow from right to left. However for lateral boundary relays, forward designated flow from the lateral tap point on the main feeder to the end of the lateral, and reverse is vice-versa. These directions were implemented in simulation based on the measurements of the directional sequence elements. Table 20 summarizes the fault current direction methodology based on the measurement of the sequence elements.

Table 20 Fault Current Direction Based on Directional Sequence Element Measurements

Direction / Element	Forward	Reverse
Negative Sequence	$Z_2 < Z_2$ FWD or negative	$Z_2 > Z_2$ REV or more positive
Positive Sequence	$-17.31^0 < \beta < 162.9^0$	$\beta < -17.31^0$ or $\beta > 162.9^0$

5.3 Simulation Cases for Proposed Directional Overcurrent Protection

The proposed protection approach was tested on the multi-feeder test system. Case 1 examined the response of the protection approach in isolating the faulted zones for several faults on the multi-feeder test system. In case 2, an exhaustive study was conducted for various fault types and locations in all zones defined on the multi-feeder test system. The results of case 2 studies are summarized in tables. At the start of the transient simulations for all cases, the DGs were operated as simple 3-phase ideal voltage sources, and then were switched to machine mode at 0.8 s. The DGs reached 60 Hz system frequency at about 3 s. The frequency response of the DGs on the two feeders is depicted in Fig. 23.

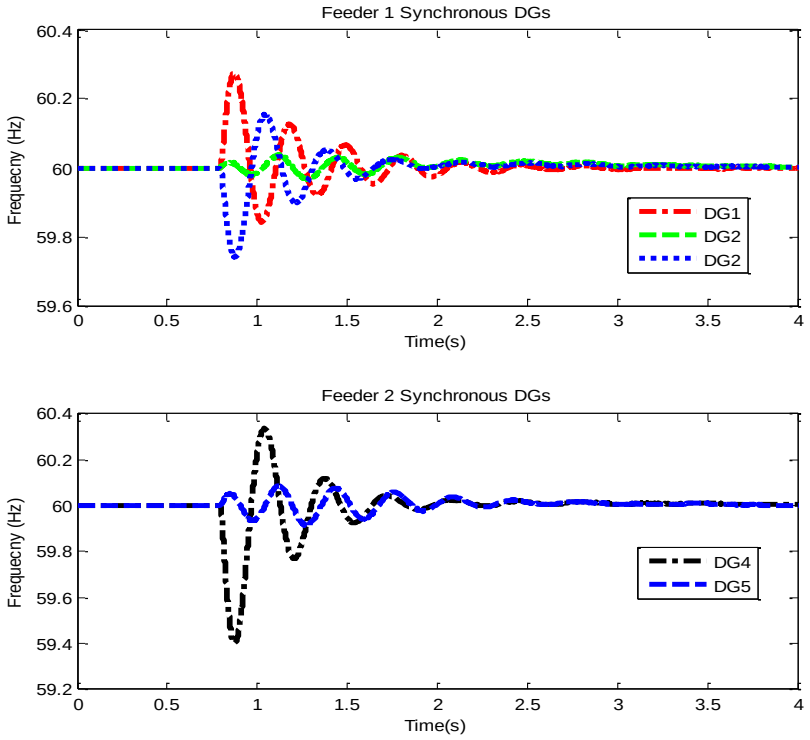

Fig. 23 Frequency for Five DGs Operating as Synchronous Machines in Multi-feeder Test System

5.3.1 Case 1– Test of Proposed Directional Overcurrent Protection Scheme

This case investigated the response of the proposed protection approach to a select number of balanced and unbalanced faults. The studies focused on the performance of the directional sequence elements of the boundary protective relays to accurately detect the faulted zones and communicate their fault direction detection status to other neighboring zonal protective relays.

5.3.1.1 Case 1.1: A-N fault on Feeder 1

In this test scenario, an A-N fault was staged between nodes 816 and 824 on feeder 1. Since the fault was unbalanced, the negative sequence directional component determined the fault direction as presented in the solution methodology. The fault was applied at 4 s. Fig. 24 displays the response of the negative sequence directional

elements of the boundary protective elements (CB1, CB2, CB3 and CB4) on feeder 1. CB2, CB3 and, CB4 negative sequence directional elements shows positive impedance values while CB1 shows a negative impedance value. The positive impedance values of CB2, CB3 and CB4, and the fact that they are all greater than their reverse impedance threshold, implies reverse fault current detection. On the other hand, CB1 negative impedance value infers forward fault current detection as described in Table 20.

Fig. 25 shows the status of the forward and reverse current direction of each of the zonal boundary protective elements. The logic flow in Fig. 21 ensured that at any given point only one fault direction of the zonal boundary element had the level "1" logic. A level "1" for either the forward or reverse direction indicates the active status of the fault current. In Fig. 25, CB2 forward status goes from active (level "1") to inactive (level "0") at 4 s while its reverse status goes from inactive (level "0") to active (level "1"). CB1 forward direction however stayed active (level "1") before and during the fault. The active path of the fault current seen by CB3 and CB4 remained as reverse (level "1") due to the DGs in their protected zone. The momentarily change of the reverse status of CB3 from "1" to "0" was due to the transients imposed on the DGs during to the fault.

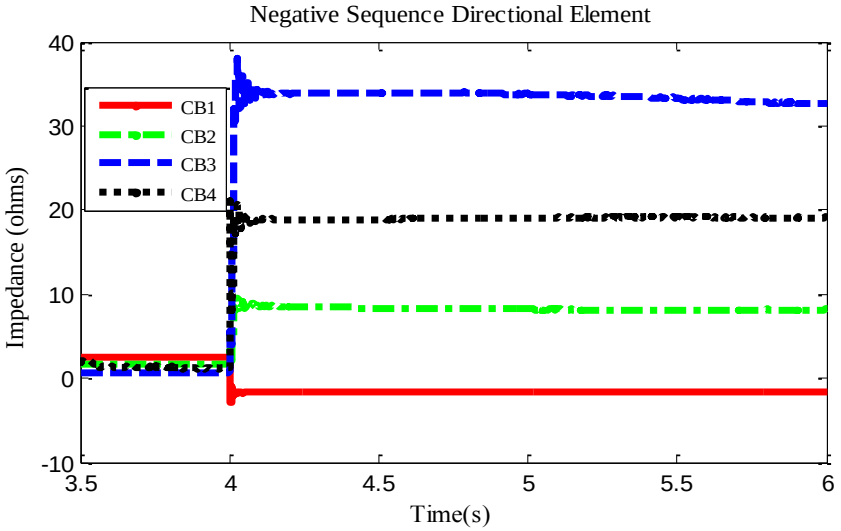

Fig. 24 Negative Sequence Elements Impedance for an A-N Fault on Feeder 1.

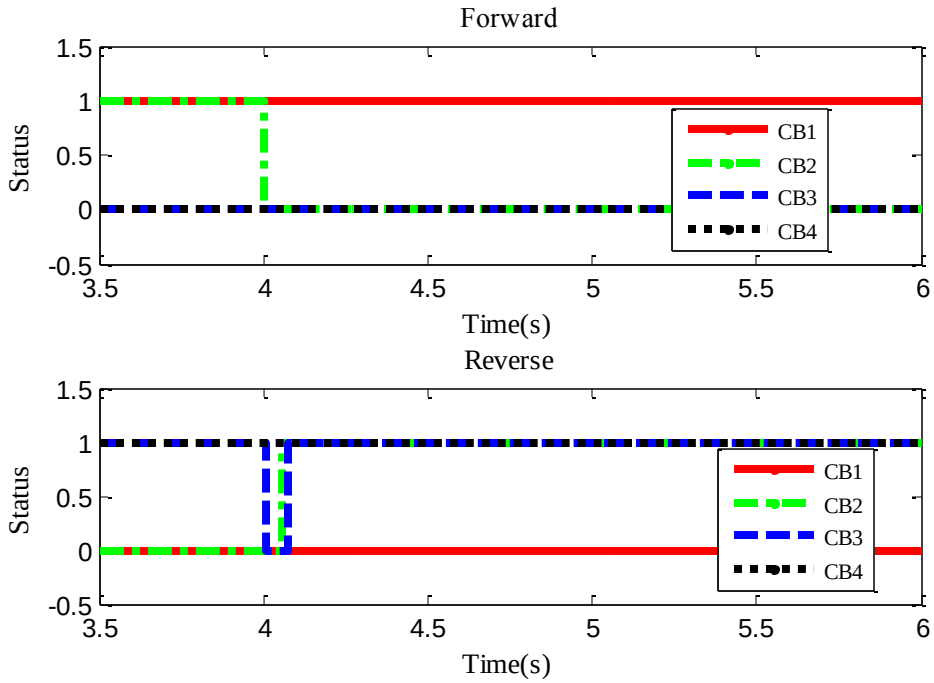

Fig. 25 Fault Direction Detection by Negative Sequence Elements for A-N Fault on Feeder 1.

The fault direction status of all zonal boundary elements was exchanged via a radio communication link. As shown in Fig. 25, CB1 indicated a forward fault and CB2 indicated a reverse fault. This shows that the fault was determined to be in zone 1. This caused the relays of both elements to proceed to trip their breakers as depicted in Fig. 26. Since the breakers of CB1 and CB2 were the only ones that tripped, it confirms that the fault was in zone 1.

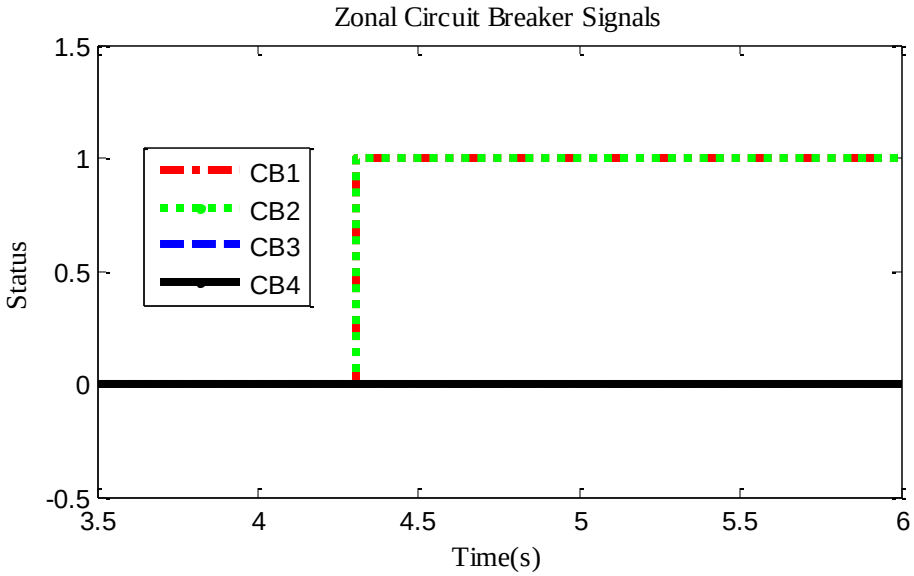

Fig. 26 Zonal Circuit Breakers Trip Status for an A-N Fault on Feeder 1.

5.3.1.2 Case 1.2: B-C Fault on Feeder 2

This case illustrates the response of the protection approach to a B-C fault staged on the line segment between nodes 808 and 812 on feeder 2. This fault is also unbalanced so the negative sequence directional element reacted to indicate the fault current direction. The fault was applied at 4 s. Fig. 27 displays the impedances of the negative sequence elements of the zonal boundary protective elements during the fault. The impedance of CB5 decreased from 2.63 Ω to -1.73 Ω during the fault. CB6 impedance value increased in its positive magnitude to about 10.31 Ω when the fault was staged. The impedance value of CB7 also increased to a steady state value of about 16.81 Ω during the fault.

From the designation of the fault current direction by the negative sequence element in Table 20, CB5 detected a forward fault while CB6 and CB7 detected a reverse fault. This condition is corroborated by the forward and reverse active fault direction status of these elements in Fig. 28. It is seen that CB6 changed its active status from forward to reverse during the fault at about 4.05 s while CB5 maintained its forward direction status during the fault.

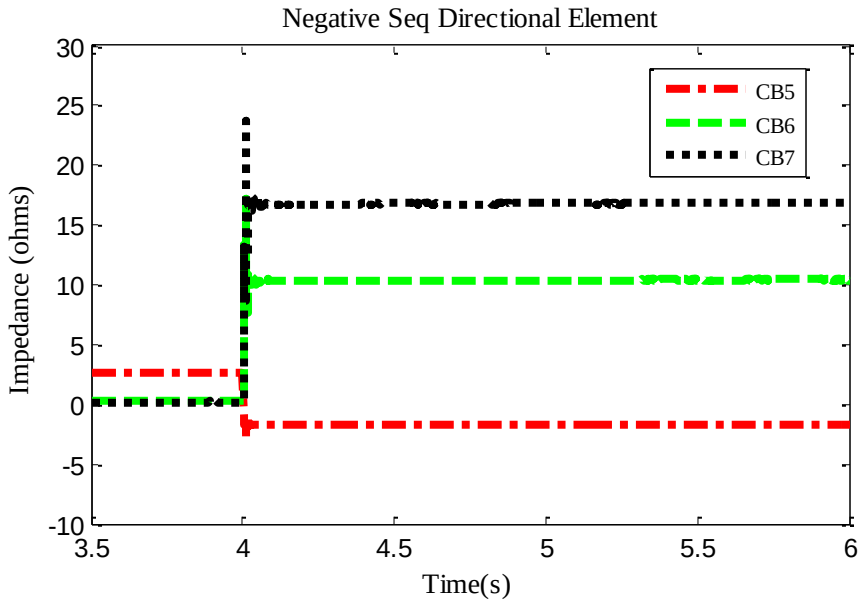

Fig. 27 Negative Sequence Elements Impedance for a B-C Fault on Feeder 2.

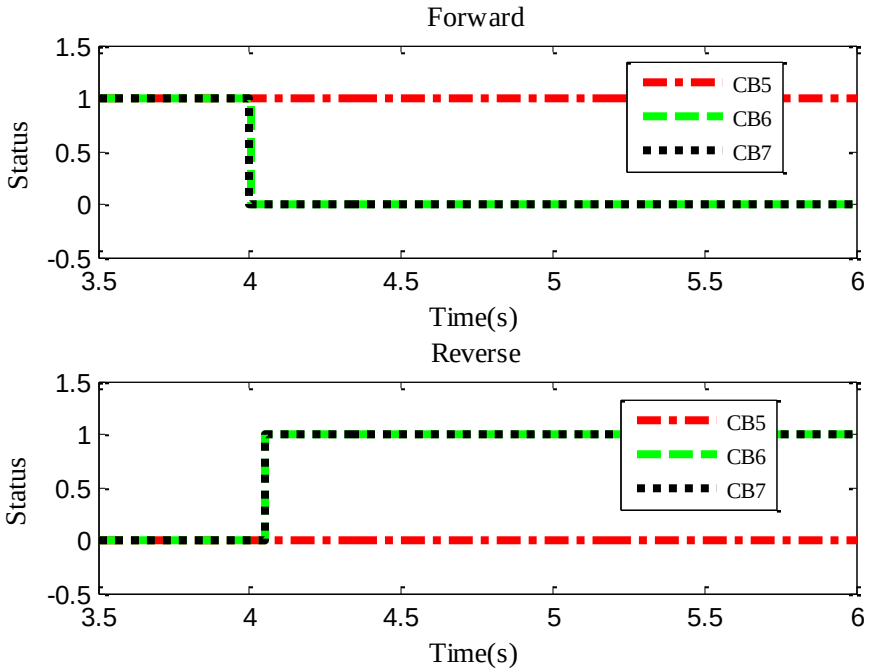

Fig. 28 Fault Direction Detection by Negative Sequence Elements for a B-C Fault on Feeder 2.

With the fault detected to be in zone 5 due to the incongruous active fault direction status of CB5 and CB6, CB5 relay at zone 5's entrance tripped the breaker. CB6 also tripped its breaker to prevent DG4 from sourcing the fault. This response is shown in Fig. 29 where both elements have their circuit breaker trip status at level "1". Since the breaker of CB7 did not trip, zone 6 and zone 7 operated together as an intentional island.

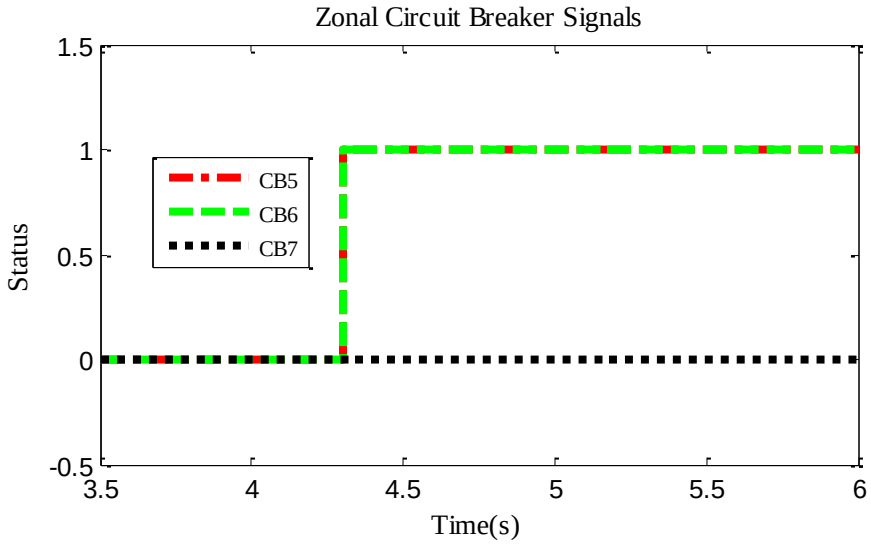

Fig. 29 Zonal Circuit Breakers Trip Status for a B-C Fault on Feeder 2.

5.3.1.3 Case 1.3: ABCN Fault on Feeder 1

This test scenario examines the response of the protection approach to a balanced three phase fault. An ABCN fault was applied between nodes 834-860 on feeder 1 of Fig. 22. The time that the fault was staged was again 4s. Fig. 30 illustrates the response of the directional elements on feeder 1. Since the fault was balanced, the positive sequence directional elements responded to make the ultimate fault direction detection decision as presented in the solution methodology. It can be noticed that the angle detected by CB1, CB2, and CB3 are positive and falls within the forward region defined

in Table 20. However, CB4 shows a negative angle in the reverse operating region. Thus, during the fault, CB4 reverse status was active (“level 1’) and the remaining boundary elements (CB1, CB2, and CB3) all had their active status as forward as shown in Fig. 31.

The reverse fault direction status of the positive sequence element of CB4 compared to the forward fault direction status of that of CB2 and CB3 when shared among their relays allowed the relays to identify the fault to be within zone 3. Therefore, CB3 tripped its breaker. Fig. 32 indicates that CB3’s breaker was the only breaker that tripped to isolate the faulted zone. Since zone 3 was the only zone that got isolated, the extent of the outage experienced by the customers on feeder 1 was reduced.

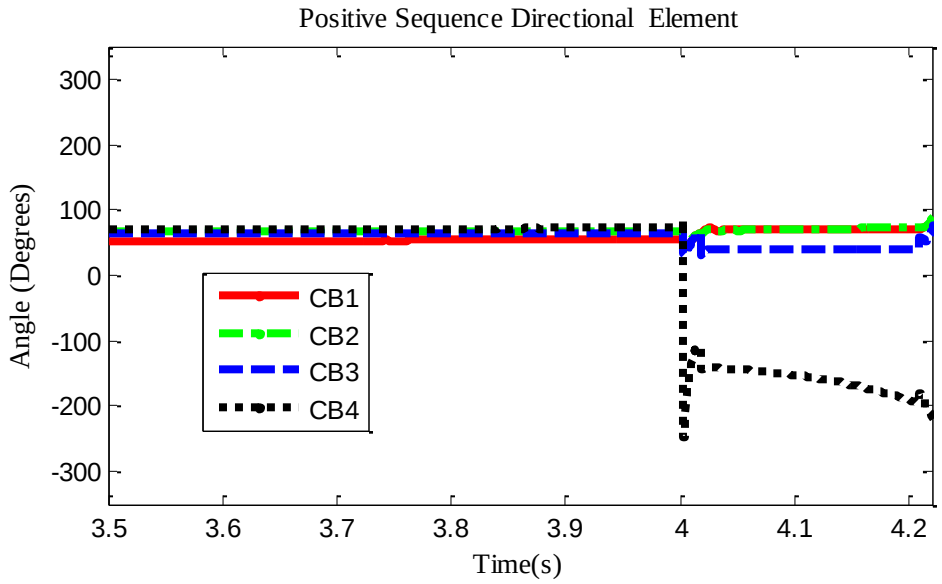

Fig. 30 Positive Sequence Elements Angles for an ABCN Fault on Feeder 1

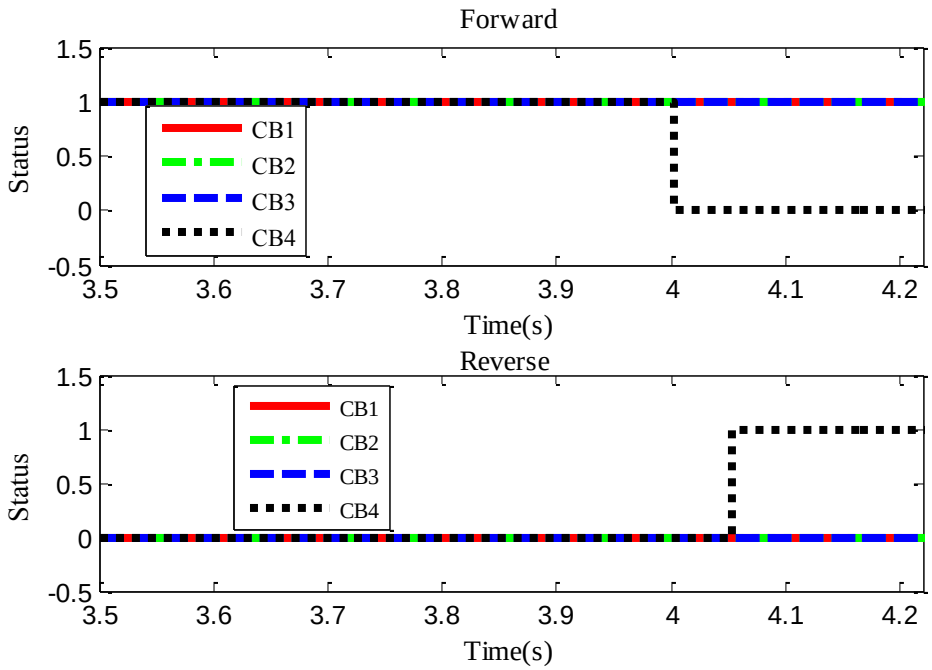

Fig. 31 Fault Direction Detection by Positive Sequence Elements for ABCN Fault on Feeder 1.

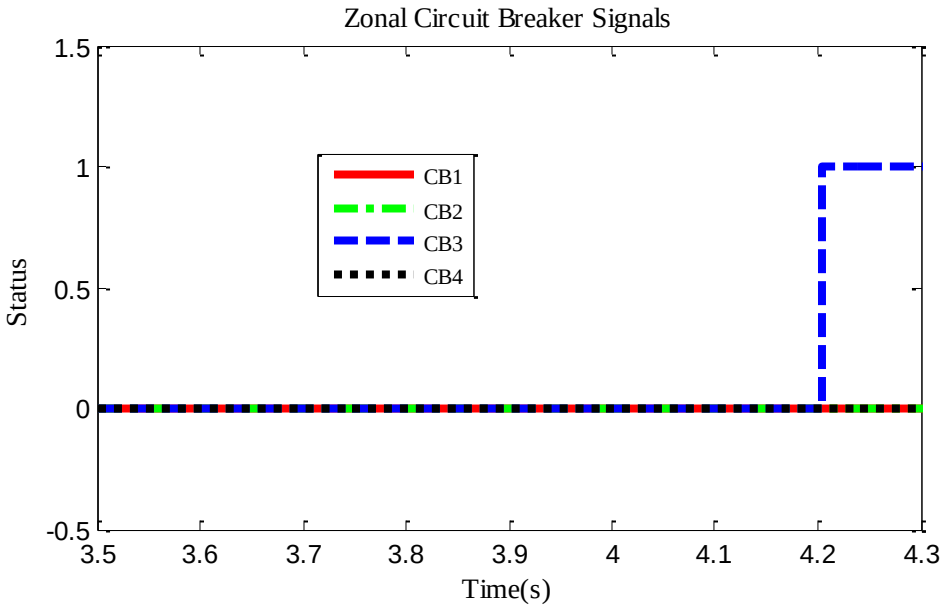

Fig. 32 Zonal Circuit Breakers Trip Status for an ABCN Fault on Feeder 1.

5.3.1.4 Case 1.4: ABCN Fault on Feeder 2

This case also shows how the protection approach performed against a balanced fault on feeder 2. An ABCN fault was applied at 4 s on the line segment between nodes 852 and 832. Fig. 33 shows the angles of the positive sequence components of the zonal boundary protective elements on feeder 2. CB6 and CB7 measured negative angles at values of -107.1 ^{0} and -123.8 ^{0}, respectively. The angle detected by CB5 was 70.07 ^{0} as depicted in Fig. 33. Consequently, CB5 detected the fault as forward while CB6 and CB7 sensed the fault as reverse. The active (level '1') fault direction status of the three zonal boundary protective elements during the fault are shown in Fig. 34. CB5 at the beginning of zone 5 compared its active fault direction status with that received from CB6 over the communication channel and subsequently caused a tripping of its breaker. CB6's breaker was also tripped to prevent the DGs in zones 6 and 7 from energizing the fault in zone 5. The breakers' trip status can be seen in Fig. 35. For this fault condition, all DGs remained connected to the system to supply the loads in zones 6 and 7.

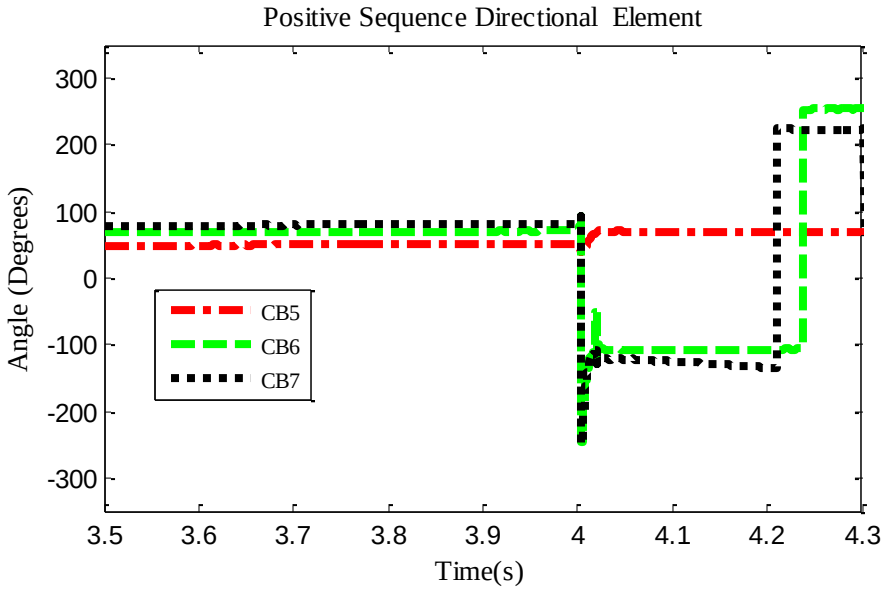

Fig. 33 Positive Sequence Elements Angles for an ABCN Fault on Feeder 2.

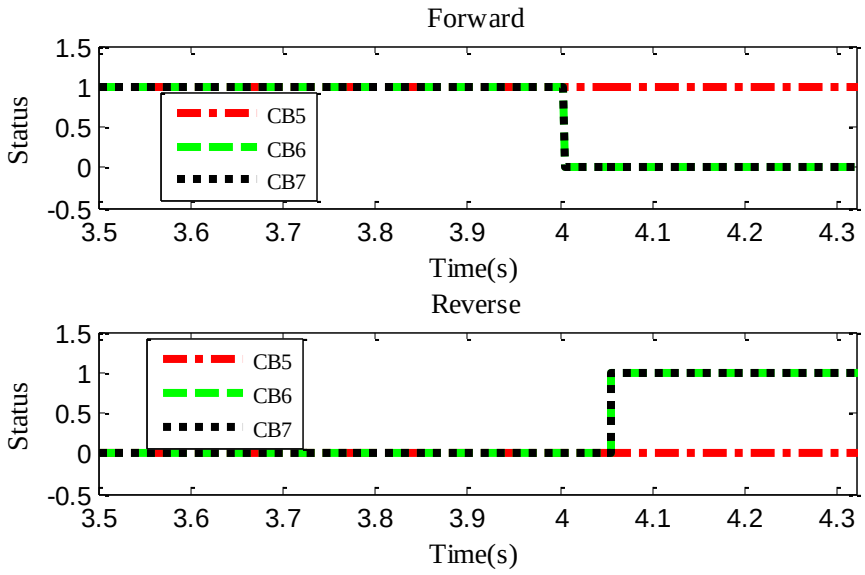

Fig. 34 Fault Direction Detection by Positive Sequence Elements for ABCN Fault on Feeder 2.

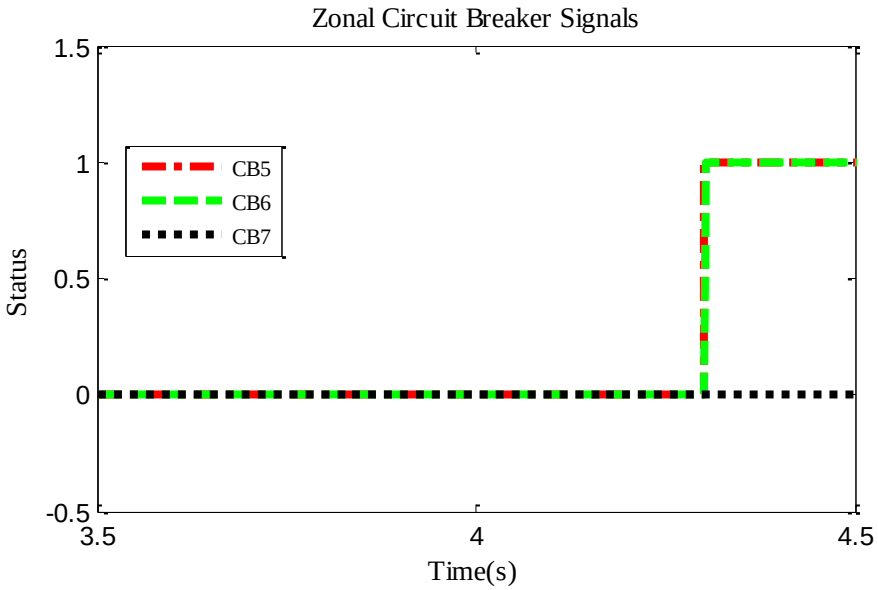

Fig. 35 Zonal Circuit Breakers Trip Status for an ABCN Fault on Feeder 2.

5.3.2 Case 2 – Exhaustive Test of Proposed Directional Overcurrent Approach

A series of tests were simulated for different fault types at different locations in the zones of the multi-feeder test system. The fault locations within a zone were selected to span the main feeder and the laterals. A given zone's faults on the main feeder were selected to be close to the entrance of the zone, at the middle, and close to the end of the zone. The results of the zonal boundary protective elements (ZBEs) fault direction detection for the staged faults are summarized in tables.

Table 21 provides the response of the ZBEs to a number of faults studied in zone 1 of the multi-feeder test system. Column 1 of the table provides the line segments on which the faults were staged. Column 2 shows the fault types simulated. Column 3 indicates the ZBEs whose negative sequence and positive sequence directional elements were monitored. The measured and expected impedances of the negative sequence directional elements of the individual ZBEs during the fault are shown in columns 4 and 5 respectively. Columns 6 and 7 provide the measured and the expected angles of the positive sequence directional elements during the fault. In columns 8 and 9, the indicated fault directions of the ZBEs are given. A "1" for either column 8 or column 9 represents the established direction during the fault. The last column shows the ZBE breakers that opened to isolate the faulted zone.

The zonal boundary elements with one asterisk signify the conditions where their measured quantity for both the positive and negative sequence elements did not corroborate each other on the fault current direction. However, the direction decision priority of the sequence elements depending on the fault type resolves the differing decisions made separately by each of these sequence elements. For instance, in Table 21, the A-N fault between nodes 820-822 caused the negative sequence element of CB2 to indicate a reverse fault (more positive impedance value as expected) while the positive sequence element detected a forward fault (angle is more than expected) as described in Table 20. The erroneous indication by the positive sequence element of CB2 was due to the relatively long distance between the fault point and the DGs. Because the fault occurred on a single phase lateral, the substation still supplied power through the

remaining healthy phases of CB2, therefore its positive sequence element recognized the current as forward. Nonetheless, for unbalanced faults, the decision of the negative sequence element has priority over the decision of the positive sequence element as discussed in the solution methodology. This caused CB2 to select the negative sequence response as its final indicated direction. Thus, CB2 indicated the fault direction as reverse since the measured impedance satisfies the conditions given in Table 20. For balanced faults, the decision of the positive sequence element has priority over the decision of the negative sequence element. Thus, for the balanced fault type simulated on the line segments for nodes 824-828 and 802-806, the positive sequence element angles were used in establishing the reverse indicated fault direction for CB2, CB3, and CB4, and the forward indicated direction for CB1. For the case shown in Table 21, the appropriated CBs opened.

Table 21 Directional Sequence Elements Response for Zone-1 Faults

Fault Loc.	**Fault Type**	**Zonal Boundary Elements**	**Negative Seq. Element Imped. (Ohms)**		**Positive Seq. Element Angle (Degrees)**		**Zonal Boundary Element Indicated Fault Direction**		**CBs opened**
			Measured	**Expected**	**Measured**	**Expected**	**Forward**	**Reverse**	
820-822	A-N	CB1	-1.72	< 0	54.3	< 162. 9	1	0	CB1 CB2
		CB2*	7.24	> 1.0	50	< -17.31	0	1	
		CB3	22.11	> 0.26	-147.58	< -17.31	0	1	
		CB4	17.72	> 0.21	-76.03	< -17.31	0	1	
808-810	B-N	CB1	7.1	< 0	74.66	< 162. 9	1	0	CB1 CB2
		CB2	23.4	> 1.0	-168.24	< -17.31	0	1	
		CB3*	19.91	> 0.26	72.01	< -17.31	0	1	
		CB4	7.1	> 0.21	-118.16	< -17.31	0	1	
806-808	C-N	CB1	-1.74	< 0	80.4	< 162. 9	1	0	CB1 CB2
		CB2	9.9	> 1.0	-162.71	< -17.31	0	1	
		CB3	46.87	> 0.26	-246.06	< -17.31	0	1	
		CB4	22.13	> 0.21	-121.3	< -17.31	0	1	
812-814	BC	CB1	-1.72	< 0	78.41	< 162. 9	1	0	CB1 CB2
		CB2	8.52	> 1.0	-150	< -17.31	0	1	
		CB3	32.48	> 0.26	-168	< -17.31	0	1	
		CB4	20.68	> 0.21	-132.38	< -17.31	0	1	

Table 21 Continued

Fault Loc.	Fault Type	Zonal Boundary Elements	Negative Seq. Element Imped. (Ohms)		Positive Seq. Element Angle (Degrees)		Zonal Boundary Element Indicated Fault Direction		CBs opened
			Measured	Expected	Measured	Expected	Forward	Reverse	
824-828	AB	CB1	-1.72	< 0	76.51	< 162. 9	1	0	CB1 CB2
		CB2	7.87	> 1.0	-149.06	< -17.31	0	1	
		CB3	30.36	> 0.26	-188.5	< -17.31	0	1	
		CB4	19.1	> 0.21	-129.35	< -17.31	0	1	
850-816	AC	CB1	-1.72	< 0	78.61	< 162. 9	1	0	CB1 CB2
		CB2	9.164	> 2.68	-161.15	< -17.31	0	1	
		CB3	41.41	> 0.26	-190.47	< -17.31	0	1	
		CB4	20.23	> 0.21	-135.53	< -17.31	0	1	
824-828	ABCN	CB1*	2.45	< 0	70.76	< 162. 9	1	0	CB1 CB2
		CB2*	1.65	> 1.0	-107.06	< -17.31	0	1	
		CB3*	0.35	> 0.26	-141.73	< -17.31	0	1	
		CB4*	0.115	> 0.21	-83.04	< -17.31	0	1	
802-806	ABCN	CB1*	2.45	< 0	49.942	< 162. 9	1	0	CB1 CB2
		CB2	1.65	> 1.0	-108.65	< -17.31	0	1	
		CB3*	0.25	> 0.26	-134.92	< -17.31	0	1	
		CB4*	0.115	> 0.21	-78.901	< -17.31	0	1	

The results of zone 2 faults are shown in Table 22. The ZBE with double asterisks in this case represented a scenario where the priority sequence element failed to produce the correct indicated fault direction. For instance, the AB fault in Table 22 represents a situation where the unbalanced fault staged was on the secondary side of the in-line transformer. Since the fault is unbalanced, the negative sequence has the higher priority is establishing the fault direction. However, the negative sequence element of CB2 incorrectly indicated the detected fault direction as reverse since the measured impedance value did not match the expected value. This erroneous indication by CB2 can be attributed to the fact that, a fault on the secondary side of the in-line transformer results in less significant contribution from the substation due to the connected generation sources. Nevertheless, the exchange of the indicated fault directions of CB1 and CB3 with that of CB2 through the use of the binary state signals ensured that the proper faulted zone, zone 2, was identified and eventually isolated.

Table 22 Directional Sequence Elements Response for Zone-2 Faults

Fault Loc.	Fault Type	Zonal Boundary Elements	Negative Seq. Element Imped. (Ohms)		Positive Seq. Element Angle (Degrees)		Zonal Boundary Element Indicated Fault Direction		CBs opened
			Measured	Expected	Measured	Expected	Forward	Reverse	
854-852	A-N	CB1	-1.75	< 0	75.87	< 162. 9	1	0	CB2 CB3 CB4
		CB2	-4.54	< 0	81.04	< 162.9	1	0	
		CB3	36.03	> 0.26	-240.77	< -17.31	0	1	
		CB4	19.18	> 0.21	-121.11	< -17.31	0	1	
852-832	B-N	CB1	-1.732	< 0	75.77	< 162. 9	1	0	CB2 CB3 CB4
		CB2	-5.07	< 0	86.54	< 162.9	1	0	
		CB3	26.9	> 0.26	-197.87	< -17.31	0	1	
		CB4	19.85	> 0.21	-130.51	< -17.31	0	1	
832-858	C-N	CB1	-1.73	< 0	76.79	< 162. 9	1	0	CB2 CB3 CB4
		CB2	-4.83	< 0	85.74	< 162.9	1	0	
		CB3	40.27	> 0.26	-180.57	< -17.31	0	1	
		CB4	21.28	> 0.21	-127.11	< -17.31	0	1	
858-834	BC	CB1	-1.74	< 0	77.87	< 162. 9	1	0	CB2 CB3 CB4
		CB2	-5.21	< 0	88.8	< 162.9	1	0	
		CB3	33.41	> 0.26	-171.42	< -17.31	0	1	
		CB4	20.33	> 0.21	-138.97	< -17.31	0	1	
888-890	AB	CB1	-1.75	< 0	60.17	< 162. 9	1	0	CB2 CB3 CB4
		CB2**	1.65	< 0	69.45	< 162.9	0	1	
		CB3	14.17	> 0.26	64.6	< -17.31	0	1	
		CB4	18.78	> 0.21	69	< -17.31	0	1	
832-858	AC	CB1	-1.74	< 0	77.85	< 162. 9	1	0	CB2 CB3 CB4
		CB2**	1.65	< 0	88.51	< 162.9	0	1	
		CB3	36.2	> 0.26	-225	< -17.31	0	1	
		CB4	20.38	> 0.21	-192.89	< -17.31	0	1	
830-854	ABCN	CB1*	2.45	< 0	70.36	< 162. 9	1	0	CB2 CB3 CB4
		CB2*	1.65	< 0	73.84	< 162.9	1	0	
		CB3	0.57	> 0.26	-128.88	< -17.31	0	1	
		CB4*	0.12	> 0.21	-84	< -17.31	0	1	
858-834	ABCN	CB1*	2.45	< 0	70.63	< 162. 9	1	0	CB2 CB3 CB4
		CB2*	1.65	< 0	73.82	< 162.9	1	0	
		CB3	0.571	> 0.26	-157.03	< -17.31	0	1	
		CB4*	0.12	> 0.21	-68.59	< -17.31	0	1	

Table 23 provides the results of the various faults in zone 3 that were studied. Again, the negative sequence component of some of the zonal boundary elements (ZBEs) did not respond appropriately to the ABCN faults as their measured values did not satisfy the expected. One asterisk is placed beside these ZBEs in the table. However, for unbalanced faults, the sequence element with the higher priority to make the indicated fault direction decisions is the positive sequence element. Thus, for the ABCN faults, the measured angles of the positive elements were equivalent to the expected angles; and therefore the appropriate faulted zone was determined by the ZBEs regardless of the negative sequence elements response.

Table 23 Directional Sequence Elements Response for Zone-3 Faults

Fault Loc.	**Fault Type**	**Zonal Boundary Elements**	**Negative Seq. Element Imped. (Ohms)**		**Positive Seq. Element Angle (Degrees)**		**Zonal Boundary Element Indicated Fault Direction**		**CB opened**
			Measured	**Expected**	**Measured**	**Expected**	**Forward**	**Reverse**	
860-836	A-N	CB1	-1.73	< 0	76.07	< 162. 9	1	0	CB3
		CB2	-4.51	< 0	82.37	< 162.9	1	0	
		CB3	-6.25	< 0	78.91	< 162.9	1	0	
		CB4	19.29	> 0.21	-124.96	< -17.31	0	1	
862-838	B-N	CB1	-1.73	< 0	72.31	< 162. 9	1	0	CB3
		CB2	-5.18	< 0	79.94	< 162.9	1	0	
		CB3	-6.87	< 0	77.67	< 162.9	1	0	
		CB4	19.71	> 0.21	-126	< -17.31	0	1	
836-840	C-N	CB1	-1.74	< 0	76.08	< 162. 9	1	0	CB3
		CB2	-4.86	< 0	84.96	< 162.9	1	0	
		CB3	-6.89	< 0	80.95	< 162.9	1	0	
		CB4	21.24	> 0.21	-125.65	< -17.31	0	1	
860-836	AB	CB1	-1.75	< 0	74.9	< 162. 9	1	0	CB3
		CB2	-4.66	< 0	80.34	< 162.9	1	0	
		CB3	-6.31	< 0	78.79	< 162.9	1	0	
		CB4	19.2	> 0.21	-128.08	< -17.31	0	1	
836-840	AC	CB1	-1.74	< 0	76.4	< 162. 9	1	0	CB3
		CB2	-4.76	< 0	82.98	< 162.9	1	0	
		CB3	-6.71	< 0	77.24	< 162.9	1	0	
		CB4	20.26	> 0.21	-137.53	< -17.31	0	1	

Table 23 Continued

Fault Loc.	Fault Type	Zonal Boundary Elements	Negative Seq. Element Imped. (Ohms)		Positive Seq. Element Angle (Degrees)		Zonal Boundary Element Indicated Fault Direction		CB opened
			Measured	Expected	Measured	Expected	Forward	Reverse	
836-862	BC	CB1	-1.73	< 0	77.28	< 162. 9	1	0	CB3
		CB2	-5.14	< 0	87.54	< 162.9	1	0	
		CB3	-7.08	< 0	81.94	< 162.9	1	0	
		CB4	20.46	> 0.21	-136.6	< -17.31	0	1	
834-860	ABCN	CB1*	2.45	< 0	70.42	< 162. 9	1	0	CB3
		CB2*	1.65	< 0	74..53	< 162.9	1	0	
		CB3	-0.6	< 0	55	< 162.9	1	0	
		CB4	3.94	> 0.21	-182.27	< -17.31	0	1	
836-840	ABCN	CB1*	2.45	< 0	70.42	< 162. 9	1	0	CB3
		CB2*	1.65	< 0	74.53	< 162.9	1	0	
		CB3	-0.6	< 0	55	< 162.9	1	0	
		CB4	3.5	> 0.21	-222.27	< -17.31	0	1	

Table 24 provides the results of zone 4 staged faults. The ZBEs with one asterisk again indicate the conditions where their positive sequence directional element response and their negative sequence directional response did not corroborate each other on the fault direction. As an example, the measured impedance of CB1 did not match the expected value, while the measured angle matched the expected value. Since the measured angle matched the expected value, and it is the response of the positive sequence element that has the higher priority for this fault condition, CB1 correctly indicated the detected fault direction as forward as described in Table 20. The double asterisks by CB2 show the scenario where its higher priority directional sequence element (negative sequence) for that fault type produced the wrong detected fault direction. This is because its measured impedance did not satisfy the condition for a forward fault direction. Nonetheless, the exchange of the fault current direction information of CB1 and CB3 with CB4 caused the tripping of the desired circuit breaker.

Table 24 Directional Sequence Elements Response for Zone-4 Faults

Fault Loc.	Fault Type	Zonal Boundary Elements	Negative Seq. Element Imped. (Ohms)		Positive Seq. Element Angle (Degrees)		Zonal Boundary Element Indicated Fault Direction		CB opened
			Measured	Expected	Measured	Expected	Forward	Reverse	
846-848	A-N	CB1	-1.74	< 0	76.3	< 162. 9	1	0	CB4
		CB2	-5.08	< 0	86.53	< 162.9	1	0	
		CB3	27.19	> 0.26	-195.39	< -17.31	0	1	
		CB4	-4.46	< 0	84.48	< 162.9	1	0	
844-846	B-N	CB1	-1.73	< 0	76.38	< 162. 9	1	0	CB4
		CB2	-4.58	< 0	81.67	< 162.9	1	0	
		CB3	38.04	> 0.26	-217.97	< -17.31	0	1	
		CB4	-4.48	< 0	79.41	< 162.9	1	0	
842-844	C-N	CB1	-1.73	< 0	76.74	< 162. 9	1	0	CB4
		CB2	-4.81	< 0	85.92	< 162.9	1	0	
		CB3	39.8	> 0.26	-177.81	< -17.31	0	1	
		CB4	-4.863	< 0	79.67	< 162.9	1	0	
844-846	BC	CB1	-1.73	< 0	77.684	< 162. 9	1	0	CB4
		CB2	-5.18	< 0	88.47	< 162.9	1	0	
		CB3	33.34	> 0.26	-173.12	< -17.31	0	1	
		CB4	-4.86	< 0	82.94	< 162.9	1	0	
846-848	AB	CB1	-1.73	< 0	76.65	< 162. 9	1	0	CB4
		CB2**	1.65	< 0	90	< 162.9	0	1	
		CB3	28.22	> 0.26	-200	< -17.31	0	1	
		CB4	-3.78	< 0	94.8	< 162.9	1	0	
842-844	AC	CB1	-1.75	< 0	76.54	< 162. 9	1	0	CB4
		CB2	-4.72	< 0	84.14	< 162.9	1	0	
		CB3	40	> 0.26	-187.8	< -17.31	0	1	
		CB4	-4.72	< 0	73.29	< 162.9	1	0	
842-844	ABCN	CB1*	2.45	< 0	70.75	< 162. 9	1	0	CB4
		CB2*	1.65	< 0	74.15	< 162.9	1	0	
		CB3*	0.165	> 0.26	-200	< -17.31	0	1	
		CB4*	0.012	< 0	48.49	< 162.9	1	0	
846-848	ABCN	CB1*	2.45	< 0	71.02	< 162. 9	1	0	CB4
		CB2*	1.65	< 0	74.72	< 162.9	1	0	
		CB3	0.73	> 0.26	-214.31	< -17.31	0	1	
		CB4*	4.58	< 0	63.08	< 162.9	1	0	

Similar fault types at various locations were studied on feeder 2 zones of the multi-feeder test system. The main feeder fault locations were again selected to be close to the zones entrances', the middle, and the end of the zones. Table 25 shows the results for the fault cases simulated in zone 5. From the table, it can be seen that all the measured values of the directional sequence elements for the unbalanced faults met the expected values. However, because the negative sequence directional elements assume the higher priority for these fault types, the indicated fault directions were determined based on the negative sequence element using the conditions in Table 20. The ZBEs with the one asterisk represents the fault conditions where their negative sequence element did not respond correctly. However, the higher priority of the positive sequence element for these fault types ensured that the indicated fault directions by the ZBEs were correct.

Table 25 Directional Sequence Elements Response for Zone-5 Faults

Fault Loc.	Fault Type	Zonal Boundary Elements	Negative Seq. Element Imped. (Ohms)		Positive Seq. Element Angle (Degrees)		Zonal Boundary Element Indicated Fault Direction		CBs opened
			Measured	Expected	Measured	Expected	Forward	Reverse	
812-814	A-N	CB5	-1.74	< 0	71	< 162.9	1	0	CB5 CB6
		CB6	10.6	> 0.32	-182.47	< -17.3	0	1	
		CB7	18.81	> 0.21	-218	< -17.3	0	1	
808-810	B-N	CB5	-1.74	< 0	70.51	< 162.9	1	0	CB5 CB6
		CB6	8.55	> 0.32	-104.18	< -17.3	0	1	
		CB7	12.82	> 0.21	-237.28	< -17.3	0	1	
852-854	C-N	CB5	-1.78	< 0	72.57	< 162.9	1	0	CB5 CB6
		CB6	12.01	> 0.32	-157.36	< -17.3	0	1	
		CB7	20.54	> 0.21	-181.89	< -17.3	0	1	
852-832	AB	CB5	-1.74	< 0	74.31	< 162.9	1	0	CB5 CB6
		CB6	9.73	> 0.32	-161.18	< -17.3	0	1	
		CB7	16.32	> 0.21	-181.26	< -17.3	0	1	
808-812	AC	CB5	-1.72	< 0	79.67	< 162.9	1	0	CB5 CB6
		CB6	11.51	> 0.32	-163.96	< -17.3	0	1	
		CB7	20.85	> 0.21	-182.18	< -17.3	0	1	
828-830	BC	CB5	-1.74	< 0	76.24	< 162.9	1	0	CB5 CB6
		CB6	10.51	> 0.32	-180.56	< -17.3	0	1	
		CB7	17.63	> 0.21	-198.8	< -17.3	0	1	

Table 25 Continued

Fault Loc.	Fault Type	Zonal Boundary Elements	Negative Seq. Element Imped. (Ohms)		Positive Seq. Element Angle (Degrees)		Zonal Boundary Element Indicated Fault Direction		CBs opened
			Measured	Expected	Measured	Expected	Forward	Reverse	
806-808	ABCN	CB5*	3.42	< 0	70.02	< 162.9	1	0	CB5 CB6
		CB6*	0.27	> 0.32	-108.61	< -17.3	0	1	
		CB7*	0.67	> 0.21	-132.16	< -17.3	0	1	
888-890	ABCN	CB5*	3.42	< 0	63.71	< 162.9	1	0	CB5 CB6
		CB6*	0.27	> 0.32	-171.37	< -17.3	0	1	
		CB7*	0.67	> 0.21	-200	< -17.3	0	1	

Table 26 shows the result of the various faults simulated in zone 6. Column 1 provides the line segments where the faults were staged. Column 2 shows the simulated fault type. Columns 4 and 5, respectively, indicate the measured and expected impedances of the negative sequence directional component for the individual zonal boundary elements given in column 3. Columns 6 and 7 correspondingly provide their positive sequence directional elements measured and expected angles. Column 8 provides the indicated forward fault direction during the fault. Column 9 provides the indicated reverse fault direction during the fault. A “1” in either column 8 or column 9 shows the identified fault direction by the CBs. Finally, column 10 provides the zonal protective circuit breakers that were tripped to isolate the faulted zone. The one asterisk represents the conditions where the positive sequence element rather than the negative sequence element indicated the correct fault direction and consequently the faulted zone.

Table 26 Directional Sequence Elements Response for Zone-6 Faults

Fault Loc.	Fault Type	Zonal Boundary Elements	Negative Seq. Element Imped. (Ohms)		Positive Seq. Element Angle (Degrees)		Zonal Boundary Element Indicated Fault Direction		CBs opened
			Measured	Expected	Measured	Expected	Forward	Reverse	
858-864	A-N	CB5	-1.74	< 0	73.93	< 162.9	1	0	CB6 CB7
		CB6	-5.83	< 0	81.95	< 162.9	1	0	
		CB7	19.83	> 0.21	-187.44	< -17.3	0	1	
846-848	B-N	CB5	-1.72	< 0	73.99	< 162.9	1	0	CB6 CB7
		CB6	-5.7	< 0	82.44	< 162.9	1	0	
		CB7	19.62	> 0.21	-186.15	< -17.3	0	1	
834-842	C-N	CB5	-1.75	< 0	75.16	< 162.9	1	0	CB6 CB7
		CB6	-6.41	< 0	86.87	< 162.9	1	0	
		CB7	19.56	> 0.21	-187.56	< -17.3	0	1	
844-846	AB	CB5	-1.75	< 0	73.33	< 162.9	1	0	CB6 CB7
		CB6	-5.78	< 0	84.44	< 162.9	1	0	
		CB7	16.34	> 0.21	-175.53	< -17.3	0	1	
846-848	AC	CB5	-1.74	< 0	74.98	< 162.9	1	0	CB6 CB7
		CB6	-6.08	< 0	83.9	< 162.9	1	0	
		CB7	19.87	> 0.21	-182.01	< -17.3	0	1	
842-844	BC	CB5	-1.74	< 0	76.2	< 162.9	1	0	CB6 CB7
		CB6	-4.94	< 0	98.73	< 162.9	1	0	
		CB7	19.08	> 0.21	-190.99	< -17.3	0	1	
846-848	ABCN	CB5*	3.42	< 0	69.57	< 162.9	1	0	CB6 CB7
		CB6*	0.27	< 0	74.85	< 162.9	1	0	
		CB7*	0.16	> 0.21	-212.15	< -17.3	0	1	
858-834	ABCN	CB5*	3.42	< 0	69.95	< 162.9	1	0	CB6 CB7
		CB6*	0.27	< 0	51.17	< 162.9	1	0	
		CB7*	0.29	> 0.21	-108.21	< -17.3	0	1	

Table 27 provides the results of zone 7 faults. Again, the zonal boundary elements, ZBEs, with one asterisk were for the faults conditions where the high priority directional sequence element (positive sequence under this case) resulted in determining the correct fault direction.

Table 27 Directional Sequence Elements Response for Zone-7 Faults

Fault Loc.	Fault Type	Zonal Boundary Elements	Negative Seq. Element Imped. (Ohms)		Positive Seq. Element Angle (Degrees)		Zonal Boundary Element Indicated Fault Direction		CB opened
			Measured	Expected	Measured	Expected	Forward	Reverse	
860-836	A-N	CB5	-1.73	< 0	74.21	< 162.9	1	0	CB7
		CB6	-5.7	< 0	82.15	< 162.9	1	0	
		CB7	-4.82	< 0	89.7	< 162.9	1	0	
862-838	B-N	CB5	-1.72	< 0	71.76	< 162.9	1	0	CB7
		CB6	-6.4	< 0	84.11	< 162.9	1	0	
		CB7	-5.19	< 0	82.76	< 162.9	1	0	
836-862	C-N	CB5	-1.72	< 0	74.57	< 162.9	1	0	CB7
		CB6	-6.37	< 0	86.19	< 162.9	1	0	
		CB7	-5.3	< 0	84.71	< 162.9	1	0	
860-836	AB	CB5	-1.72	< 0	73.44	< 162.9	1	0	CB7
		CB6	-6.4	< 0	83.44	< 162.9	1	0	
		CB7	-4.755	< 0	81.88	< 162.9	1	0	
836-840	AC	CB5	-1.72	< 0	75.74	< 162.9	1	0	CB7
		CB6	-6.4	< 0	82.89	< 162.9	1	0	
		CB7	-5.03	< 0	80.03	< 162.9	1	0	
836-862	BC	CB5	-1.75	< 0	75.16	< 162.9	1	0	CB7
		CB6	-6.61	< 0	88.97	< 162.9	1	0	
		CB7	-5.41	< 0	85.7	< 162.9	1	0	
860-836	ABCN	CB5*	3.42	< 0	69.5	< 162.9	1	0	CB7
		CB6*	0.27	< 0	64.4	< 162.9	1	0	
		CB7*	0.16	< 0	57.36	< 162.9	1	0	
836-862	ABCN	CB5*	3.42	< 0	69.09	< 162.9	1	0	CB7
		CB6*	0.27	< 0	59.59	< 162.9	1	0	
		CB7*	0.15	< 0	48.38	< 162.9	1	0	

5.4 Summary of Results

The implemented protection approach modifies the method for isolating faulted zones in [27] and [28] by decentralizing the control of the zonal boundary breakers. Single phase, double phase, and three-phase faults were staged at the various line segments spanning the beginning, the middle, and the end of the individual zones of the multi-feeder test system.

For some of the simulated fault types, the negative sequence directional element and the positive sequence directional element of the zonal boundary elements (ZBEs)

indicated opposing fault directions. These conditions occurred for three-phase faults simulated in all zones of the multi-feeder test system. For these faults, the measured negative sequence directional element impedance values of the ZBEs did not match the expected impedance values. On the other hand, the positive sequence directional element angles for the ZBEs matched the expected angle values. The erroneous response of the negative sequence directional element is due to the negligible negative sequence voltage and currents produced for three phase faults. Other fault types that showed a similar discrepancy included the A-N and B-N faults in zone 1. For these two faults, it was rather the measured angles of the positive sequence directional elements of CB2 and CB3 that did not match the expected angle values. Because the A-N and B-N faults occurred on a single phase lateral, power continued to flow through the remaining healthy phases of CB2 and CB3 during the fault, thereby causing their positive sequence directional elements to recognize the fault as forward instead of reverse. However, of the two directional sequence elements (positive and negative), the one with the higher priority for the particular fault type was able to determine the correct fault direction, resulting in the isolation of the appropriate faulted zone.

For other fault types, the higher priority directional sequence element indicated an incorrect fault direction. This happened to the negative sequence directional element of CB2 for AB and AC faults staged in zone 2, and an AB fault staged in zone 4. The AB fault in zone 2 was on the secondary side of the in-line transformer while the zone 2 AC fault and the zone 4 AB fault were at locations relatively distant from CB2. The incorrect fault direction by the negative sequence element of CB2 for a fault on the secondary side of the in-line transformer or at the distant locations is as a result of the small contribution from the substation due to the DGs connections. The small contribution from the substation resulted in less fault current flowing through CB2, thereby causing CB2 to indicate an incorrect fault direction. Notwithstanding these challenges, the fact that the indicated fault direction decisions of CB1, CB3, and CB4 is shared with CB2 using binary state signals resulted in the proper isolation of the faulted zone.

The exhaustive fault types simulated at the various locations of the individual zones of the multi-feeder test system shows that the protection approach worked for a large number of the faults by selectively identifying the correct fault direction to cause the eventual isolation of the faulted zones.

5.5 Proposed Methodology for Smart Meter Data Usage for Overcurrent Protection

Distribution customers can be classified as residential, commercial or industrial. Each of these customers may be supplied by a primary circuit protected by a relay. The power that flows through the relay may be made available to the customers through a secondary distribution transformer depending on the customers' voltage utilization level. In a smart distribution grid, it is expected that distribution customers will have smart meters installed at their facility. The proposed methodology for smart meter data usage for OC protection is to be applied to the substation relay after the zonal boundary protective elements has operated to isolate the faulted zones downstream the zone of the multi-feeder test system whose main supply is from the substation. The method, therefore, seeks to aggregate the individual customer load demand from the smart meter measurements for each secondary transformer in the unfaulted zone connected to the substation and eventually determine the demand the flows through the substation relay. This technique is to help determine the demand pattern over a given time duration for the substation OC protective relay. The pickup setting of the substation relay is then adapted over a day depending on the maximum loading levels identified from the demand pattern obtained using the smart meter measurements from the previous day. The steps below outline the proposed methodology for using the smart meter load demand measurements.

1. Obtain the individual customer, i, power demands as recorded by the smart meter over a given time interval. For this work, 30-minute demand over a 24-hour period was assumed. Most manufactured smart meters are capable of providing this information to the AMI headend. Equation (9) shows the customer power demands in vector form.

$$\mathbf{H}_i(\Delta t) = \begin{bmatrix} D(\Delta t_1) \\ D(\Delta t_2) \\ D(\Delta t_3) \\ \vdots \\ D(\Delta t_m) \end{bmatrix}_{m\times 1} \quad \text{kW} \tag{9}$$

$\mathbf{H}_i(\Delta t)$ = Customer i's power demand vector over the selected time interval

D = 30-minute power demand

Δt = 30-minute interval

m = Number of 30-minute intervals over a 24-hour time duration

2. Compute the 30-minute diversified demand for each phase of the secondary transformer, k, serving a group of customers, using the demands acquired in step 1 using (10).

$$\mathbf{T}_k^p(\Delta t) = \left[\sum_{i=1}^{n} \mathbf{H}_i(\Delta t) \right]_{m\times 1} \quad \text{kW} \tag{10}$$

$\mathbf{T}_k$ = Transformer k's 30-minute diversified demand vector of size m x 1

p = phase of transformer

n = Number of customers fed by transformer

3. Sum the 30-minute diversified demands for each phase of the secondary transformers over the corresponding time intervals to obtain the demand seen by the relay at the substation using (11). Since a distribution system may have several laterals of various phases, the diversified demand for each phase of the transformers serving the customers on a particular lateral is determined, and then added to the corresponding phase of the diversified demands of the transformers on the main feeder in order to obtain the demand seen by the substation relay.

$$\mathbf{R}(\Delta t) = \left[\sum_{k=1}^{N} \left[\mathbf{T}^{p}_{main,\,k}(\Delta t)\right] + \sum_{k=1}^{M} \left[\mathbf{T}^{p}_{lat,\,k}(\Delta t)\right] \right]_{m\times 1} \text{ kW} \tag{11}$$

$\mathbf{R}(\Delta t)$ = Relay demand vector of size m x 1

$\mathbf{T}^{p}_{main}$ = Main feeder transformer 30-minute diversified demand

$\mathbf{T}^{p}_{lat}$ = Lateral transformer 30-minute diversified demand

N = Number of main feeder transformers fed by substation

M = Number of lateral transformers fed by substation

p = phase of transformer

4. Divide the relay demand vector over the 24-hour time duration into two time intervals, 12-hours each, using (12). This results in a vector of size m/2 x 1.

$$\text{First 12-hour Interval, } \mathbf{R}_1(\Delta t) = [\mathbf{R}(\Delta t)]_{\frac{m}{2}\times 1} = \begin{bmatrix} \mathbf{R}(\Delta t_1) \\ \mathbf{R}(\Delta t_2) \\ \vdots \\ \vdots \\ \mathbf{R}(\Delta t_{\frac{m}{2}}) \end{bmatrix} \tag{12}$$

$$\text{Second 12-hour Interval, } \mathbf{R}_2(\Delta t) = [\mathbf{R}(\Delta t)]_{\frac{m}{2}\times 1} = \begin{bmatrix} \mathbf{R}(\Delta t_{\frac{m}{2}+1}) \\ \vdots \\ \vdots \\ \vdots \\ \mathbf{R}(\Delta t_m) \end{bmatrix}$$

5. Determine the maximum diversified demand in each time interval of step 4 using (13).

$$M_1 = \max(\mathbf{R}_1(\Delta t)) \qquad M_2 = \max(\mathbf{R}_2(\Delta t)) \tag{13}$$

M_1 = maximum diversified in first 12-hour time interval

M_2 = maximum diversified in second 12-hour time interval

6. Set the substation's phase overcurrent relay pickup value as 1.5 times the corresponding current of the maximum diversified demand in each time interval using (14).

$$I_{p1} = 1.5 \times I(M_1) \qquad I_{p2} = 1.5 \times I(M_2) \tag{14}$$

I_{p1} = pickup setting for first 12-hour interval

I_{p2} = pickup setting for second 12-hour interval

$I(M_1)$ = Corresponding current of M_1

$I(M_2)$ = Corresponding current of M_2

Step 1 is readily obtainable in most commercial smart meters. Commercial smart meters have the capability to be programmed to compute the customer demand at selectable intervals of 5, 10, 15, 20, 30 and 60 minutes [46]. Steps 2 to 6 are expected to be handled by the computing facilities at the AMI headend. The assumptions made in this solution methodology are:

1. The customers' energy usage pattern has been carefully monitored and understood over the given time duration.
2. The two 12-hour time interval divisions are as a result of the customers' energy usage peaking in the morning and in the evening.
3. In setting the pickup value for each 12-hour time interval, the previous day's maximum diversified demand during that interval is used. The assumption is that the utility's prediction of the current day's power demands using the information from the smart meters for the previous day is relatively consistent with the previous day.

The proposed methodology can be illustrated using the example radial distribution feeder shown in Fig. 36. On the mains of the feeder are two secondary transformers serving a total of 8 customers. Transformer 1, T1, between nodes 3 and 4 supplies the distributed load customers H1-H4. Transformer 2, T2, supplies customers

H5-H8. The feeder has a single phase lateral between nodes 6 to 8 with a secondary transformer T3, supplying the distributed load customers H9 and H10. Each customer shown is considered to be on the same phase of the secondary distribution transformers and have a smart meter installed at their site. The following steps outline the procedure:

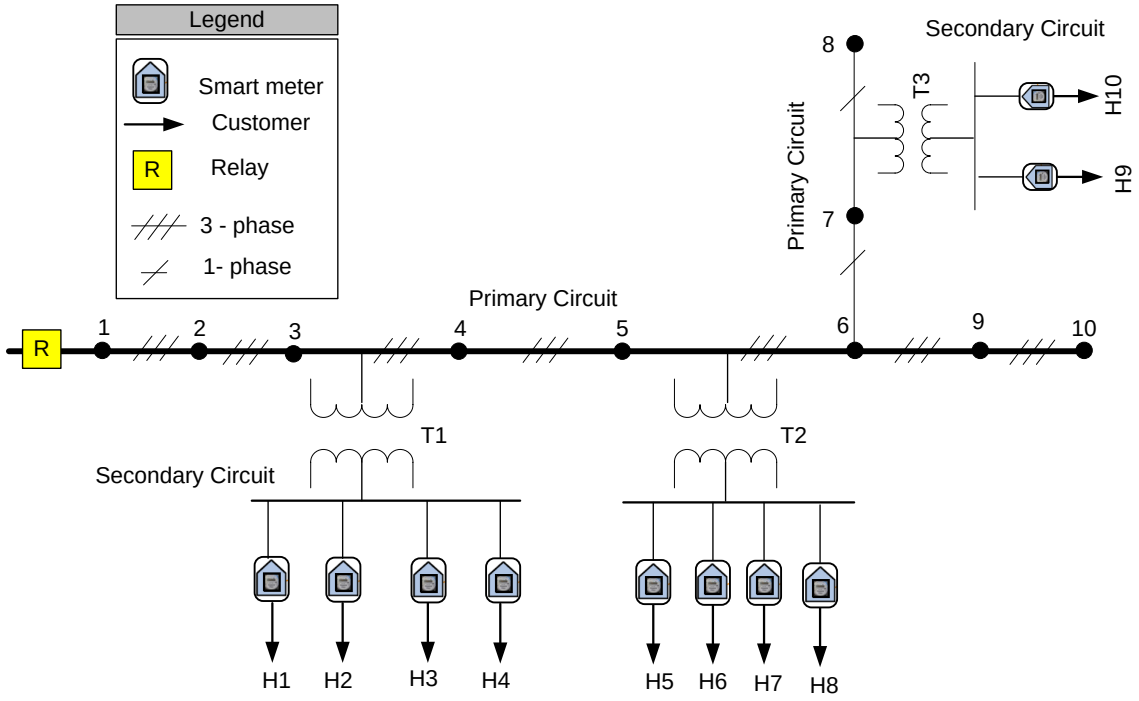

Fig. 36 A Simple Radial Distribution Feeder to Illustrate Smart Meter Information Usage.

Step 1: The smart meter demand measurements of customers are obtained as described in section 3.4. Let the sample 30-minute, Δt, demand measurements obtained from the smart meters for customers H1 to H4 over a 24-hour time duration be as given in Fig. 37, Fig. 38, Fig. 39, and Fig. 40 respectively.

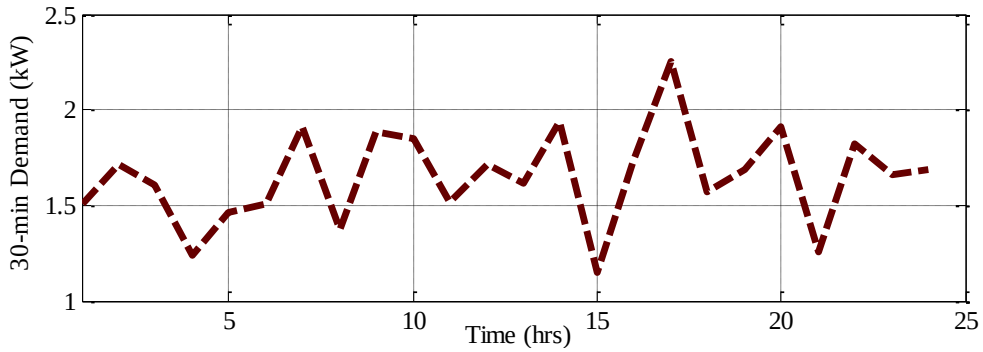

Fig. 37 A Sample 30-minute Demand Measurements for Customer #1

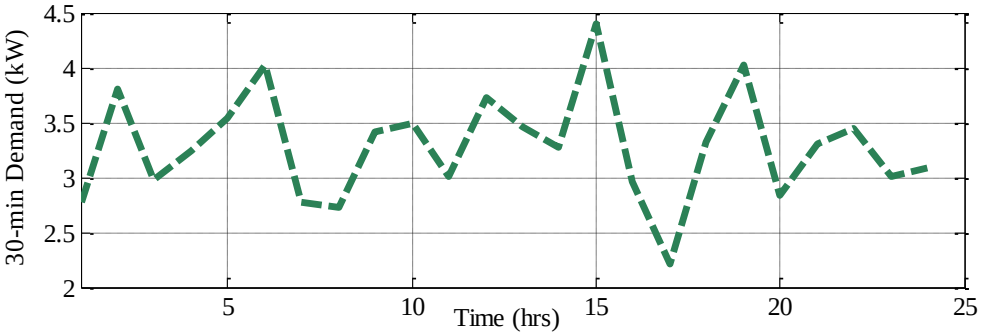

Fig. 38 A Sample 30-minute Demand Measurements for Customer #2

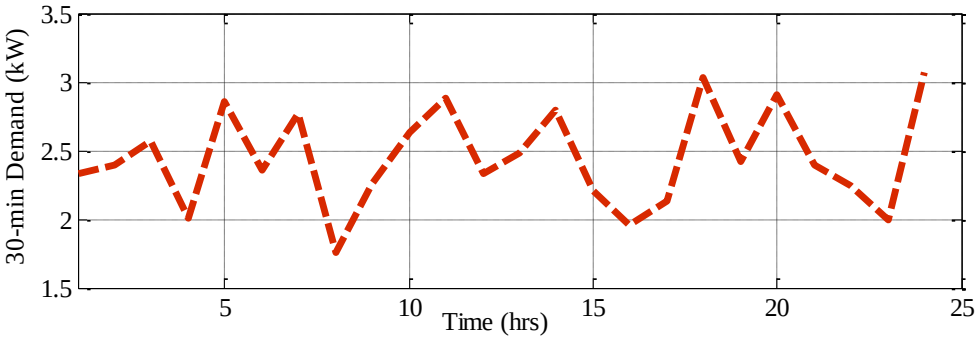

Fig. 39 A Sample 30-minute Demand Measurements for Customer #3

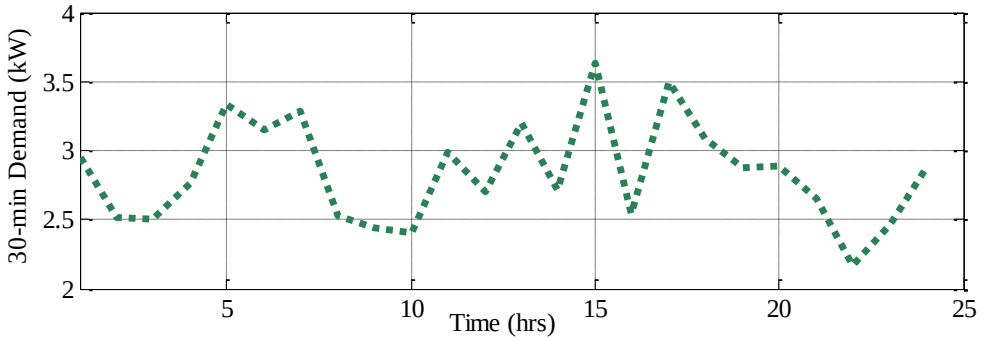

Fig. 40 A Sample 30-minute Demand Measurements for Customer #4

Step 2: Transformer 1 diversified demand for its four customers (H1-H4) is obtained by summing the corresponding 30-minute demands of the customers using (10). The resultant diversified demand vector for T1 is shown as a curve in Fig. 41. The diversified demand vector curves for transformers T2 and T3 is obtained from similar samples of 30-minute demand measurements by the smart meters located at their respective customer locations and applying (10). Fig. 42 and Fig. 43 respectively show the diversified demand for transformer 2 and transformer 3 obtained from a sample demand measurements of their customers smart meters.

$$\mathbf{T}_1^{a}(\Delta t) = \sum_{i=1}^{4} \mathbf{H}_i(\Delta t) = \mathbf{H}_1(\Delta t) + \mathbf{H}_2(\Delta t) + \mathbf{H}_3(\Delta t) + \mathbf{H}_4(\Delta t)$$

$$\mathbf{T}_2^{a}(\Delta t) = \sum_{i=1}^{4} \mathbf{H}_i(\Delta t) = \mathbf{H}_5(\Delta t) + \mathbf{H}_6(\Delta t) + \mathbf{H}_7(\Delta t) + \mathbf{H}_8(\Delta t)$$

$$\mathbf{T}_3^{a}(\Delta t) = \sum_{i=1}^{2} \mathbf{H}_i(\Delta t) = \mathbf{H}_9(\Delta t) + \mathbf{H}_{10}(\Delta t)$$

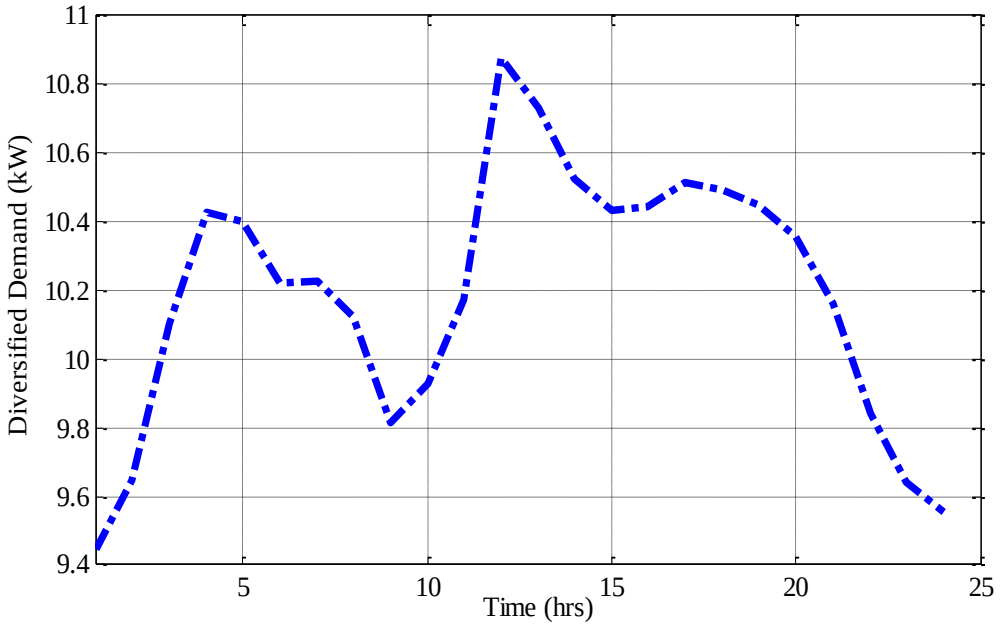

Fig. 41 Transformer 1 Diversified Demand Curve

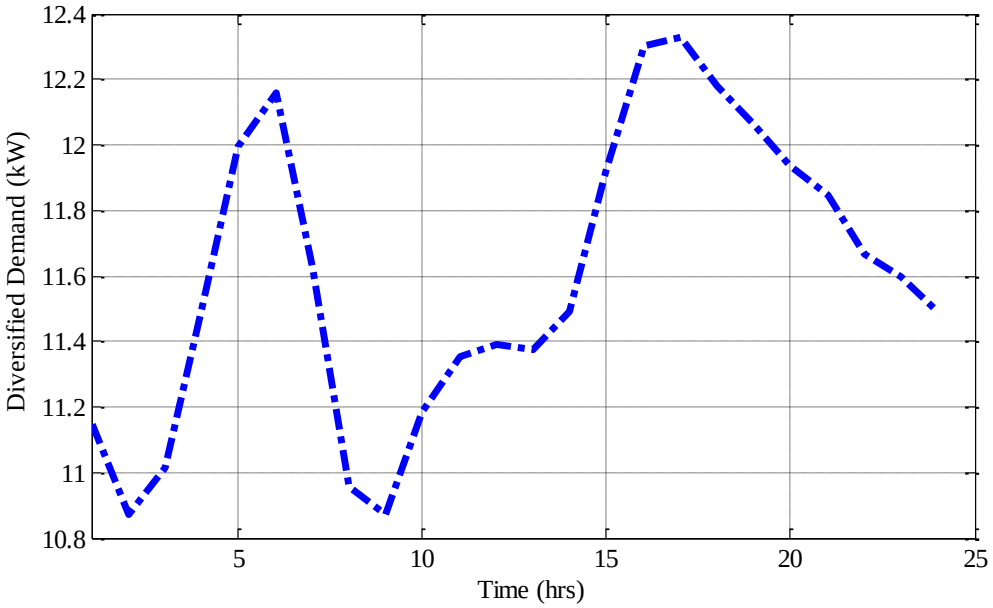

Fig. 42 Transformer 2 Diversified Demand Curve

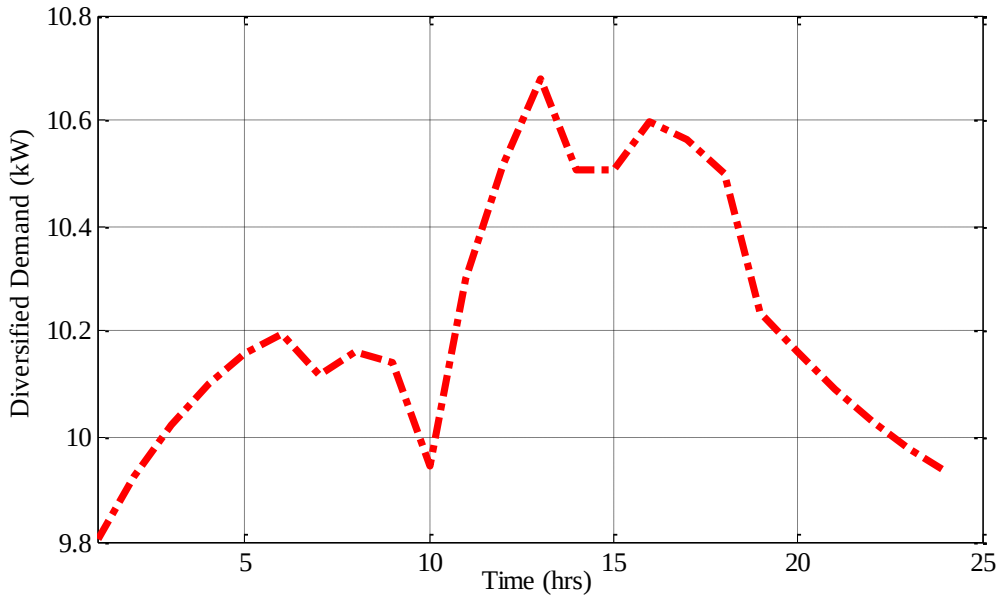

Fig. 43 Transformer 3 Diversified Demand Curve

Step 3: The demand seen by the substation relay, R, on the primary circuit of Fig. 36 over the 24-hour time interval is determined using (11). Fig. 44 shows the demand curve of the relay. The demand seen by the relay varies from hour-to-hour, which is a representative of a typical distribution load variation pattern.

$$\mathbf{R}(\Delta t) = \sum_{k=1}^{2} \left[\mathbf{T}^{p}_{main,\,k}(\Delta t)\right] + \sum_{k=1}^{1} \left[\mathbf{T}^{p}_{lat,\,k}(\Delta t)\right]$$

$$\mathbf{R}(\Delta t) = \left[\, \mathbf{T}^{a}_{1}(\Delta t) + \mathbf{T}^{a}_{2}(\Delta t) \,\right] + \left[\mathbf{T}^{a}_{3}(\Delta t) \,\right]$$

Steps 4 and 5: The 24-hour time interval is divided into the two 12-hour intervals as proposed in the solution methodology. The maximum diversified demand for each interval is determined as shown in Fig. 44.

Step 6: The pickup value of the relay is set as 1.5 times the current corresponding to the maximum diversified demands in each of the two time intervals. This current can be obtained by taken a ratio of the maximum diversified demand power to the primary relay voltage or running an offline load flow using the maximum diversified powers. Assuming the demand at the relay has been established to follow the pattern in Fig. 44, then before the commencement of each time interval for the next day, the relay pickup setting is updated to reflect the maximum diversified demand expected within that time interval.

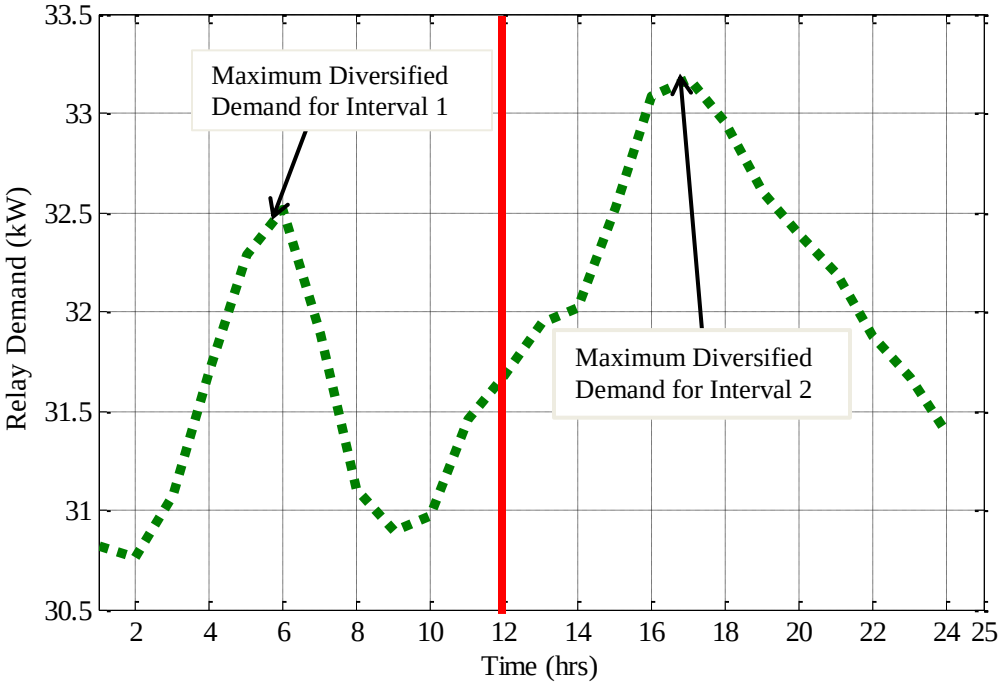

Fig. 44 Relay Demand Curve over a 24-hour Time Interval

5.5.1 Secondary Level Distribution Design for Multi-feeder Test system

The secondary level of the multi-feeder test system was configured as either a common secondary main transformer or a single service individual transformer. Common secondary main transformer feed a group of residential customers. The single service individual transformers were modeled to feed a single commercial or industrial customer or a single residential customer depending on the mean displacement obtained using (4). Fig. 45 shows the secondary distribution design using the customers between nodes 860-836 for feeder 1 and feeder 2, as an example. From the groupings in Table 11, one common secondary transformer (Transformer 1) supplied 12 residential customers and another transformer, T2, supplied the remaining 4 residential customers. The selected voltages for the secondary level were 120/240V single phase, or 277/480V three phase, which is typical of the United States. The connection of the commercial load at node 860 was made at the primary node point using the single service transformer configuration (Transformer 3). The service for customers is monitored via the smart meters as shown in the figure.

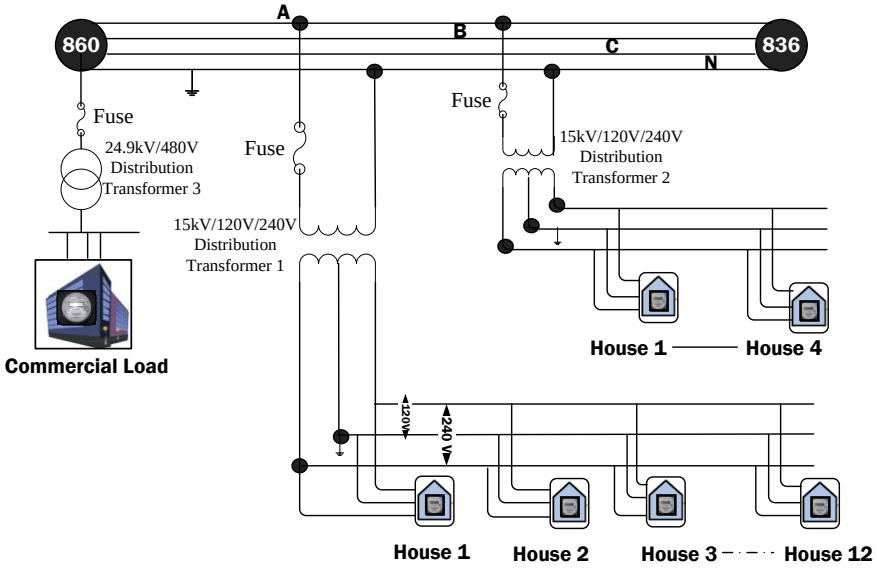

Fig. 45 Secondary Distribution Design between Nodes 860 and 836 for Feeder 1 and Feeder 2

5.6 Simulation Cases for Smart Meter Data Usage

The methodology outlined in section 5.5 was tested on the substation relay on the multi-feeder test system through simulation studies performed in PSCAD. Two case studies were performed which concentrated on zone 1. Fig. 46 shows zone 1 of the multi-feeder test system on which the methodology of the smart meter information usage for the substation relay was studied. The studies were performed after the zonal boundary elements had operated due to a fault in zone 2, causing zone 1 to be only zone connected to the substation. In each of the two cases, several fault types were staged and simulated on selected line segments on the main feeder and laterals within zone 1. The faults on the main feeder line segments spanned the beginning, the middle, and the end of the zone. For each fault type, both a bolted (zero impedance) and a high impedance fault were simulated. The high impedance fault involved a 20 Ω resistance. The trip times of the substation relay for the bolted and the high impedance faults were monitored using a pickup setting obtained based on the maximum loading of the zone (using the conventional approach for determining pickup setting, henceforth referred to as the old pickup), and a pickup setting that uses the proposed methodology of the maximum diversified demands of the two 12-hour intervals (henceforth referred to as the new pickup). The zone 1 loads variation pattern were randomly developed in matlab.

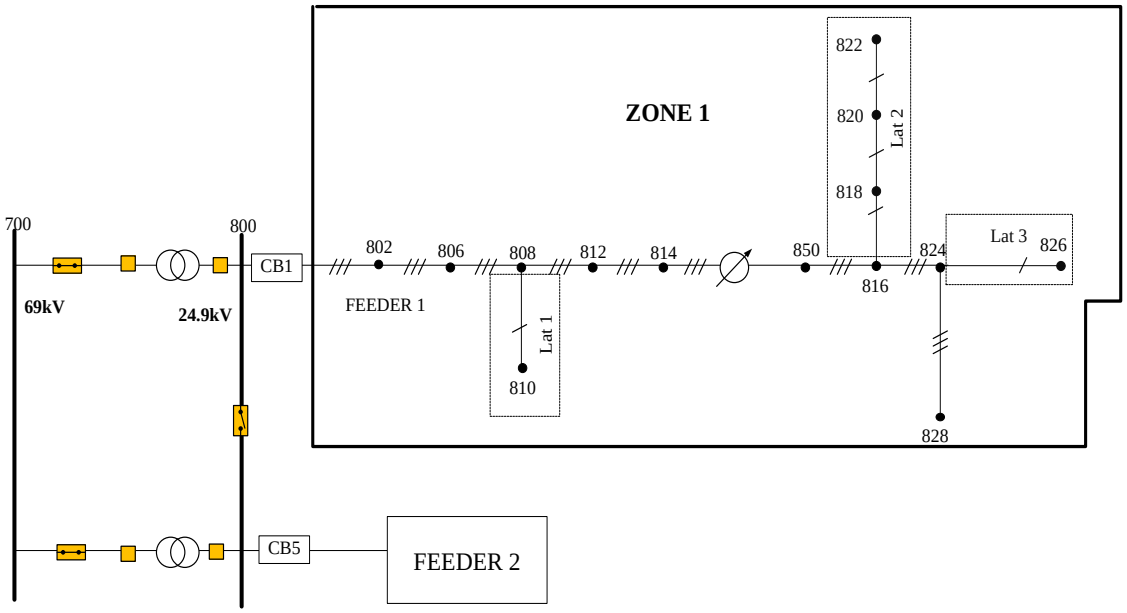

Fig. 46 Zone 1 of Multi-feeder Test System for Substation OC Relay Adaptive Pickup Study

5.6.1 Case 3 – Adaptive Pickup Study

Loads on the secondary distribution level on laterals 1, 2 and 3 were randomly varied to be within the bounds of the average and the maximum demands estimated for the multi-feeder test system as given in appendix A. The individual demands by the smart meters were used to obtain the diversified demands of the transformers on these laterals. Fig. 47 shows the individual diversified demands of the transformers on line segment 808-810 of lateral 1. The number of secondary transformers on this line segment is seven following the transformer allocation method discussed in section 5.2 as seen in appendix A. Lateral 2 has two line segments on which loads are connected, lines 818-820 and 820-822, with a total of six and nine secondary transformers for each line, respectively. Fig. 48 and Fig. 49 show the diversified demands obtained for all the transformers on lines 818-820 and 820-822, respectively. From the figures, it is seen that the peak loading of each transformer did not occur at the same time. This is a typical feature of distribution systems due to the diversity in energy usage by customers. Fig. 50

shows the diversified demands of the transformers on line segment 824-826 obtained from the random load variations.

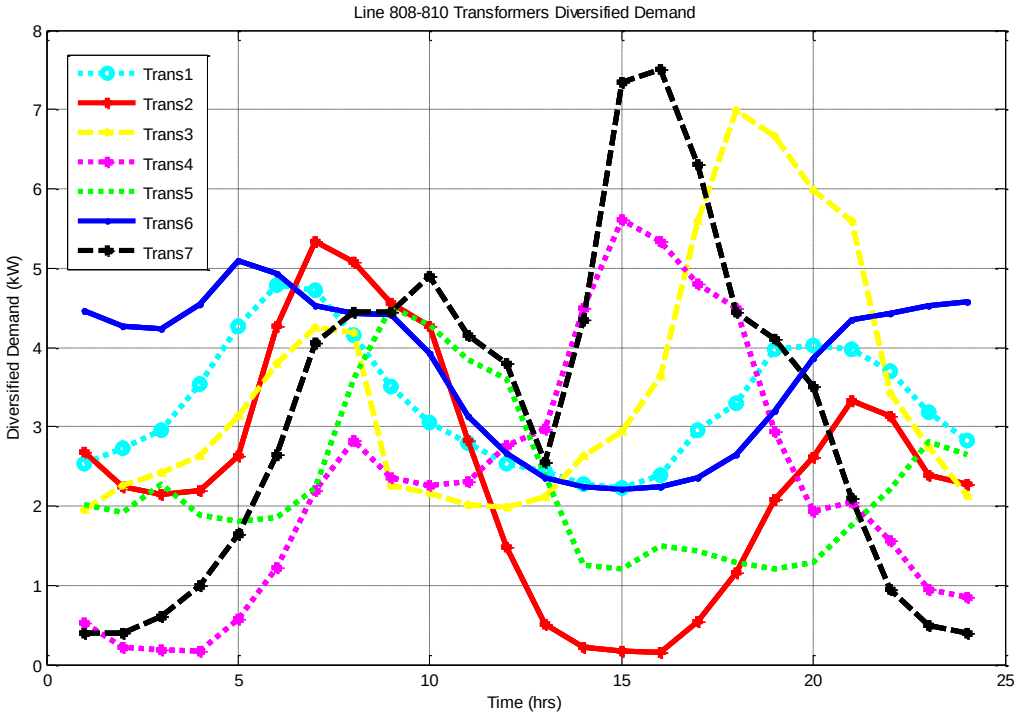

Fig. 47 Case 3: Diversified Demand of Transformers on Line Segment 808-810.

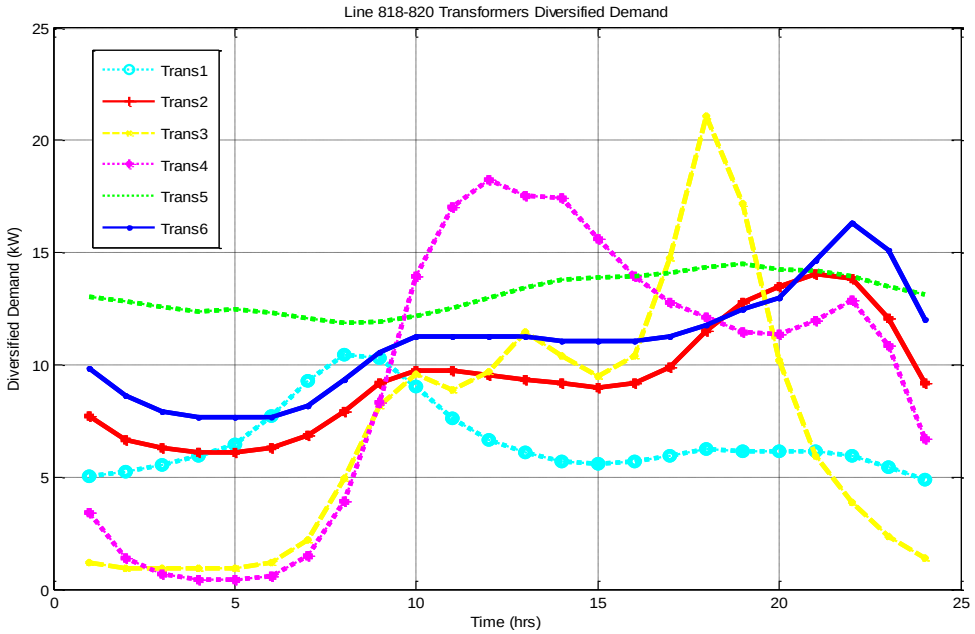

Fig. 48 Case 3: Diversified Demand of Transformers on Line Segment 818-820.

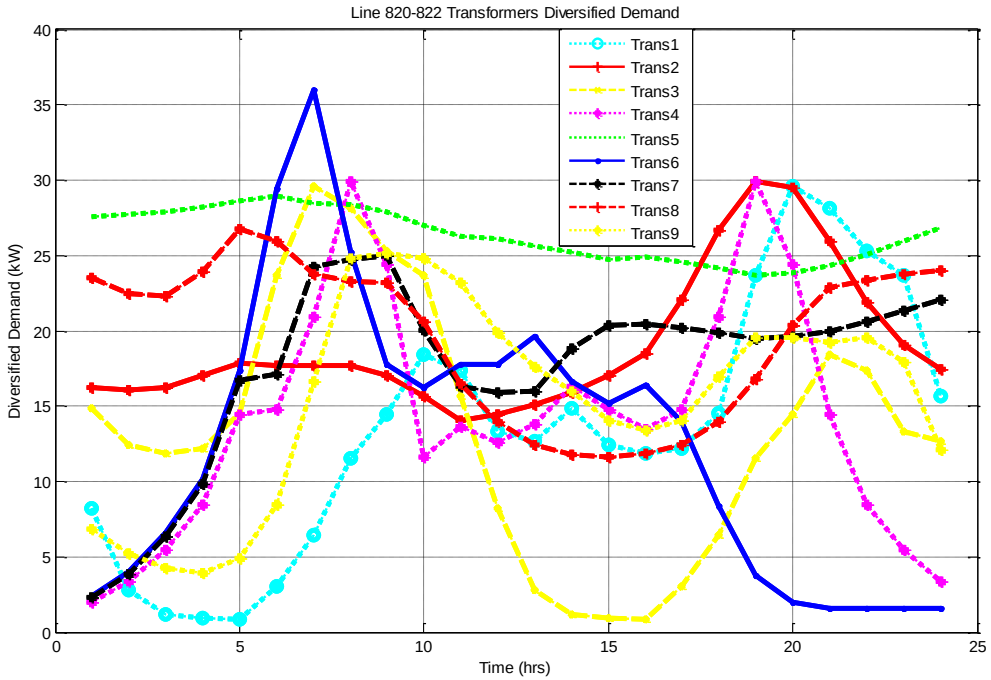

Fig. 49 Case 3: Diversified Demand of Transformers on Line Segment 820-818.

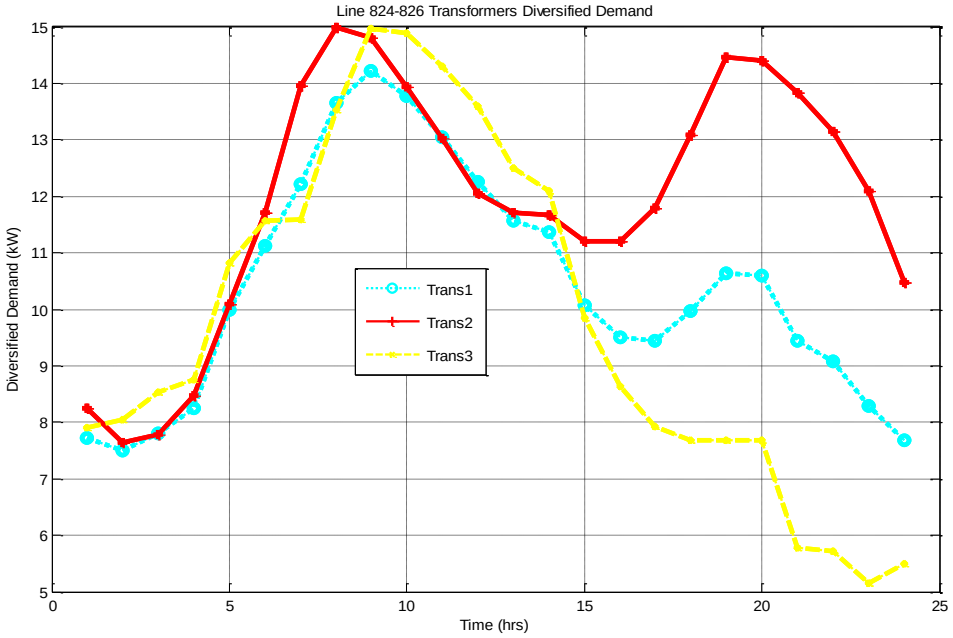

Fig. 50 Case 3: Diversified Demand of Transformers on Line Segment 824-826.

From the individual transformers' diversified demands of the laterals, the contribution to the substation relay demand was computed as the sum of all transformer diversified demands on that lateral using the second term in (11). Fig. 51 depicts lateral 1 contribution which was aggregated from the transformers diversified demand information. The load curve shows two peaks, one occurring in the morning and the other occurring in the evening, typical of a distribution residential load pattern. The morning demand peaks at 8:00 at a value of 28.2 kW, and the evening demand peaks at 18:00 at a value of 24.33 kW. In Fig. 52, the two maximum demands of lateral 2's contribution occurred at values of 262 kW and 253 kW at 8:00 and 19:00, respectively. Fig. 53 shows that lateral 3's contribution had a morning demand peak of 43.96 kW at 9:00 and an evening peak of 32.79 kW at 19:00. To obtain the substation relay demand, (11) was used to add the corresponding phases of the main feeder individual transformer diversified demands to the contribution of the lateral transformers.

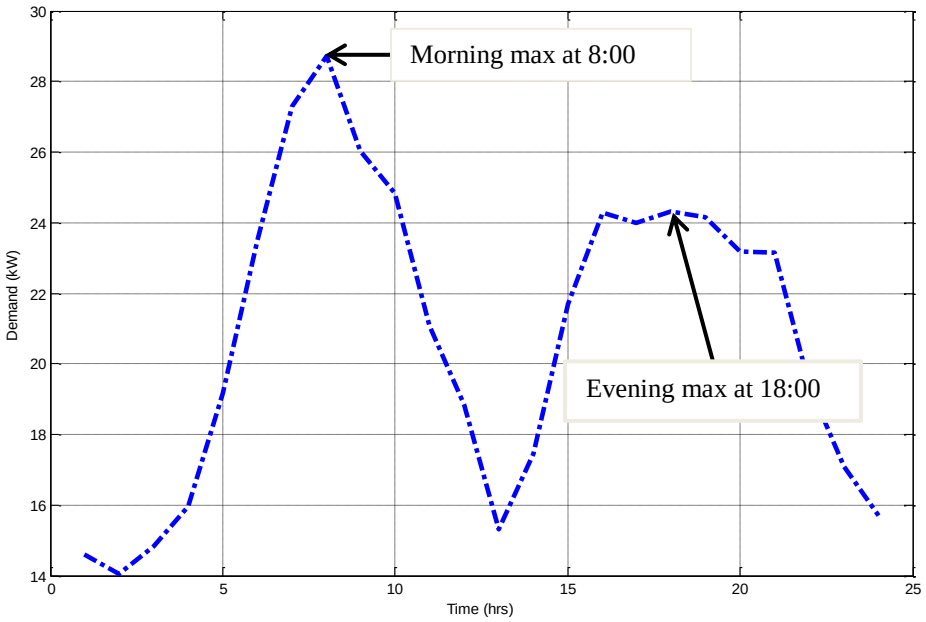

Fig. 51 Case 3: Lateral 1 Demand Contribution Curve.

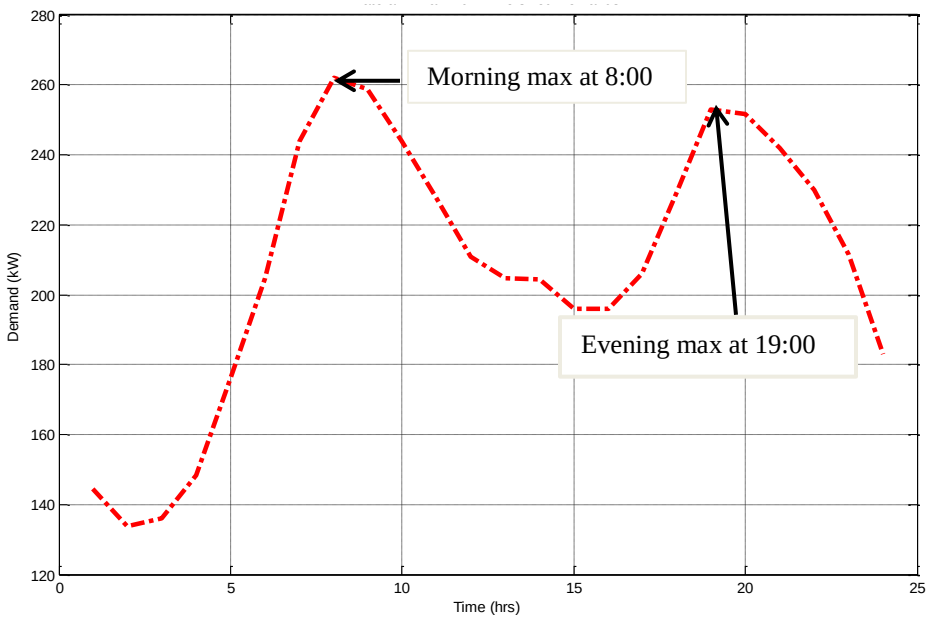

Fig. 52 Case 3: Lateral 2 Demand Contribution Curve.

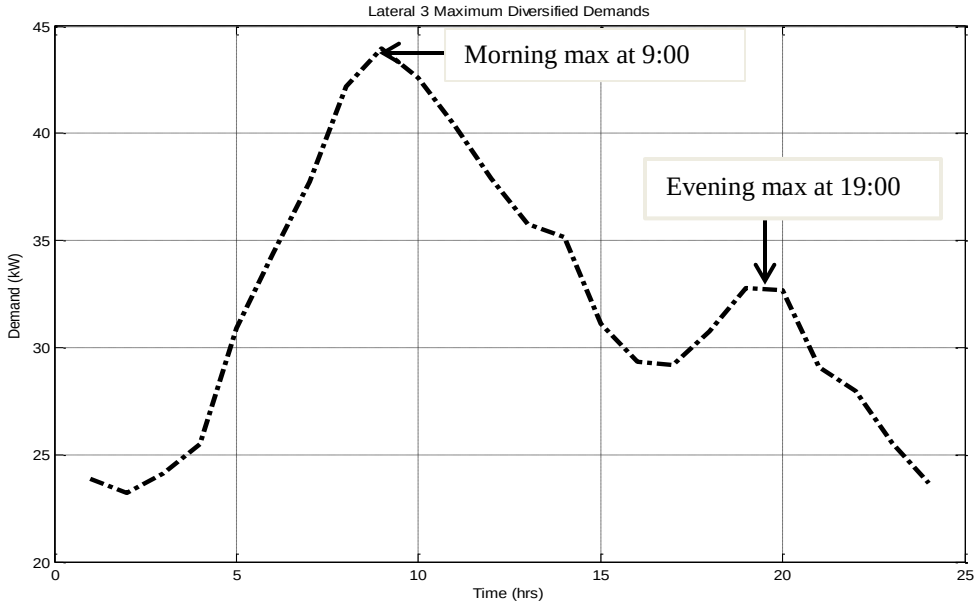

Fig. 53 Case 3: Lateral 3 Demand Contribution Curve.

Table 28 shows the comparison of the substation OC relay trip times using the old pickup setting (94.3 A) to the trip times using its new pickup setting (32.84 A) for the first 12-hour interval. The first column of the table indicates the faulted line sections. The second column represents the fault types that were simulated. Columns 3 and 4 provide the measured bolted and high impedance fault currents, respectively, for the associated fault types in column 2. The fifth and sixth columns indicate the measured trip times for the bolted and the impedance faults using the old pickup setting value of 94.3 A. The trips times for the new pickup setting (32.84 A) as recorded for the same bolted and impedance faults are shown in columns 7 and 8, respectively. The sensitivity improvement of the zone 1 substation OC relay in using the new pickup setting for each fault type and condition was computed as the difference between the old pickup trip times and the new pickup trip times expressed as a percentage of the old pickup trip times. The table shows that for each fault type and fault condition, the relay tripped faster when the new pickup setting was used than when the old pickup setting was used. The differences in the tripping times between the old and new pickup settings were

higher for the high impedance faults than the bolted faults. The table shows that, in using the new pickup setting, the substation OC relay had at least a 26% more improvement in its sensitivity for the bolted faults. For the high impedance faults, the minimum sensitivity improvement of the substation OC relay was 33%. This improvement is as a result of the faster speed of operation of the relay when using the new pickup setting.

Table 28 Case 3: Pickup Variation Study for Maximum Diversified Demand in 1st 12-hour Interval

Fault Location	Fault Type	Fault Current (A)		Old Pickup Trip Times (s)		New Pickup Trip Times (s)		Sensitivity Improvement	
		Bolted Fault	High Imped. Fault	Bolted Fault	High Imped. Fault	Bolted Fault	High Imped. Fault	Bolted Fault	High Imped. Fault
820-822	A-N	333.75	266.95	1.072	1.293	0.604	0.664	44%	49%
808-810	B-N	782.85	512.14	0.658	0.812	0.454	0.517	31%	36%
824-826	B-N	406.34	328.56	0.944	1.085	0.564	0.608	40%	44%
806-808	C-N	1273.53	641.06	0.543	0.722	0.399	0.481	27%	33%
816-824	AB	561.9	482.67	0.748	0.819	0.492	0.519	34%	37%
814-850	AC	560.17	487.44	0.770	0.719	0.501	0.480	35%	33%
802-806	ABC	1301.12	652.47	0.538	0.715	0.396	0.478	26%	33%
814-850	ABC	665.25	467.94	0.704	0.855	0.474	0.533	33%	38%
824-828	ABC	599.52	441.75	0.739	0.885	0.488	0.544	34%	39%

In Table 29, the results for the old pickup setting of 94.3 A are contrasted with that of the new pickup setting of 31.59 A determined for the second 12-hour interval. Again, the new pickup trip times were smaller compared to the old pickup trip times. From the table, it can be observed that the substation relay also shows higher percentage sensitivity improvement in responding to almost all the high impedance faults than it does to the bolted faults.

A comparison of the tripping times using the new pickup settings for the first 12-hour interval to that of the second 12-hour interval shows that the first 12-hour interval has longer tripping times for all fault conditions than the second 12-hour interval.

However, the difference in the tripping times is not very pronounced. The largest difference between the two 12-hour intervals for the new pickup tripping times for the bolted faults is 0.009 s for an A-N between nodes 820-822. For the high impedance faults, the largest difference is 0.011 s, and it is for a fault that occurs between the same two nodes.

Table 29 Case 3: Pickup Variation Study for Maximum Diversified Demand in 2nd 12-hour Interval

Fault Location	Fault Type	Fault Current (A)		Old Pickup Trip Times (s)		New Pickup Trip Times (s)		Sensitivity Improvement	
		Bolted Fault	High Imped. Fault	Bolted Fault	High Imped. Fault	Bolted Fault	High Imped. Fault	Bolted Fault	High Imped. Fault
820-822	A-N	333.7	267.0	1.072	1.292	0.595	0.653	44%	49%
808-810	B-N	783.1	511.2	0.658	0.813	0.449	0.511	32%	37%
824-826	B-N	408.8	328.3	0.945	1.094	0.556	0.601	41%	45%
806-808	C-N	1274.6	642.2	0.543	0.721	0.395	0.475	27%	34%
816-824	AB	559.8	480.0	0.747	0.818	0.486	0.513	35%	37%
814-850	AC	560.5	487.6	0.770	0.719	0.495	0.474	36%	34%
802-806	ABC	1301.5	652.3	0.538	0.715	0.393	0.473	27%	34%
814-850	ABC	664.4	466.8	0.705	0.856	0.468	0.526	34%	39%
824-828	ABC	599.3	438.8	0.739	0.889	0.482	0.538	35%	40%

5.6.2 Case 4- Adaptive Pickup Study

This case involved generating a new set of demands by the smart meters for the customers at the secondary distribution level of zone 1. Again, each customer on the laterals of the zone had the power randomly varied to be within the average and the maximum demand as given in appendix A. Fig. 54 shows the diversified demand for the seven transformers on lateral 1, line segment 808-810. Fig. 55 and Fig. 56, respectively, represent the diversified demands of the transformers on the line segments 818-820 and 820-822 of lateral 2. Fig. 57 shows the diversified demand of the three transformers on lateral 3, line segment 824-826.

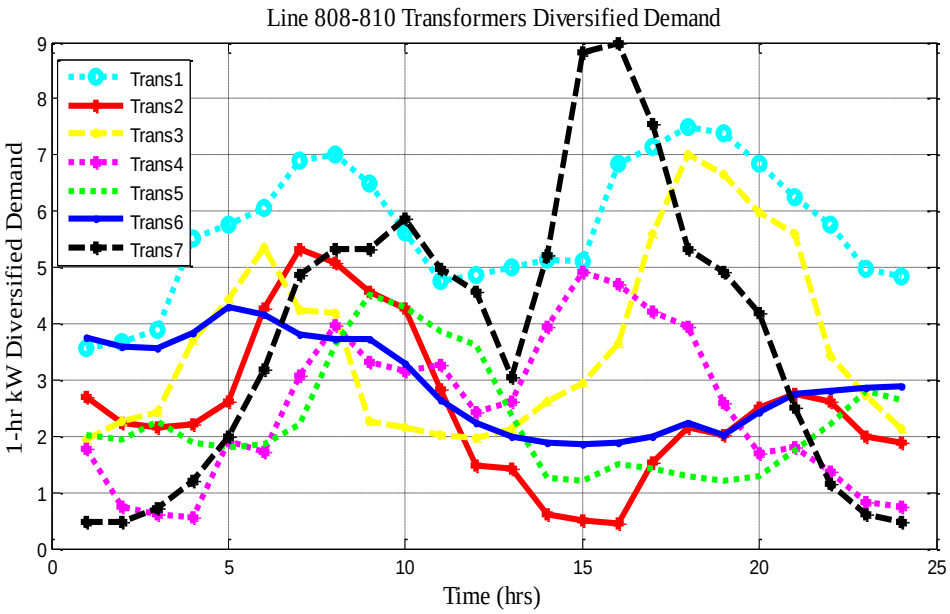

Fig. 54 Case 4: Diversified Demand of Transformers on Line Segment 808-810.

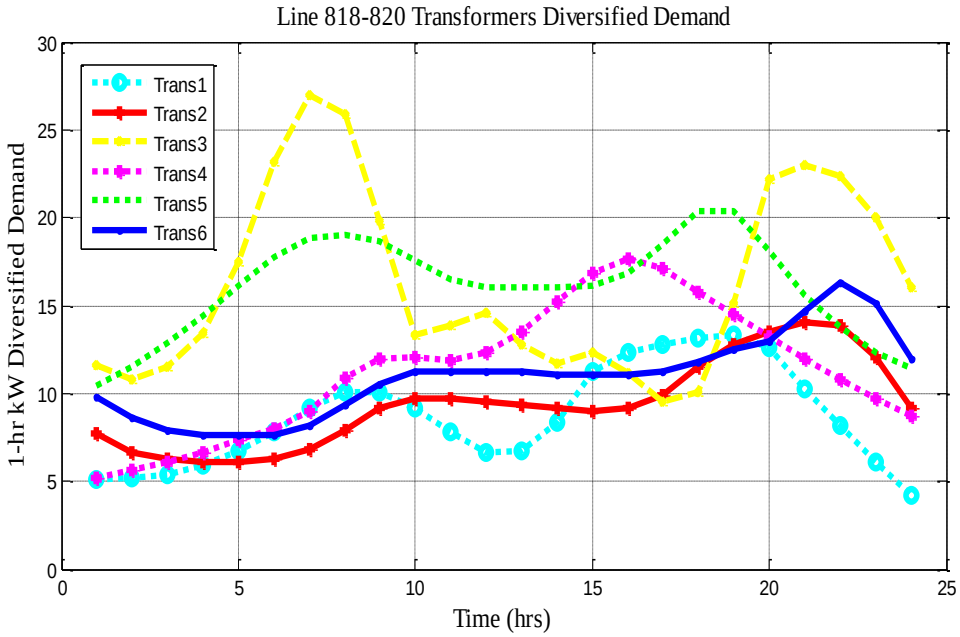

Fig. 55 Case 4: Diversified Demand of Transformers on Line Segment 818-820.

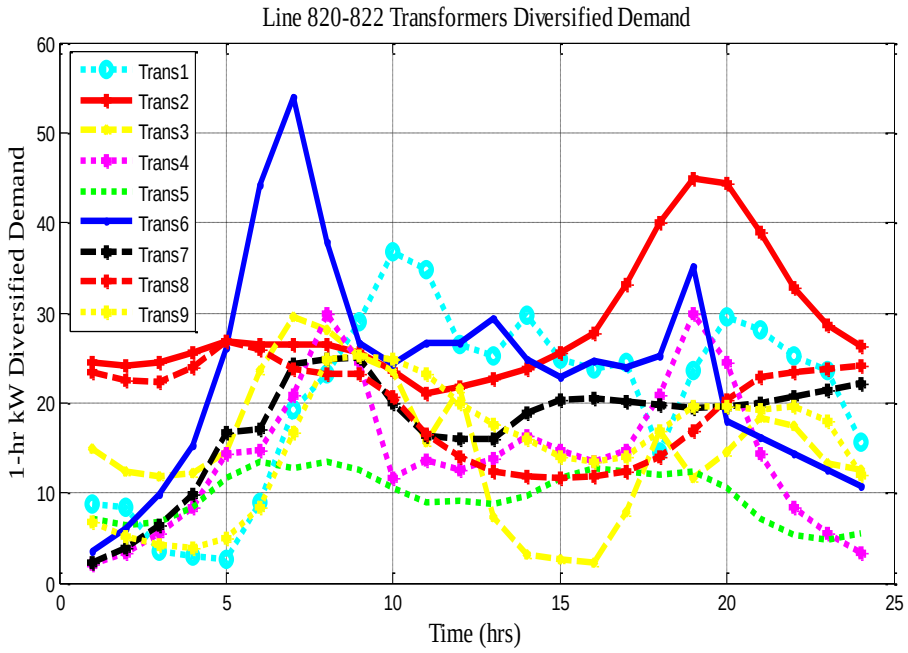

Fig. 56 Case 4: Diversified Demand of Transformers on Line Segment 820-822.

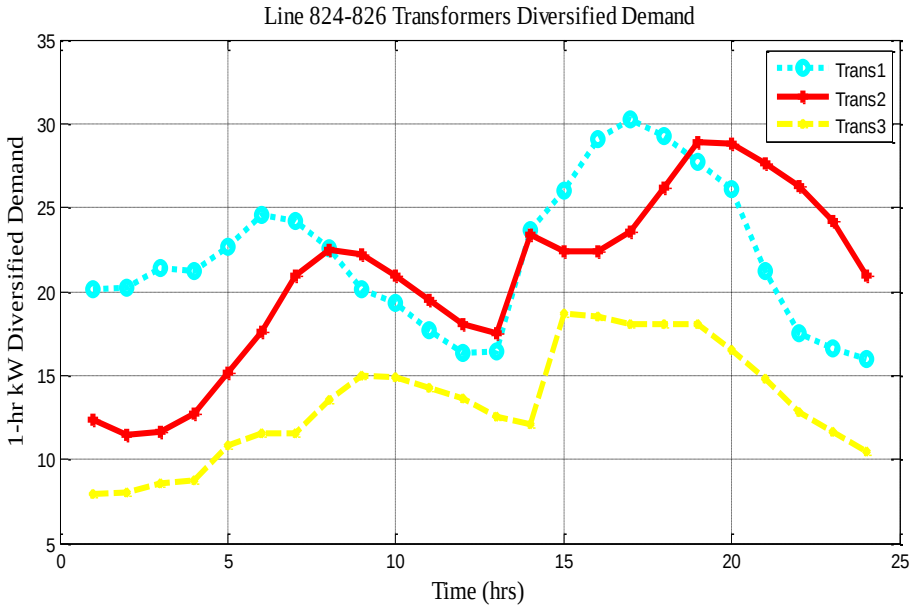

Fig. 57 Case 4: Diversified Demand of Transformers on Line Segment 824-826.

The contribution of the laterals' transformers diversified demands to the substation relay demand was obtained as the sum of the individual lateral transformer diversified demands using the second term in (11). Fig. 58 shows lateral 1's contribution to the substation relay demand. The morning demand peak occurred at 8:00 at a value of 32.92 kW. The evening demand peak value is 29.47 kW and occurred at 17:00. Fig. 59 shows the contributions made by lateral 2's transformers. The peak demand for the morning is higher with a value of 315 kW and occurred at 8:00. The evening demand peak value is 301.9 kW, which is seen to occur at 19:00. The demand contribution by the transformers on lateral 3 is shown in Fig. 60. The morning demand has a peak value of 58.59 kW and occurred at 8:00, and the evening peak value is 74.76 kW and occurred at 19:00.

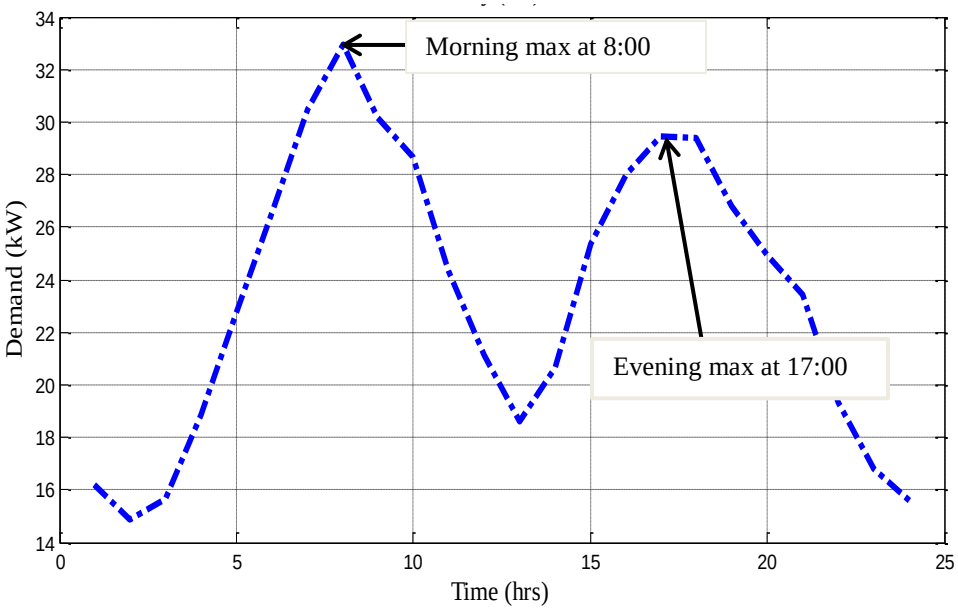

Fig. 58 Case 4: Lateral 1 Demand Contribution Curve.

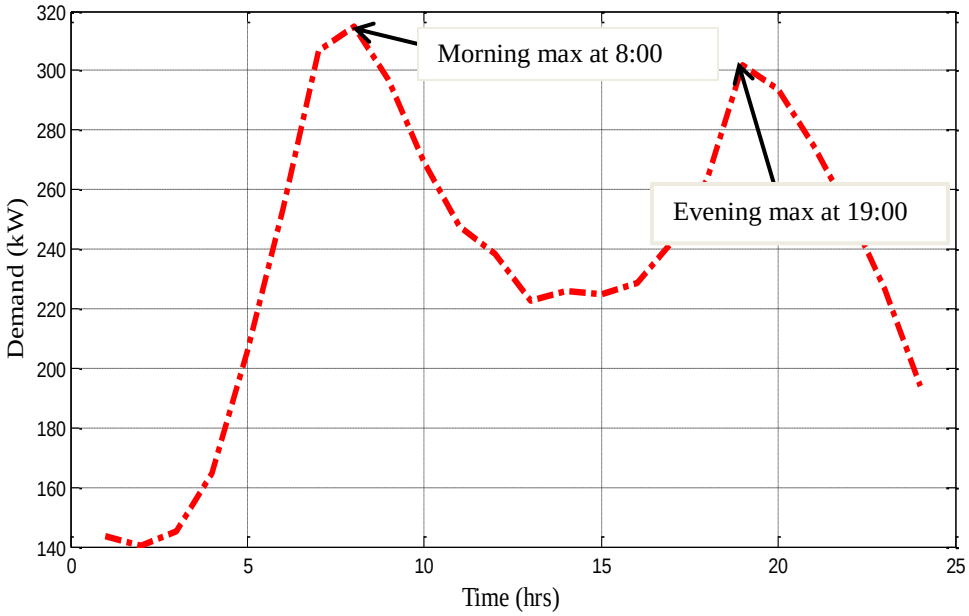

Fig. 59 Case 4: Lateral 2 Demand Contribution Curve.

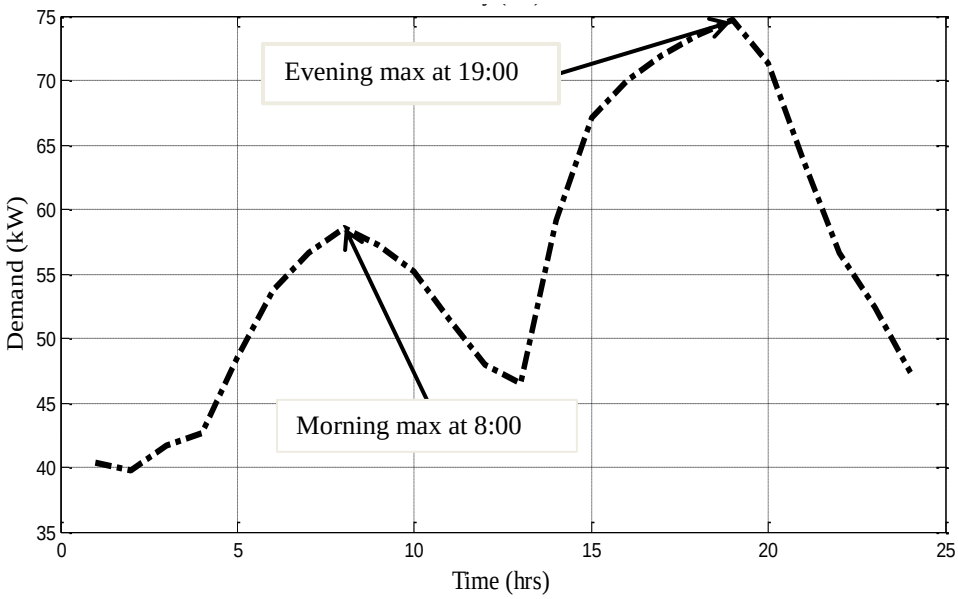

Fig. 60 Case 4: Lateral 3 Demand Contribution Curve.

Again, the substation OC relay trip times in using the new pickup setting in each 12-hour interval are compared to that of the old pickup setting (94.3 A) for bolted and high impedance fault scenarios. Table 30 shows a comparison of the trip times using the new pickup setting (39.12 A) for the first 12-hour interval to the trip times using the old pickup setting. The table also indicates the faulted line sections and the fault types that were simulated. The sensitivity improvement of the substation relay in using the first 12-hour interval pickup setting (new pickup) over the old pickup setting is also shown. This sensitivity improvement was computed as the difference between the old pickup trip times and the new pickup trip times expressed as a percentage of the old pickup trip times. The table shows that there is at least a 23% improvement in the sensitivity of the substation OC relay in responding to bolted faults, and at least a 29% sensitivity improvement by the substation relay in responding to the high impedance faults. The new pickup trip times are also smaller and therefore more desirable than the old pickup trip times.

Table 30 Case 4: Pickup Variation Study for Maximum Diversified Demand in 1st 12-hour Interval

Fault Location	Fault Type	Fault Current (A)		Old Pickup Trip Times (s)		New Pickup Trip Times (s)		Sensitivity Improvement	
		Bolted Fault	High Imped. Fault	Bolted Fault	High Imped. Fault	Bolted Fault	High Imped. Fault	Bolted Fault	High Imped. Fault
820-822	A-N	333.37	267.36	1.073	1.291	0.650	0.720	39%	44%
808-810	B-N	783.19	513.99	0.658	0.810	0.477	0.548	27%	32%
824-826	B-N	409.35	329.38	0.941	1.083	0.602	0.654	36%	40%
806-808	C-N	1272.17	642.06	0.543	0.721	0.417	0.508	23%	30%
816-824	AB	554.08	470.01	0.744	0.808	0.519	0.548	30%	32%
814-850	AC	565.4	491.24	0.769	0.718	0.530	0.507	31%	29%
802-806	ABC	1302.77	654.74	0.538	0.713	0.414	0.504	23%	29%
814-850	ABC	664.6	470.57	0.704	0.852	0.500	0.566	29%	34%
824-828	ABC	599.87	440.19	0.738	0.887	0.516	0.581	30%	35%

Table 31 presents the comparison of the tripping times for the substation relay for the second 12-hour interval using its corresponding new pickup setting (37.59 A) to that of the old pickup setting for the bolted and high impedance faults staged at various fault locations. Again, it can be seen that changing the substation OC relay pickup setting from its old pickup setting to its new pickup setting for the second 12-hour interval shows significant reduction in the times at which the bolted and high impedance faults were isolated.

By comparing the tripping times of the substation OC relay during the first 12-hour interval to that of the second 12-hour interval, it can be seen that there was a much faster response in isolating the faults that occurred in the second 12-hour interval than those that occurred in the first 12-hour interval. The largest difference in the tripping times of the two time intervals for the bolted and high impedance faults in this case is 0.033 s and 0.031 s, respectively. The faulted line section that resulted in this difference was between nodes 824-826.

Table 31 Case 4: Pickup Variation Study for Maximum Diversified Demand in 2nd 12-hour Interval

Fault Location	Fault Type	Fault Current (A)		Old Pickup Trip Times (s)		New Pickup Trip Times (s)		Sensitivity Improvement	
		Bolted Fault	High Imped. Fault	Bolted Fault	High Imped. Fault	Bolted Fault	High Imped. Fault	Bolted Fault	High Imped. Fault
820-822	A-N	333.79	267.61	1.072	1.290	0.639	0.706	40%	45%
808-810	B-N	783.41	531.24	0.658	0.795	0.472	0.534	28%	33%
824-826	B-N	446.25	355.31	0.880	1.023	0.569	0.622	35%	39%
806-808	C-N	1284	641.03	0.541	0.722	0.412	0.502	24%	30%
816-824	AB	557.69	479.55	0.747	0.814	0.513	0.542	31%	33%
814-850	AC	562.18	490.31	0.772	0.718	0.524	0.500	32%	30%
802-806	ABC	1300.66	654.94	0.538	0.713	0.410	0.498	24%	30%
814-850	ABC	666.24	469.43	0.704	0.853	0.494	0.559	30%	35%
824-828	ABC	598.72	440.99	0.738	0.886	0.509	0.572	31%	36%

5.7 Summary of Results

The smart meter demand measurements from a load variation pattern randomly developed in matlab for the loads in zone 1 of the multi-feeder test system were used to determine a 24-hour time duration demand that the substation OC relay monitors. The 24-hour time duration demands of the substation OC relay was divided into two 12-hour time intervals. The trip times of the substation relay for bolted and high impedance faults in the zone were monitored using a pickup setting obtained based on the maximum loading of zone 1 (following the conventional approach for determining pickup setting), and a pickup setting that uses the proposed methodology of the maximum diversified demands of the two 12-hour intervals. The bolted and the high impedance faults on the main feeder line segments spanned the beginning, the middle, and the end of the zone.

The case studies revealed that changing the pickup setting of the substation relay from the maximum loading using the conventional approach to the pickup setting corresponding to the maximum diversified demand in each 12-hour interval provided faster tripping times of the substation relay for the bolted and high impedance fault types that were simulated. The faster tripping times of the substation relay were as a result of the two 12-hour intervals pickup settings being less than the conventional approach pickup setting. The percentage improvement in the sensitivity of the substation OC relay for using the two 12-hour intervals pickup settings in responding to faults was on the average higher for the high impedance fault types than the bolted fault types. The tripping times of the second 12-hour interval showed only a slight improvement over the tripping times for the first 12-hour interval for the same faults that were studied.

6 CONCLUSIONS AND FUTURE WORK

6.1 Conclusions

This thesis discusses a method for identifying faulted zones and reducing the extent of customers' affected by faults due to DGs influence on overcurrent protection for radial distribution systems (RDSs). A technique for using smart metering load information in adapting the pickup setting of the substation overcurrent relay was also discussed. The IEEE 34 Node Radial Test Feeder was expanded into a multi-feeder test system and a secondary distribution level was designed for the multi-feeder. The multi-feeder test system, along with its components, was modeled in EMTP™/PSCAD®. The multi-feeder implementation was verified with transient analysis studies. Five DGs were connected at selected nodes on the multi-feeder test system. The substation overcurrent (OC) relay trip times for a zone that was supplied by the multi-feeder system substation was studied using the smart meters power demand measurements.

The implemented overcurrent protection approach modified the scheme presented in [27] and [28], that uses a zoning concept to isolate faulted areas in RDS with DGs. The multi-feeder test system was divided into various zones, and each zone was separated from the other by a zonal boundary protective element that included a directional overcurrent relay and a circuit breaker. The directional element in the OC relay uses both positive sequence and negative sequence components to detect the direction of fault current. The negative sequence element is given a higher priority to indicate the fault direction for unbalanced faults while the positive sequence element has the higher priority in identifying the direction of balanced faults. The status of the fault current direction of each zonal boundary relay is communicated to other zonal boundary relays using binary state signals over a radio frequency communication medium. Any two adjoining zonal boundary relays that show a difference in their communicated fault current direction provide an indication of the faulted zone to the installed relays. The effectiveness of the approach in detecting faults and reducing the extent of impact on distribution customers was shown through a number of case studies. By decentralizing

the control of the zonal breakers, the single point of failure that a central relay may present was eliminated. In some instances, the higher priority directional sequence element indicated an incorrect fault direction. This was shown for faults that occurred on the secondary side of the in-line transformer of the multi-feeder test system and in some cases where the fault occurred further away from the zonal boundary elements. Notwithstanding these challenges, the fact that the zonal boundary elements shared indicated fault direction decisions using binary state signals resulted in the proper isolation of the faulted zone.

The technique for the usage of the smart meter load information in OC protection involved sequentially determining the demand at the substation's relay location using previous day's smart meter demand measurements. The load information from the smart meters installed at the secondary distribution level over a 24-hour time duration was aggregated to obtain the substation's relay demands. The substation's relay demand over the 24-hour time duration was divided into two 12-hour intervals and the maximum diversified demand in each time interval was determined. The zone 1 substation OC relay pickup setting was then set as 1.5 times the current corresponding to the maximum diversified demand in each of the two 12-hour intervals. The trip times of the two 12-hour pickup values were compared to that of the pickup value corresponding to the maximum demand of the zone.

The results from case studies for bolted and high impedance fault types showed that the sensitivity of the substation OC relay was improved. The sensitivity improvement resulted from using the pickup settings of the maximum diversified demands for the two 12-hour intervals, as opposed to the pickup setting which was based on the maximum demand in zone 1. However, by comparing the tripping times obtained for the two 12-hour intervals pickup settings, it was noticed that they did not vary substantially from each other. The difference in variations was approximately less than 0.1 s for the bolted and high impedance faults that were studied. The difference suggests that for a more conservative approach for the usage of the smart meter data in OC protection, only one of the two time interval pickup settings can be adopted for each day

of operation of the multi-feeder distribution system. The presented technique for smart meter information usage also devises a possible alternative for determining the loading downstream of a protective relay at regular time intervals. This approach may help distribution operators track the day-to-day maximum loading levels due to the determination of the maximum diversified demands of the substation overcurrent relay. Another benefit from the technique may be to help distribution system operators in planning operations once a record of the maximum diversified demands over a longer time during duration is reviewed. The technique for determining the load downstream of the relay may be computationally intensive, and therefore, the AMI headend computers may need high processing powers. However, this may not be a major concern as the computers located at the AMI headend may be fully sophisticated in a smart grid environment. In using the previous day's load demand measurements from the smart meters to set the substation relay's pickup setting, the technique may produce unnecessary tripping of the substation relay for any unforeseen weather conditions that may cause significant changes in customer energy usage in the current day. This is as a result of potentially setting the pickup of the substation OC relay to a value that may be less than the current day's maximum diversified demand.

6.2 Future Work

Future research is recommended to continue in applying the smart meter load demands to two or more zones supplied by the multi-feeder substation. A more heavily loaded test feeder is also recommended to be used in advancing the technique on the possible use of smart meter load demand information in an adaptive overcurrent protection.

REFERENCES

[1] N. Kouka. Electromagnetic field, Oct. 16, 2011. [Online]. Available: http://brain101.info/EMF.php

[2] L. M. Faulkenberry and W. Coffer, *Electrical Power Distribution and Transmission*. Englewood Cliffs, NJ: Prentice Hall, 1996.

[3] T. A. Short, *Electric Power Distribution Handbook*. Boca Raton, FL: CRC Press, 2003.

[4] IEEE guide for protective relay applications to distribution Lines, *IEEE Standard C37.230-2007*, pp. 1-100, 2007.

[5] IEEE standard for relays and relay systems associated with electric power apparatus, *IEEE Std C37.90-2005 (Revision of IEEE Std C37.90-1989)*, pp. 1-19, 2006.

[6] S. H. Horowithz and A. G. Phadke, *Power System Relaying*, 3rd ed.Chichester, England: John Wiley & Sons Ltd, 2008.

[7] M. Prica and M. Ilic, "A novel fault-dependent-time-settings algorithm for overcurrent relays," in *Proc. 2009 IEEE Power and Energy Soc. General Meeting*, Calgary, AB, Canada, Jul. 2009, pp. 1-9.

[8] J. L. Blackburn and T. J. Domin, *Protective Relaying Principles and Applications*, 3rd ed. Boca Raton, FL: CRC Press, 2007.

[9] P. Dondi, D. Bayoumi, C. Haederli, D. Julian, and M. Suter, "Network integration of distributed power generation," *Journal of Power Sources*, vol. 106, pp. 1-9, Apr. 2002.

[10] K. L. Butler-Purry and M. Marotti, "Impact of distributed generators on protective devices in radial distribution systems," in *Proc. 2005/2006 IEEE PES Transmission and Distribution Conf. and Exhibition*, Dallas, TX, May 2006, pp. 87-88.

[11] T. M. de Britto, D. R. Morais, M. A. Marin, J. G. Rolim, H. H. Zurn, and R. F. Buendgens, "Distributed generation impacts on the coordination of protection

systems in distribution networks," in *Proc. 2004 IEEE PES Transmission and Distribution Conf. and Exposition: Latin America*, Sao Paulo, Brazil, Nov. 2004, pp. 623-628.

[12] R. C. Dugan and T. E. McDermott, "Distributed generation," *IEEE Industry Applications Magazine,* vol. 8, pp. 19-25, Mar. 2002.

[13] A. Girgis and S. Brahma, "Effect of distributed generation on protective device coordination in distribution system," in *Proc. 2001 Large Eng. Systems Conf. on Power Eng. (LESCOPE)*, Halifax, Canada, Jul. 2001, pp. 115-119.

[14] S. Kwon, C. Shin, and W. Jung, "Evaluation of protection coordination with distributed generation in distribution networks," in *Proc. 2010 10th IET Int. Conf. on Developments in Power System Protection (DPSP).* , Manchester, UK, Mar. 2010, pp. 1-5.

[15] J. A. Martinez and J. Martin-Arnedo, "Impact of distributed generation on distribution protection and power quality," in *Proc. 2009 IEEE Power and Energy Society General Meeting*, Calgary, AB, Canada, Jul. 2009, pp. 1-6.

[16] Summary of C37.230-2007, IEEE Guide for Protective Relay Applications to Distribution Lines, *IEEE Std C37.230-2007*.

[17] L. Zhongwei, T. Weiming, L. Fengge, and F. Shenghu, "Study on adaptive protection system of power supply and distribution line," in *Proc. 2006 Int. Conf. on Power System Technology(PowerCon)*, Chongqing, China, Oct. 2006, pp. 1-6.

[18] G. Tang and M. R. Iravan, "Application of a fault current limiter to minimize distributed generation impact on coordinated relay protection," in *Proc. Int. Conf. Power Systems Transients*, Montreal, QC, Canada, Jun. 2005.

[19] A. Agheli, H. A. Abyaneh, R. M. Chabanloo, and H. H. Dezaki, "Reducing the impact of DG in distribution networks protection using fault current limiters," in *Proc. 4th Int. Power Eng. and Optimization Conf.* , Selangor, Malaysia, Jun. 2010, pp. 298-303.

[20] S. M. Brahma and A. A. Girgis, "Microprocessor-based reclosing to coordinate fuse and recloser in a system with high penetration of distributed generation," in

Proc. 2002 IEEE Power Eng. Soc. Winter Meeting, New York, USA, Jan. 2002, vol. 1, pp. 453-458.

[21] A. Zamani, T. Sidhu, and A. Yazdani, "A strategy for protection coordination in radial distribution networks with distributed generators," in *Proc. 2010 IEEE Power and Energy Society General Meeting*, Minneapolis, MN, USA, Jul. 2010, pp. 1-8.

[22] H. B. Funmilayo and K. L. Butler-Purry, "An approach to mitigate the impact of distributed generation on the overcurrent protection scheme for radial feeders," in *Proc. 2009 IEEE PES Power Systems Conf. and Exposition (PSCE)*, Piscataway, NJ, USA, Mar. 2009, p. 11.

[23] A. Conde and E. Vazquez, "Operation logic proposed for time overcurrent relays," *IEEE Trans. Power Del.*, vol. 22, pp. 2034-2039, Oct. 2007.

[24] N. A. Laway and H. O. Gupta, "A method for adaptive coordination of overcurrent relays in an interconnected power system," in *Proc. 1993. 5th Int. Conf. on Developments in Power System Protection*, York, UK, Mar. 1993, pp. 240-243.

[25] M. Jing, L. Jinlong, and W. Zengping, "An adaptive distance protection scheme for distribution system with distributed generation," in *Proc. 2010 5th Int. Conf. on Critical Infrastructure (CRIS)*, Beijing, China, Sept. 2010, pp. 1-4.

[26] Y. Han, X. Hu, and D. Zhang, "A new adaptive current protection scheme of distribution networks with distributed generation," in *Proc. 2009 Int. Conf. on Sustainable Power Generation and Supply (SUPERGEN)*, Nanjing, China, Apr. 2009, pp. 1-5.

[27] S. M. Brahma and A. A. Girgis, "Development of adaptive protection scheme for distribution systems with high penetration of distributed generation," *IEEE Trans. Power Delivery*, vol. 19, pp. 56-63, Jan. 2004.

[28] S. A. M. Javadian and M. R. Haghifam, "Implementation of a new protection scheme on a real distribution system in presence of DG," in *Proc. 2008*

POWERCON and IEEE Power India Conf. on Power System Technology, New Delhi, India, Oct. 2008, pp. 1-7.

[29] S. A. M. Javadian, R. Tamizkar, and M. R. Haghifam, "A protection and reconfiguration scheme for distribution networks with DG," in *Proc. 2009 IEEE PowerTech Bucharest,* Bucharest, Romania, Jun. 2009, pp. 1-8.

[30] J. L. Sun, Y. L. Li, S. W. Li, and Q. Jin, "A new protection scheme for distribution system with distributed generations," in *Proc. 2009 Int. Conf. on Electrical Engineering (ICEE),* Shenyang, China, Jul. 2009.

[31] M. Baran and I. El-Markabi, "Adaptive over current protection for distribution feeders with distributed generators," in *Proc. 2004 IEEE Power Systems Conf. and Exposition*, New York, USA, Oct. 2004, vol. 2, pp. 715-719

[32] N. Schaefer, T. Degner, A. Shustov, T. Keil, and J. Jaeger, "Adaptive protection system for distribution networks with distributed energy resources," in *Proc. 10th IET Intl. Conf. on Developments in Power System Protection (DPSP).* Manchester, UK, Mar. 2010, pp. 1-5.

[33] J. Sung-II, K. Kwang-Ho, P. Young-Up, C. Jung-Hwan, K. Yong-Cheol, K. San-Hee, L. Seung-Jae, O. Hideharu, and P. Jong-Keun, "An adaptive setting method for the overcurrent relay of distribution feeders considering the interconnected distributed generations," *KIEE Int.Trans. on Power Eng.*, vol. 5-A, pp. 357-365, 2005.

[34] F. A. Viawan, D. Karlsson, A. Sannino, and J. Daalde, "Protection scheme for meshed distribution systems with high penetration of distributed generation," in *Proc. 2006 Power Systems Conf. Advanced Metering, Protection, Control, Communication, and Distributed Resources*, Clemson, SC, USA, Mar. 2006, pp. 99-104.

[35] Y. Chunguang, P. Zhencun, C. Wei, and W. Wei, "The study on fault directional relay in protection system for distribution system under high DG penetration level," in *Proc. 2009 Power and Energy Engineering Conf, Asia-Pacific (APPEEC),* Chengdu, China, Mar. 2009, pp. 1-4.

[36] K. Okuyama, T. Kato, Y. Suzuoki, and T. Funabashi, "Protection relay system using information network for distribution system with DGs," *Electrical Engineering in Japan*, vol. 155, pp. 1281-1285, Apr. 2006.

[37] J. Tian, H. Gao, M. Hou, J. Liang, and Y. Zhao, "A fast current protection scheme for distribution network with distributed generation," in *Proc. 2010 10th IET Int. Conf. on Developments in Power System Protection (DPSP)*, Manchester, UK, Mar. 2010, pp. 1-4.

[38] Renesas. Efforts by Renesas toward the building of smart grids. Sept. 25, 2011. [Online]. Available: http://www.renesas.com/ecology/eco_society/

[39] DOE Smart Grid System Report, US Department of Energy, Jul. 2009. [Online]. Available: http://energy.gov/oe/smart-grid-publications-archive

[40] A systems view of the modern grid, National Energy Technology Laboratory (NETL) for the U.S. Department of Energy Office of Electricity Delivery and Energy Reliability, Jan. 2007 [Online]. Available: http://www.netl.doe.gov/smartgrid/refshelf.html#WhitePapers

[41] M. Peterson, "Role of protective relaying in the smart grid (Draft Report)," Power System Relaying Committee, System Protection Subcommittee (PSRC) WG C2, Berkeley, CA, Sept. 2010.

[42] K.U.Leuven; and K. Arenberg, "An evaluation of two-way communication means for advanced metering in Flanders," in *Proc. IEEE Int. Instrumentation and Measurement Technology Conf.*, Victoria, Vancouver Island, Canada, May 2008, pp. 900-905.

[43] Advanced metering infrastructure, National Energy Technology Laboratory (NETL) for the U.S. Department of Energy Office of Electricity Delivery and Energy Reliability, Feb. 2008 [Online]. Available: http://www.netl.doe.gov/smartgrid/refshelf.html#WhitePapers

[44] F. M. Cleveland, "Cyber security issues for advanced metering infrasttructure (AMI)," in *Proc. 2008 Power and Energy Soc. General Meeting*, Pittsburgh, USA, Jul. 2008, pp. 1-5.

[45] Final Report on evaluation of advanced metering system (AMS) deployment in Texas, Public Utility Commission of Texas, Jul. 2010. [Online]. Available: http://www.centerpointenergy.com/staticfiles/CNP/Common/SiteAssets/doc/PUCT%20Final%20Report%207-30.pdf

[46] ITRON. OpenWay® CENTRON®, Nov. 15, 2011. [Online]. Available: https://www.itron.com/na/productsAndServices/Pages/OpenWay%20CENTRON.aspx

[47] G.E. I-210+c family smart grid enabled consumer friendly metering, Aug. 15, 2011. [Online]. Available: http://www.gedigitalenergy.com/smartmetering/catalog/i210plusc.htm

[48] Elster. "AS220 - Electronic Smart Meter". Dec. 15, 2011. [Online]. Available: http://www.elstermetering.com/en/1141.html

[49] Sensus. iCon A Residential Meter, Aug. 20, 2011. [Online]. Available: http://www.sensus.com/web/usca/electric/product-line/electricity-metering/product/icon-a-residential-meter

[50] LandisGyr. E330 FOCUS® AX and E350 FOCUS® AX-SD, Aug. 29, 2011. [Online]. Available: http://www.landisgyr.com/na/en/pub/products_na.cfm?eventProducts=products.ProductDetails&ID=239&catID=32

[51] Echelon. ANSI 2S meter. Dec. 08, 2011. [Online]. Available: http://www.echelon.com/metering/datasheets/ANSI_2s.pdf

[52] D. Reilch. Smart meters on a roll in Canada, Oct. 19, 2011. [Online]. Available: http://mthink.com/utilities/knowledge/smart-meters-roll-canada

[53] A. Ukil, B. Deck, and V. H. Shah, "Smart distribution protection using current-only directional overcurrent relay," in *Proc. 2010 IEEE PES Innovative Smart Grid Technologies Conf. Europe (ISGT Europe)*, Gothenburg, Sweden, Oct. 2010, pp. 1-7.

[54] M-7651 feeder protection system smart grid ready, Jul. 15, 2011. [Online]. Available: http://www.beckwithelectric.com/products/m-7651.html

[55] Smart grid solutions from SEL, Oct. 11, 2011. [Online]. Available: http://www.selinc.com/smartsolutions/

[56] Application guide for interconnecting distributed resources with electric power systems *IEEE Standard 1547.2-2008,* pp. 1-207, 2008.

[57] K. Okuyama, T. Kato, Y. Suzuoki, and T. Funabashi, "Protection relay system using information network for distribution system with DGs," *Electrical Engineering in Japan (English translation of Denki Gakkai Ronbunshi),* vol. 155, pp. 30-35, Jun. 2006.

[58] W. H. Kersting, "Radial distribution test feeders," in *Proc. 2001 IEEE Power Engineering Soc. Winter Meeting*, Columbus, OH , USA, Jan. 2001, vol. 2, pp. 908-912.

[59] IEEE PES distribution system analysis subcommittee. Distribution test feeders, Jun. 22, 2010. [Online]. Available: http://ewh.ieee.org/soc/pes/dsacom/testfeeders/index.html

[60] W. H. Kersting; and W. H. Phillips, "Modeling and analysis of rural electric distribution feeders," *IEEE Trans. on Industry Applications,* vol. 28, pp. 767-773, Jul. 1992.

[61] W. H. Kersting, *Distribution System Modeling and Analysis*. New York: CRC Press, 2002.

[62] A. Pabla, *Electric Power Distribution.* New Dehli: Tata McGraw-Hill, 2004.

[63] "EMTP/PSCAD X4," Manitoba HVDC Research Centre Inc, Jan. 11, 2011. [Online]. Available: https://pscad.com/products/pscad/past_present_and_future/.

[64] S. Santoso, Z. Zheng, and D. Muthumuni, "Induction machine test case for the 34-bus test feeder: a wind turbine time-domain model," in *Proc. 2006 IEEE Power Eng. Soc. General Meeting* Montreal, Quebec, Canada, Oct. 2006, p. 2

[65] P. Kundur, *Power System Stability and Control*. New York: McGraw-Hill, 1994.

[66] SEL-351-5,-6,-7 protection system product literature, Aug. 17, 2011 [Online]. Available: http://www.selinc.com/literature/literature.aspx?fid=1473

[67] B. Fleming, "Negative sequence impedance directional element," Pullman, WA, USA: Schweitzer Engineering Laboratories Inc. May 5, 2011. [Online]. Available: http://www2.selinc.com/techpprs/6072.pdf

APPENDIX A

A. Secondary Distributed Load and Transformer Ratings for the Multi-feeder Test System

The listings of the secondary distributed loads and the transformer (x'fmer) ratings for each phase are provided in the tables below. Table 32, Table 33, Table 34 and provide the ratings for phase A, B and C, respectively. Each row between nodes A and B corresponds to a customer. The number of transformer(s) serving a group of customers between the nodes A and B is provided in column 3.

Table 32 Phase A Secondary Distributed Loads and Transformer Ratings

Node A	Node B	# of X'fmers	kWh per Customer	Average Demand per Customer (kW)	Max. Demand per Customer (kW)	Max Demand per Customer (kVAR)	X'fmer Rating (kVA)
818	820	6	966	1.34	9.58	4.64	10.00
			1494	2.08	14.82	7.18	15.00
			1363	1.89	13.52	6.55	15.00
			1257	1.75	14.55	7.05	15.00
			1450	2.01	18.31	8.87	15.00
			1176	1.63	11.67	5.65	10.00
820	822	1	557	0.77	5.95	3.61	25.00
			551	0.77	6.96	4.87	
			484	0.67	5.17	3.62	
			493	0.68	6.22	3.78	
			480	0.67	5.56	3.24	
			559	0.78	5.97	3.62	
			501	0.70	6.33	4.14	
			567	0.79	5.63	2.72	
			532	0.74	6.72	4.23	
			557	0.77	5.95	4.03	
			509	0.71	5.44	3.56	
			482	0.67	4.78	2.32	
		1	506	0.70	7.03	4.26	25
			505	0.70	4.68	2.61	
			498	0.69	4.61	3.23	
			553	0.77	5.12	2.98	
			583	0.81	5.40	3.15	
			475	0.66	6.00	3.20	

Table 32 Continued

Node A	Node B	# of X'fmers	kWh per Customer	Average Demand per Customer (kW)	Max. Demand per Customer (kW)	Max. Demand per Customer (kVAR)	X'fmer Rating (kVA)
			563	0.78	6.52	4.11	
			553	0.77	6.98	5.06	
			540	0.75	7.50	5.08	
			528	0.73	5.24	3.79	
			573	0.80	7.96	5.39	
			543	0.75	5.80	3.79	
820	822	1	520	0.72	7.22	3.68	25
			521	0.72	4.82	3.27	
			561	0.78	6.49	3.31	
			513	0.71	5.48	3.45	
			553	0.77	5.49	3.84	
			515	0.72	6.50	4.56	
			504	0.70	5.38	3.77	
			581	0.81	6.72	3.76	
			593	0.82	5.88	2.85	
			564	0.78	6.03	3.22	
			500	0.69	4.96	3.01	
			542	0.75	6.27	4.39	
		1	466	0.65	4.62	2.80	25
			568	0.79	7.17	3.65	
			518	0.72	6.54	4.12	
			565	0.78	7.13	3.64	
			580	0.81	5.37	2.87	
			504	0.70	5.38	3.01	
			556	0.77	6.44	3.75	
			549	0.76	7.63	5.52	
			563	0.78	7.82	5.30	
			584	0.81	5.79	3.51	
			517	0.72	5.98	3.91	
			553	0.77	6.98	3.73	
		1	527	0.73	5.63	2.87	25
			556	0.77	5.15	3.12	
			513	0.71	4.75	3.44	
			561	0.78	5.57	3.77	
			560	0.78	7.78	4.53	
			534	0.74	5.71	4.13	
			562	0.78	7.10	4.30	
			561	0.78	5.19	2.65	

Table 32 Continued

Node A	Node B	# of Xfmers	kWh per Customer	Average Demand Per Customer (kW)	Max. Demand Per Customer (kW)	Max. Demand per Customer (kVAR)	X'fmer Rating (kVA)
			550	0.76	5.88	2.85	
			509	0.71	4.71	2.75	
			488	0.68	6.16	4.32	
			574	0.80	5.31	2.71	
820	822	1	552	0.77	7.67	4.65	25
			491	0.68	6.82	4.46	
			576	0.80	6.67	3.72	
			586	0.81	6.26	3.19	
			481	0.67	4.45	2.60	
			510	0.71	6.44	3.75	
			529	0.73	4.90	3.32	
			576	0.80	5.71	2.77	
			526	0.73	7.31	4.60	
			494	0.69	6.86	4.97	
			484	0.67	6.72	3.92	
			533	0.74	7.40	4.14	
		1	450	0.63	4.46	2.92	25
			503	0.70	6.99	5.06	
			527	0.73	7.32	4.79	
			517	0.72	5.13	2.48	
			586	0.81	8.14	4.15	
			488	0.68	5.65	3.69	
			525	0.73	7.29	4.42	
			554	0.77	6.41	4.04	
			513	0.71	7.13	3.45	
			542	0.75	7.53	4.21	
			564	0.78	7.83	4.75	
			508	0.71	6.41	3.43	

Table 32 Continued

Node A	Node B	# of X'fmers	kWh per Customer	Average Demand per Customer (kW)	Max. Demand per Customer (kW)	Max. Demand per Customer (kVAR)	X'fmer Rating (kVA)
820	822	1	482	0.67	6.69	4.06	25
			561	0.78	5.57	3.64	
			507	0.70	5.87	3.70	
			501	0.70	5.35	3.37	
			494	0.69	5.72	3.19	
			584	0.81	7.37	4.12	
			577	0.80	6.16	2.99	
			504	0.70	5.83	4.22	
			558	0.78	5.54	2.96	
			551	0.77	5.89	3.29	
			522	0.73	7.25	4.22	
			516	0.72	4.78	2.55	
		1	568	0.79	7.17	3.83	15.00
			554	0.77	6.41	4.19	
			529	0.73	5.65	3.83	
			508	0.71	5.04	3.65	
			572	0.79	5.30	2.83	
828	830	5	217	0.30	2.51	1.28	5.00
			209	0.29	2.07	1.21	5.00
			214	0.30	2.97	1.94	5.00
			221	0.31	2.05	1.39	5.00
			212	0.29	2.94	1.99	5.00
832	858	10	149	0.21	1.59	0.97	5.00
			140	0.19	1.39	0.67	5.00
			125	0.17	1.45	0.70	5.00
			154	0.21	1.65	0.80	5.00
			144	0.20	1.67	1.13	5.00
			142	0.20	1.31	0.86	5.00
			142	0.20	1.31	0.86	5.00
			147	0.20	1.86	0.99	5.00
			127	0.18	1.76	0.85	5.00
			150	0.21	2.08	1.51	5.00

Table 32 Continued

Node A	Node B	# of X'fmers	kWh per Customer	Average Demand per Customer (kW)	Max. Demand per Customer (kW)	Max. Demand per Customer (kVAR)	X'fmer Rating (kVA)
858	864	2	35	0.05	0.44	0.23	5.00
			34	0.05	0.36	0.20	5.00
858	834	11	77	0.11	0.76	0.45	5.00
			68	0.09	0.79	0.53	5.00
			78	0.11	0.72	0.49	5.00
			72	0.10	1.00	0.70	5.00
			72	0.10	0.67	0.39	5.00
			73	0.10	0.72	0.46	5.00
			72	0.10	0.83	0.47	5.00
			79	0.11	0.73	0.39	5.00
			73	0.10	0.84	0.47	5.00
			71	0.10	0.66	0.43	5.00
			78	0.11	0.83	0.58	5.00
834	860	1	308	0.43	3.29	1.76	15.00
			302	0.42	3.00	1.60	
			305	0.42	3.03	1.76	
			316	0.44	2.93	1.91	
			305	0.42	3.26	1.74	
			294	0.41	3.14	1.75	
			313	0.43	4.35	2.11	
			275	0.38	3.82	2.68	
			320	0.44	2.96	1.80	
			319	0.44	2.95	1.58	
			297	0.41	4.13	2.70	
			305	0.42	3.53	1.80	
		1	321	0.45	3.18	1.86	5.00

Table 32 Continued

Node A	Node B	# of X'fmers	kWh per Customer	Average Demand per Customer (kW)	Max. Demand per Customer (kW)	Max. Demand per Customer (kVAR)	X'fmer Rating (kVA)
860	836	2	536	0.74	5.73	4.15	25.00
			500	0.69	6.31	2.89	
			457	0.64	5.77	3.50	
			458	0.64	6.36	2.80	
			498	0.69	6.92	2.64	
			459	0.64	5.31	3.08	
			500	0.69	6.94	2.85	
			488	0.68	6.16	2.47	
			506	0.70	5.02	3.88	
			453	0.63	5.24	3.82	
			461	0.64	4.27	3.09	
			459	0.64	5.80	3.44	
			523	0.73	5.59	3.15	10.00
			518	0.72	6.54	2.68	
			513	0.71	5.09	3.06	
			515	0.72	5.96	3.82	
836	840	1	839	1.17	11.65	7.62	15
			799	1.11	10.09	5.14	
			812	1.13	11.28	5.75	
			844	1.17	10.66	7.47	
842	844	1	1380	1.92	17.42	12.21	15.00

Table 33 Phase B Secondary Distributed Loads and Transformer Ratings

Node A	Node B	# of X'fmers	kWh per Customer	Average Demand per Customer (kW)	Max. Demand per Customer (kW)	Max. Demand per Customer (kVAR)	X'fmer Rating (kVA)
802	806	1	147	0.20	1.46	0.99	5.00
			155	0.22	2.15	1.46	
			158	0.22	1.46	0.75	
			156	0.22	1.67	1.13	
			156	0.22	1.55	1.08	
			147	0.20	2.04	1.19	
			151	0.21	2.10	1.37	
			145	0.20	1.34	0.78	
			146	0.20	1.35	0.85	
			152	0.21	1.62	0.99	
			159	0.22	1.47	0.82	
			158	0.22	1.83	1.02	
		1	146	0.20	1.56	1.02	5
			149	0.21	2.07	1.00	
			155	0.22	1.96	0.95	
			146	0.20	1.84	0.94	
			154	0.21	1.78	1.29	
			154	0.21	1.78	0.91	
			158	0.22	1.99	1.30	
			158	0.22	2.19	1.17	
			159	0.22	2.01	0.97	
			148	0.21	1.58	1.11	
			158	0.22	1.99	1.26	
			160	0.22	2.22	1.45	
		1	149	0.21	1.48	0.75	5
			153	0.21	1.77	1.20	
			154	0.21	1.78	1.04	
			154	0.21	1.78	0.95	
			157	0.22	2.18	1.37	
			152	0.21	1.92	1.03	
			141	0.20	1.78	1.12	
			157	0.22	2.18	1.17	

Table 33 Continued

Node A	Node B	# of X'fmers	kWh per Customer	Average Demand per Customer (kW)	Max. Demand per Customer (kW)	Max. Demand per Customer (kVAR)	X'fmer Rating (kVA)
			146	0.20	1.69	1.18	
			160	0.22	2.22	1.19	
			159	0.22	1.47	0.75	
			155	0.22	1.44	0.87	
802	806	1	152	0.21	1.92	1.25	5.00
			146	0.20	1.35	0.82	
			147	0.20	1.46	0.85	
			154	0.21	1.53	0.78	
			152	0.21	2.11	1.48	
			155	0.22	1.79	1.30	
			155	0.22	2.15	1.31	
			160	0.22	1.48	0.93	
			156	0.22	1.97	1.43	
			155	0.22	1.79	1.00	
			147	0.20	1.86	0.99	
			156	0.22	1.55	0.79	
802	806	1	145	0.20	1.68	0.98	5
			146	0.20	2.03	0.98	
			154	0.21	1.65	1.19	
			159	0.22	2.21	1.34	
			155	0.22	2.15	1.25	
			153	0.21	1.93	1.08	
			158	0.22	1.83	0.89	
			145	0.20	1.55	1.05	
			154	0.21	1.78	1.17	
			147	0.20	2.04	1.24	
			150	0.21	1.39	1.01	
			149	0.21	1.59	1.12	
802	806	1	155	0.22	2.15	1.31	5
			146	0.20	2.03	1.28	
			151	0.21	1.91	1.11	
			152	0.21	1.76	1.19	
			153	0.21	2.13	1.44	
			158	0.22	1.57	0.91	
			151	0.21	1.61	0.82	
			147	0.20	1.36	0.69	

Table 33 Continued

Node A	Node B	# of X'fmers	kWh per Customer	Average Demand per Customer (kW)	Max. Demand per Customer (kW)	Max. Demand per Customer (kVAR)	X'fmer Rating (kVA)
808	810	7	479	0.67	5.54	3.75	5.00
			535	0.74	7.43	5.03	5.00
			496	0.69	4.92	2.63	5.00
			494	0.69	5.28	3.45	5.00
			451	0.63	5.69	3.32	5.00
			477	0.66	6.02	4.22	5.00
			483	0.67	5.16	2.76	5.00
816	824	1	39	0.05	0.54	0.28	5.00
824	826	1	391	0.54	5.43	3.16	15.00
			403	0.56	3.73	2.44	
			419	0.58	4.85	3.06	
			394	0.55	3.65	2.04	
			406	0.56	3.76	2.10	
			397	0.55	4.59	2.34	
			372	0.52	3.97	2.88	
			378	0.53	3.75	1.91	
			383	0.53	4.09	2.08	
			428	0.59	4.25	2.27	
			399	0.55	3.96	2.21	
			384	0.53	3.56	1.72	
		1	365	0.51	5.07	2.95	15.00
			392	0.54	4.54	2.42	
			368	0.51	3.93	2.85	
			386	0.54	4.47	3.03	
			390	0.54	4.17	2.12	
			430	0.60	5.43	2.77	
			410	0.57	4.07	1.97	
			378	0.53	3.75	1.91	
			398	0.55	4.61	3.23	
			401	0.56	5.57	4.03	
			391	0.54	4.94	3.34	
			429	0.60	4.97	3.59	

Table 33 Continued

Node A	Node B	# of X'fmers	kWh per Customer	Average Demand per Customer (kW)	Max. Demand per Customer (kW)	Max. Demand per Customer (kVAR)	X'fmer Rating (kVA)
824	826	1	428	0.59	4.57	2.77	15.00
			425	0.59	4.22	2.25	
			407	0.57	4.71	2.97	
			425	0.59	4.22	2.04	
			416	0.58	4.44	2.91	
			380	0.53	3.77	2.38	
			364	0.51	3.61	1.84	
			366	0.51	3.91	1.99	
			408	0.57	5.15	3.00	
			380	0.53	3.77	1.83	
			424	0.59	5.35	2.59	
			410	0.57	4.75	3.10	
854	856	1	500	0.69	4.96	2.89	5.00
832	858	2	64	0.09	0.63	0.43	5.00
			63	0.09	0.88	0.61	5.00
858	834	15	203	0.28	1.88	0.91	5.00
			216	0.30	2.00	1.31	5.00
			217	0.30	2.32	1.52	5.00
			209	0.29	2.07	1.21	5.00
			229	0.32	2.65	1.79	5.00
			225	0.31	3.13	1.97	5.00
			207	0.29	1.92	1.02	5.00
			216	0.30	2.31	1.45	5.00
			220	0.31	2.55	1.54	5.00
			207	0.29	2.21	1.24	5.00
			201	0.28	1.86	1.08	5.00
			204	0.28	1.89	1.19	5.00
834	860	1	384	0.53	4.10	2.59	15.00
			429	0.60	4.26	2.88	
			382	0.53	3.79	1.84	
			365	0.51	3.90	1.89	
			440	0.61	4.37	2.44	
			392	0.54	4.95	2.52	
			405	0.56	4.33	2.62	
			406	0.56	4.70	2.28	
			397	0.55	4.59	2.79	
			436	0.61	5.51	3.47	
			379	0.53	3.51	1.87	
			384	0.53	4.10	2.97	
		1	369	0.51	4.66	3.26	5.00
			434	0.60	4.02	2.82	

Table 33 Continued

Node A	Node B	# of X'fmers	kWh per Customer	Average Demand per Customer (kW)	Max. Demand per Customer (kW)	Max. Demand per Customer (kVAR)	X'fmer Rating (kVA)
860	836	8	258	0.36	3.26	1.90	5.00
			271	0.38	2.90	1.82	5.00
			299	0.42	3.46	2.42	5.00
			255	0.35	3.54	2.32	5.00
			278	0.39	3.51	1.96	5.00
			300	0.42	4.17	2.02	5.00
			273	0.38	2.92	2.04	5.00
			301	0.42	2.99	2.02	5.00
836	840	1	671	0.93	7.77	4.15	25.00
			669	0.93	7.74	5.24	
			695	0.97	9.65	5.16	
			632	0.88	6.75	4.26	
			609	0.85	7.05	3.77	
			622	0.86	6.17	3.60	
			578	0.80	5.35	3.50	
			601	0.83	7.59	3.68	
862	838	1	224	0.31	2.22	1.13	10.00
			242	0.34	2.40	1.63	
			288	0.40	3.08	1.72	
			222	0.31	2.20	1.59	
			210	0.29	2.08	1.41	
			266	0.37	2.64	1.54	
			263	0.37	3.65	2.30	
			251	0.35	3.49	1.86	
			292	0.41	2.70	1.77	
			245	0.34	2.27	1.43	
			293	0.41	2.71	1.84	
			296	0.41	2.94	1.99	
		1	226	0.31	3.14	1.68	10.00
			247	0.34	3.12	1.51	
			233	0.32	2.70	1.70	
			294	0.41	4.08	2.28	
			293	0.41	3.70	2.07	
			274	0.38	2.54	1.29	
			267	0.37	2.47	1.56	
			270	0.38	2.68	1.56	
			278	0.39	2.57	1.68	
			225	0.31	2.08	1.01	
			296	0.41	3.74	2.44	
			255	0.35	2.36	1.32	

Table 33 Continued

Node A	Node B	# of X'fmers	kWh per Customer	Average Demand per Customer (kW)	Max. Demand per Customer (kW)	Max. Demand per Customer (kVAR)	X'fmer Rating (kVA)
862	838	1	234	0.33	2.71	1.96	10.00
			252	0.35	3.50	2.53	
			276	0.38	3.48	1.95	
			223	0.31	2.21	1.13	
			256	0.36	2.74	1.39	
			276	0.38	3.83	2.42	
			284	0.39	3.94	2.67	
			230	0.32	2.90	1.76	
			263	0.37	3.32	2.33	
			296	0.41	3.43	2.40	
844	846	1	125	0.17	1.16	0.70	5.00
			130	0.18	1.20	0.84	
			129	0.18	1.38	0.84	
			136	0.19	1.45	0.70	
			126	0.18	1.35	0.85	
			136	0.19	1.35	0.82	
			136	0.19	1.45	0.70	
			129	0.18	1.19	0.58	
			136	0.19	1.26	0.61	
			126	0.18	1.59	0.93	
			136	0.19	1.45	1.02	
			127	0.18	1.76	0.94	
		1	130	0.18	1.64	0.79	5.00
			135	0.19	1.88	1.36	
			127	0.18	1.47	1.00	
			132	0.18	1.83	1.07	
			133	0.18	1.85	0.94	
			132	0.18	1.31	0.86	
			126	0.18	1.75	1.19	
			135	0.19	1.25	0.76	
			125	0.17	1.16	0.76	
			129	0.18	1.28	0.81	
			135	0.19	1.44	0.98	
			133	0.18	1.85	1.16	
		1	132	0.18	1.53	0.78	
			127	0.18	1.76	1.07	
			124	0.17	1.57	0.99	
			126	0.18	1.59	1.04	
			134	0.19	1.33	0.96	
			135	0.19	1.34	0.68	

Table 33 Continued

Node A	Node B	# of X'fmers	kWh per Customer	Average Demand per Customer (kW)	Max. Demand per Customer (kW)	Max. Demand per Customer (kVAR)	X'fmer Rating (kVA)
844	846		134	0.19	1.69	1.07	5.00
			136	0.19	1.45	1.02	
			131	0.18	1.52	0.99	
			127	0.18	1.26	0.88	
			136	0.19	1.45	0.81	
			126	0.18	1.75	0.94	
		1	131	0.18	1.30	0.69	5.00
			105	0.15	0.97	0.70	
			135	0.19	1.88	1.18	
			129	0.18	1.38	0.70	
			133	0.18	1.42	0.69	
			130	0.18	1.29	0.75	
			131	0.18	1.21	0.88	
			125	0.17	1.45	0.95	
			128	0.18	1.27	0.71	
			132	0.18	1.22	0.59	
			124	0.17	1.72	0.88	
			132	0.18	1.41	0.89	
		1	125	0.17	1.16	0.78	5.00
			134	0.19	1.55	1.12	
			125	0.17	1.45	0.91	
			126	0.18	1.17	0.68	
			132	0.18	1.53	0.78	
			126	0.18	1.75	1.10	
			132	0.18	1.83	0.98	
			129	0.18	1.38	0.77	
			133	0.18	1.32	0.77	
			134	0.19	1.33	0.68	
			126	0.18	1.35	0.91	
			128	0.18	1.27	0.71	
844	846	1	131	0.18	1.30	0.85	5.00
846	848	2	1977	2.75	22.88	13.33	25.00
			1978	2.75	19.62	13.75	15.00

Table 34 Phase C Secondary Distributed Load and Transformer Ratings

Node A	Node B	# of X'fmers	kWh per Customer	Average Demand per Customer (kW)	Max. Demand per Customer (kW)	Max. Demand per Customer (kVAR)	X'fmer Rating (kVA)
802	806	1	123	0.17	1.31	0.92	5.00
			118	0.16	1.37	0.96	
			127	0.18	1.18	0.60	
			128	0.18	1.27	0.80	
			133	0.18	1.23	0.89	
			125	0.17	1.34	0.87	
			126	0.18	1.59	1.08	
			134	0.19	1.55	0.79	
			122	0.17	1.13	0.82	
			132	0.18	1.53	0.89	
			129	0.18	1.49	1.05	
			124	0.17	1.32	0.74	
802	806	1	127	0.18	1.36	0.89	5
			116	0.16	1.07	0.55	
			122	0.17	1.69	0.91	
			123	0.17	1.22	0.65	
			127	0.18	1.60	0.82	
			128	0.18	1.62	0.94	
			114	0.16	1.13	0.77	
			120	0.17	1.39	0.84	
			128	0.18	1.48	0.97	
			115	0.16	1.23	0.86	
			133	0.18	1.68	1.22	
			139	0.19	1.76	0.89	
802	806	1	135	0.19	1.34	0.91	5
			124	0.17	1.23	0.63	
			125	0.17	1.58	0.80	
			130	0.18	1.64	1.19	
			127	0.18	1.26	0.76	
			121	0.17	1.20	0.87	
			136	0.19	1.26	0.85	
			137	0.19	1.73	1.13	

Table 34 Continued

Node A	Node B	# of X'fmers	kWh per Customer	Average Demand per Customer (kW)	Max. Demand per Customer (kW)	Max. Demand per Customer (kVAR)	X'fmer Rating (kVA)
			114	0.16	1.44	0.70	
			131	0.18	1.40	0.85	
			128	0.18	1.27	0.62	
			116	0.16	1.24	0.69	
802	806	1	123	0.17	1.31	0.64	5.00
			120	0.17	1.19	0.75	
			138	0.19	1.60	1.04	
			134	0.19	1.24	0.90	
			120	0.17	1.52	0.73	
			130	0.18	1.39	0.91	
			134	0.19	1.24	0.69	
			114	0.16	1.13	0.79	
			127	0.18	1.18	0.66	
			126	0.18	1.35	0.88	
			118	0.16	1.17	0.57	
			121	0.17	1.29	0.81	
802	806	1	124	0.17	1.44	0.94	5.00
			116	0.16	1.61	1.02	
			137	0.19	1.27	0.68	
			121	0.17	1.53	0.74	
			135	0.19	1.88	1.09	
			130	0.18	1.39	0.67	
			120	0.17	1.28	0.72	
			119	0.17	1.38	0.87	
			132	0.18	1.53	0.96	
			125	0.17	1.16	0.70	
			129	0.18	1.63	0.95	
			124	0.17	1.44	0.94	
802	806	1	129	0.18	1.49	0.83	5.00
			134	0.19	1.86	1.13	
			130	0.18	1.39	0.81	
			135	0.19	1.25	0.67	
			134	0.19	1.43	0.69	
			116	0.16	1.07	0.68	
			133	0.18	1.54	1.01	

Table 34 Continued

Node A	Node B	# of X'fmers	kWh per Customer	Average Demand per Customer (kW)	Max. Demand per Customer (kW)	Max. Demand per Customer (kVAR)	X'fmer Rating (kVA)
824	828	3	130	0.18	1.81	0.87	5.00
			140	0.19	1.62	0.87	5.00
			120	0.17	1.11	0.70	5.00
832	858	4	216	0.30	3.00	2.03	5.00
			210	0.29	2.08	1.06	5.00
			205	0.28	2.59	1.75	5.00
			233	0.32	3.24	1.89	5.00
858	834	14	229	0.32	2.12	1.29	5.00
			227	0.32	2.25	1.58	5.00
			230	0.32	2.90	1.97	5.00
			217	0.30	2.32	1.24	5.00
			237	0.33	2.35	1.48	5.00
			216	0.30	2.14	1.30	5.00
			233	0.32	3.24	2.12	5.00
			246	0.34	2.63	1.53	5.00
			253	0.35	3.19	1.71	5.00
			234	0.33	2.95	1.86	5.00
			242	0.34	2.59	1.87	5.00
			227	0.32	2.10	1.32	5.00
			218	0.30	2.02	1.27	5.00
			224	0.31	2.83	2.05	5.00
834	860	1	388	0.54	4.49	2.83	15.00
			401	0.56	3.71	2.69	
			410	0.57	4.38	2.34	
			389	0.54	4.16	2.22	
			373	0.52	3.70	1.98	
			433	0.60	6.01	3.06	
			439	0.61	5.08	3.68	
			403	0.56	3.73	2.70	
			385	0.53	4.11	2.59	
			411	0.57	3.81	2.58	
			438	0.61	5.07	3.67	
			424	0.59	5.89	3.15	

Table 34 Continued

Node A	Node B	# of X'fmers	kWh per Customer	Average Demand per Customer (kW)	Max. Demand per Customer (kW)	Max. Demand per Customer (kVAR)	X'fmer Rating (kVA)
834	860	1	393	0.55	4.20	2.14	15.00
			416	0.58	3.85	1.87	
			377	0.52	3.49	1.87	
			388	0.54	4.15	2.81	
			444	0.62	4.11	2.30	
			392	0.54	3.63	2.63	
			393	0.55	4.20	2.74	
			430	0.60	3.98	1.93	
			373	0.52	4.71	2.86	
			391	0.54	4.94	2.88	
			404	0.56	4.68	3.28	
			414	0.58	4.11	2.29	
		1	422	0.59	4.19	2.44	15.00
			431	0.60	5.99	3.49	
			412	0.57	3.81	2.76	
			433	0.60	6.01	4.35	
			416	0.58	5.78	2.94	
			431	0.60	5.99	4.19	
			407	0.57	4.35	2.43	
			396	0.55	3.93	2.00	
			376	0.52	4.35	2.95	
			444	0.62	6.17	3.29	
			441	0.61	4.71	2.86	
			395	0.55	4.22	2.15	
		1	409	0.57	3.79	2.56	15.00
			442	0.61	5.12	3.58	
			397	0.55	3.94	2.76	
			441	0.61	5.57	3.24	
			419	0.58	5.82	4.08	
			412	0.57	5.72	2.77	
			455	0.63	5.74	3.89	
			463	0.64	5.85	3.68	
			407	0.57	3.77	2.01	
			441	0.61	5.57	3.64	

Table 34 Continued

Node A	Node B	# of X'fmers	kWh per Customer	Average Demand per Customer (kW)	Max. Demand per Customer (kW)	Max. Demand per Customer (kVAR)	X'fmer Rating (kVA)
834	860		403	0.56	4.31	2.41	
			428	0.59	4.25	2.97	
		1	460	0.64	4.26	2.78	15.00
			394	0.55	4.97	3.02	
			400	0.56	3.97	2.41	
			439	0.61	4.06	2.75	
			459	0.64	5.80	2.95	
			443	0.62	5.59	3.39	
			372	0.52	5.17	3.26	
			426	0.59	4.55	3.19	
			446	0.62	6.19	3.16	
			373	0.52	5.18	2.64	
			397	0.55	5.51	3.34	
			412	0.57	4.77	3.01	
		1	382	0.53	4.08	2.18	15.00
			383	0.53	4.43	2.37	
			381	0.53	3.78	2.65	
			385	0.53	4.86	3.52	
			424	0.59	5.89	3.71	
			373	0.52	5.18	3.02	
			399	0.55	4.62	3.24	
			383	0.53	3.80	2.03	
			395	0.55	3.92	2.09	
			426	0.59	4.23	2.96	
			412	0.57	4.77	3.34	
			442	0.61	4.09	2.87	
		1	419	0.58	3.88	1.98	15.00
			433	0.60	4.30	2.40	
			430	0.60	3.98	2.79	
			450	0.63	5.68	3.85	

Table 34 Continued

Node A	Node B	# of X'fmers	kWh per Customer	Average Demand per Customer (kW)	Max. Demand per Customer (kW)	Max. Demand per Customer (kVAR)	X'fmer Rating (kVA)
834	860		439	0.61	4.69	2.27	
			420	0.58	5.30	3.22	
			384	0.53	3.81	1.85	
			405	0.56	4.69	3.06	
			398	0.55	5.03	2.81	
			392	0.54	3.89	2.08	
			460	0.64	4.56	3.30	
			406	0.56	4.34	3.14	
		1	419	0.58	4.48	3.03	15.00
			391	0.54	3.62	1.75	
			460	0.64	6.39	3.26	
			411	0.57	4.39	3.08	
			431	0.60	4.60	2.57	
			378	0.53	3.50	1.78	
			420	0.58	5.30	3.34	
			377	0.52	3.74	2.18	
			406	0.56	5.64	2.87	
			415	0.58	5.24	2.67	
			452	0.63	4.19	2.03	
			397	0.55	5.51	3.21	
		1	388	0.54	4.90	3.43	15.00
			450	0.63	6.25	3.18	
			384	0.53	4.85	2.47	
			450	0.63	4.81	3.37	
			414	0.58	5.75	3.49	
			450	0.63	4.17	2.82	
			383	0.53	3.80	2.03	
			437	0.61	4.34	2.32	
860	836	1	939	1.30	11.86	7.19	50.00
			888	1.23	9.49	5.30	
			802	1.11	9.28	4.50	
			842	1.17	9.00	6.09	
			860	1.19	8.53	5.38	
			962	1.34	13.36	9.36	

Table 34 Continued

Node A	Node B	# of X'fmers	kWh per Customer	Average Demand per Customer (kW)	Max. Demand per Customer (kW)	Max. Demand per Customer (kVAR)	X'fmer Rating (kVA)
860	836		902	1.25	8.95	5.43	
			824	1.14	11.44	6.11	
			863	1.20	9.22	4.47	
			828	1.15	9.58	5.58	
			940	1.31	10.88	7.88	
			875	1.22	11.05	6.96	
860	836	1	947	1.32	8.77	4.47	10.00
			897	1.25	8.90	5.19	
844	846	1	191	0.27	2.41	1.17	10.00
			206	0.29	2.04	1.34	
			202	0.28	2.00	1.40	
			202	0.28	2.00	1.02	
			199	0.28	2.13	1.24	
			197	0.27	1.82	0.88	
			208	0.29	2.22	1.50	
			208	0.29	1.93	0.98	
			193	0.27	2.68	1.50	
			191	0.27	1.89	1.24	
			195	0.27	1.93	1.22	
			197	0.27	2.49	1.39	
844	846	1	202	0.28	2.81	1.57	10.00
			180	0.25	1.92	1.07	
			191	0.27	2.21	1.50	
			217	0.30	2.74	1.40	
			207	0.29	1.92	1.34	
			185	0.26	1.98	1.20	
			198	0.28	2.29	1.28	
			184	0.26	1.83	1.24	
			179	0.25	2.26	1.53	
			192	0.27	2.67	1.55	
			179	0.25	2.26	1.26	
			209	0.29	2.42	1.41	

Table 34 Continued

Node A	Node B	# of X'fmers	kWh per Customer	Average Demand per Customer (kW)	Max. Demand per Customer (kW)	Max. Demand per Customer (kVAR)	X'fmer Rating (kVA)
844	846	1	192	0.27	2.67	1.42	10
			200	0.28	2.31	1.12	
			205	0.28	2.37	1.66	
			217	0.3	2.74	1.4	
			204	0.28	2.36	1.71	
			179	0.25	2.07	1.06	
			216	0.3	2.5	1.4	
			195	0.27	2.71	1.77	
			205	0.28	2.37	1.55	
			201	0.28	2.15	1.3	
			208	0.29	2.89	1.54	

APPENDIX B

B. Multi-feeder Test System Data

The multi-feeder test system data uses some of the data for the IEEE 34 Node Radial Test Feeder, which was downloaded from [59]. The spot loads on the multi-feeder test system were maintained as they are on the IEEE 34 node Test Radial Feeder. The line segments lengths and configuration names also remained unaltered. Table 35 provides the multi-feeder test system line segment data.

Table 35 Multi-feeder Test System Line Segments Data

Node A	Node B	Configuration	Length (ft)
800	802	300	2580
802	806	300	1730
806	808	300	32230
808	810	303	5804
808	812	300	37500
812	814	300	29730
814	850	301	10
816	818	302	1710
816	824	301	10210
818	820	302	48150
820	822	302	13740
824	826	303	3030
824	828	301	840
828	830	301	20440
830	854	301	520
832	858	301	4900
832	888	XFM-1	0
834	860	301	2020
834	842	301	280
836	840	301	860
836	862	301	280
842	844	301	1350
844	846	301	3640
846	848	301	530
850	816	301	310
852	832	301	10
854	856	303	23330
854	852	301	36830
858	864	303	1620

Table 35 continued

Node A	Node B	Configuration	Length (ft)
858	834	301	5830
860	836	301	2680
862	838	304	4860
888	890	300	10560

Table 36 Multi-feeder Test System Transformer Data

	kVA	kV-high	kV-low	R - %	X - %
Substation:	5000	69 - D	24.9 -Gr. W	1	8
XFM -1	500	24.9 - Gr.W	4.16 - Gr. W	1.9	4.08

The impedance and susceptance of the line configurations were changed to match the new load ratings of the multi-feeder test system due to the secondary distribution loads. The following section of the appendix provides the impedance and susceptance matrix of the line configurations.

Configuration 300 and 301

$$Z + jR = \begin{bmatrix} 0.3465 + j1.0179 & 0.1560 + j0.5017 & 0.1580 + j0.4236 \\ 0.1560 + j0.5017 & 0.3375 + j1.0478 & 0.1535 + j0.3849 \\ 0.1580 + j0.4236 & 0.1535 + j0.3849 & 0.3414 + j1.0348 \end{bmatrix} \Omega/\text{mile} \quad (15)$$

$$B = \begin{bmatrix} 6.2998 & -1.9958 & -1.2595 \\ -1.9958 & 5.9597 & -0.7417 \\ -1.2595 & -0.7417 & 5.6386 \end{bmatrix} \mu S/\text{mile} \quad (16)$$

Configuration 302

$$Z + jR = \begin{bmatrix} 1.3292+j1.3475 & 0 & 0 \\ 0 & 0 & 0 \\ 0 & 0 & 0 \end{bmatrix} \Omega/\text{mile} \quad (17)$$

$$B = \begin{bmatrix} 4.5193 & 0.0 & 0.0 \\ 0.0 & 0.0 & 0.0 \\ 0.0 & 0.0 & 0.0 \end{bmatrix} \mu S/mile \quad (18)$$

Configuration 303 and 304

$$Z + jR = \begin{bmatrix} 0 & 0 & 0 \\ 0 & 1.3292 + j1.3475 & 0 \\ 0 & 0 & 0 \end{bmatrix} \Omega/mile \quad (19)$$

$$B = \begin{bmatrix} 0.0 & 0.0 & 0.0 \\ 0.0 & 4.5193 & 0.0 \\ 0.0 & 0.0 & 0.0 \end{bmatrix} \mu S/mile \quad (20)$$

VITA

Fred Agyekum Ituzaro received his Bachelor of Science degree in electrical/electronic engineering from Kwame Nkrumah University of Science and Technology at Kumasi, Ghana, in 2008. He entered the electrical engineering program at Texas A&M University in September 2009 and received his Master of Science degree in May 2012.

Mr. Agyekum may be reached at the Department of Electrical and Computer Engineering, 214 Zachry Engineering Center, Texas A&M University, College Station, TX 77843-3128. His email is fgyekum@gmail.com.